

**Atrial remodelling in hypertensive heart disease:  
role of Na<sup>+</sup> homeostasis and contractility**

Dissertation

zur

Erlangung des Doktorgrades  
der Naturwissenschaften  
(Dr. rer. nat.)

dem

Fachbereich Pharmazie der  
Philipps-Universität Marburg  
vorgelegt von

**Yulia Nikonova**

aus **Moskau, Russische Föderation**

Marburg/Lahn **2016**

Erstgutachter: **Prof. Dr. Jens Kockskämper**

Zweitgutachter: **Prof. Dr. Moritz Bünemann**

Eingereicht am **31.03.16**

Tag der mündlichen Prüfung am **19.05.2016**

Hochschulkenziffer: 1180

To my beloved sister

Anna Nikonova

# 1. Table of contents

1. Summary .....	5
2. Zusammenfassung.....	7
3. Introduction .....	10
<b>3.1. Arterial hypertension, heart failure and atrial fibrillation .....</b>	<b>10</b>
3.1.1. Hypertensive heart disease .....	10
3.1.2. Left ventricular hypertrophy .....	11
3.1.3. Heart failure .....	11
3.1.4. Atrial fibrillation.....	13
3.1.5. Conclusions and role of hypertension for the maintenance and development of heart failure and atrial fibrillation.....	19
<b>3.2. Neurohormonal systems involved in the regulation of blood pressure and atrial remodelling.....</b>	<b>21</b>
3.2.1. Renin-angiotensin-aldosterone system (RAAS) .....	21
3.2.2. Sympathetic nervous system .....	22
3.2.3. Endothelin-1 system.....	22
<b>3.3. Regulation of intracellular Ca<sup>2+</sup> concentration in cardiac myocytes.....</b>	<b>24</b>
3.3.1. Excitation-contraction coupling .....	24
3.3.2. Ca <sup>2+</sup> handling in atrial myocytes.....	25
<b>3.4. Intracellular Na<sup>+</sup> regulation and its role in cardiac myocytes .....</b>	<b>26</b>
3.4.1. Na <sup>+</sup> and excitation contraction coupling.....	27
3.4.2. Na <sup>+</sup> current, action potential formation, late Na <sup>+</sup> current.....	28
3.4.3. Na <sup>+</sup> and Ca <sup>2+</sup> regulation .....	29
3.4.4. Na <sup>+</sup> and pH regulation.....	30
3.4.5. Na <sup>+</sup> /K <sup>+</sup> -ATPase (NKA).....	30
3.4.6. Na <sup>+</sup> and regulation of cardiac metabolism.....	31
3.4.7. Intracellular Na <sup>+</sup> homeostasis in cardiac disease .....	32
3.4.8. Intracellular Na <sup>+</sup> homeostasis in atrial fibrillation and remodelling .....	32
<b>3.5. Spontaneously hypertensive rats (SHR) as a model for hypertensive heart disease .....</b>	<b>34</b>

3.5.1. Pathophysiological changes induced by hypertension in SHR.....	35
<b>3.6. Aims of the study .....</b>	<b>37</b>
<b>4. Materials and methods .....</b>	<b>39</b>
<b>4.1. Animals .....</b>	<b>39</b>
<b>4.2. Non-invasive blood pressure and heart rate measurements in rats .....</b>	<b>39</b>
<b>4.3. Isolation of rat atrial myocytes.....</b>	<b>41</b>
4.3.1. Chemicals and reagents.....	41
4.3.2. Solutions for atrial myocyte isolation .....	41
4.3.3. Isolation procedure.....	43
4.3.4. Plating of isolated atrial myocytes .....	45
<b>4.4. Measurements of intracellular Na<sup>+</sup> concentration and contractility of atrial myocytes .....</b>	<b>45</b>
4.4.1. Loading the atrial myocytes with SBFI-AM .....	48
4.4.2. Intracellular SBFI calibration and intracellular Na <sup>+</sup> measurements .....	48
4.4.3. Ion Optix setup and atrial myocyte Na <sup>+</sup> and contractility measurements ....	50
<b>4.5. Analysis of protein expression .....</b>	<b>54</b>
4.5.1. Tissue collection .....	54
4.5.2. Homogenization.....	54
4.5.3. Quantification of protein amount .....	55
4.5.4. Western blot analysis .....	56
<b>4.6. Statistical analysis.....</b>	<b>66</b>
<b>5. Results.....</b>	<b>67</b>
<b>5.1. Characterization of atrial remodelling in early hypertension.....</b>	<b>67</b>
5.1.1. Blood pressure and heart rate measurements, gravimetric assessment of hypertrophy .....	67
5.1.2. Measurements of contractility .....	68
5.1.3. Intracellular Na <sup>+</sup> measurements .....	70
5.1.4. Expression of Na <sup>+</sup> regulating proteins in left and right atria from SHR and WKY rats .....	73
<b>5.2. Characterization of atrial remodelling in advanced hypertension.....</b>	<b>80</b>
5.2.1. Blood pressure and heart rate measurements; gravimetric assessment of hypertrophy .....	80

5.2.2. Contractility measurements.....	82
5.2.3. Intracellular Na <sup>+</sup> measurements .....	89
5.2.4. Expression of Na <sup>+</sup> -handling proteins.....	92
<b>5.3. Expression of Na<sup>+</sup>-handling proteins in human atrial fibrillation.....</b>	<b>99</b>
5.3.1. Patient characteristics .....	99
5.3.2. Western blot analysis of Na <sup>+</sup> -handling proteins.....	101
<b>5.4. Effect of macitentan on blood pressure, heart rate, Ca<sup>2+</sup>- handling and endothelin-1 signalling proteins in left atria of SHR .....</b>	<b>106</b>
5.4.1. Blood pressure and heart rate measurements in SHR treated with macitentan or doxazosin.....	107
5.4.2. Effects of macitentan or doxazosin treatment on the expression and phosphorylation of Ca <sup>2+</sup> -handling proteins in left atrium of SHR.....	108
5.4.3. Effects of macitentan or doxazosin treatment on the expression of proteins involved in endothelin-1 signalling.....	112
<b>6. Discussion .....</b>	<b>115</b>
<b>6.1. Cardiovascular changes, unaffected contractility and unchanged [Na<sup>+</sup>]<sub>i</sub> in early hypertension .....</b>	<b>115</b>
6.1.1. Cardiovascular changes in early hypertension .....	115
6.1.2. Unaffected contractility of atrial myocytes in early hypertension .....	116
6.1.3. Unchanged [Na <sup>+</sup> ] <sub>i</sub> in atrial myocytes in early hypertension .....	117
6.1.4. Subtle changes in Na <sup>+</sup> -handling protein expression in early hypertension	118
<b>6.2. Progression of cardiovascular impairment, reduced atrial myocyte contractile function and decreased [Na<sup>+</sup>]<sub>i</sub> in advanced hypertensive heart disease .....</b>	<b>121</b>
6.2.1. Cardiovascular changes.....	121
6.2.2. Reduction in contractile function of atrial but not ventricular myocytes in advanced hypertensive heart disease .....	122
6.2.3. Decrease in [Na <sup>+</sup> ] <sub>i</sub> in atrial but not ventricular myocytes from SHR in advanced hypertensive heart disease .....	123
6.2.4. Up-regulation of Na <sup>+</sup> influx protein expression in the atria in advanced hypertensive heart disease .....	124

6.2.5. Up-regulation of NKA expression in the atria in advanced hypertensive heart disease .....	126
<b>6.3. Unaltered expression of Na<sup>+</sup>-handling proteins in human atrial fibrillation</b>	<b>129</b>
<b>6.4. Macitentan treatment did not markedly affect atrial Ca<sup>2+</sup> remodelling in SHR</b>	<b>132</b>
6.4.1. Macitentan treatment did not lower blood pressure in SHR.....	132
6.4.2. Macitentan treatment did not alter expression of key Ca <sup>2+</sup> -handling proteins in left atria of SHR.....	133
6.4.3. Expression of proteins involved in endothelin-1 signalling is not affected by macitentan treatment .....	134
<b>7. References.....</b>	<b>136</b>
<b>8. Abbreviations .....</b>	<b>150</b>
<b>9. List of Figures.....</b>	<b>154</b>
<b>10. List of tables.....</b>	<b>156</b>
<b>11. Publications .....</b>	<b>157</b>
<b>11.1. Original papers .....</b>	<b>157</b>
<b>11.2. Abstracts and poster presentations.....</b>	<b>158</b>
<b>Curriculum vitae.....</b>	<b>160</b>
<b>12. Acknowledgements .....</b>	<b>161</b>

## 2. Summary

Arterial hypertension causes hypertensive heart disease. Constant mechanical stress and activation of neurohormonal systems cause structural and functional changes in the myocardium termed “remodelling”. Remodelling is beneficial in the beginning of the disease development; however, with time it becomes detrimental and impairs cardiac function. Remodelling of the myocardium occurs in hypertension, atrial fibrillation and heart failure. These cardiac diseases are tightly linked by the mechanisms of pathological remodelling and induce development and maintenance of one another.

Ventricular remodelling has been studied intensively in hypertensive heart disease, however, atrial remodelling has been studied much less and is only poorly understood. Physiology of cardiac myocytes relies on balanced intracellular  $\text{Na}^+$  homeostasis.  $\text{Na}^+$  is involved in many cellular processes, such as action potential initiation,  $\text{Ca}^{2+}$  homeostasis, intracellular pH, metabolism and contractility.

In the first part of the thesis I investigated ionic ( $\text{Na}^+$  homeostasis) and functional (contractility) atrial remodelling in an animal model of hypertensive heart disease – spontaneously hypertensive rats (SHR). In early hypertension, SHR exhibited elevated blood pressure and isolated left ventricular hypertrophy. The atria were not hypertrophied. Contractility of atrial myocytes and intracellular  $\text{Na}^+$  concentration ( $[\text{Na}^+]_i$ ) were both unaltered. Expression of most  $\text{Na}^+$ -handling proteins was unaffected in the atria of SHR.

In advanced hypertension, SHR exhibited further progression of left ventricular hypertrophy and signs of heart failure. Left atria were hypertrophied. The contractility of atrial myocytes was reduced.  $[\text{Na}^+]_i$  was significantly decreased together with increased expression of the  $\alpha 1$  subunit of  $\text{Na}^+/\text{K}^+$ -ATPase. Expression of  $\text{Na}^+/\text{H}^+$ -exchanger was increased, suggesting activation of pro-hypertrophic pathways.

Comparison of SHR with and without signs of heart failure (i.e. increased lung weight) revealed development of right ventricular hypertrophy and progression of bi-atrial hypertrophy in SHR with heart failure. Moreover, the impairment of atrial myocyte contractility progressed. However,  $[\text{Na}^+]_i$  and the expression of major  $\text{Na}^+$ -handling proteins were not changed during the transition to heart failure. In addition to studies on atrial myocytes, we performed measurements of  $[\text{Na}^+]_i$  and contractility of



ventricular myocytes from old SHR. In contrast to our findings in the atria, no impairment of contractility or changes in  $[Na^+]_i$  were observed in the ventricular myocytes, indicating atria-specific remodelling.

Taken together, the presented results indicate that in early hypertension no significant signs of atrial remodelling in terms of contractility and  $Na^+$  homeostasis were found. However, in advanced hypertensive heart disease there was atria-specific functional atrial remodelling, which might contribute to the transition from compensated left ventricular hypertrophy to heart failure.

Atrial ionic remodelling is an important factor in the development and maintenance of atrial fibrillation. The role of intracellular  $Na^+$  homeostasis in these processes is not understood. In the second part of the thesis, I investigated expression of  $Na^+$ -handling proteins in right atrial tissue of patients suffering from paroxysmal and chronic atrial fibrillation compared to patients with sinus rhythm. The results indicated that the expression of  $Na^+$ -handling proteins, including  $Na^+$  channels,  $Na^+/H^+$  exchanger, alpha subunits of  $Na^+/K^+$ -ATPase, phospholemman, was not altered in either paroxysmal or chronic atrial fibrillation. The expression of  $\beta$  1 subunit of  $Na^+/K^+$ -ATPase was significantly reduced in chronic atrial fibrillation. However, the functional consequences of this change require further investigation.

Endothelin-1 plays an important role in the regulation of blood pressure and cardiac physiology. Enhancement of endothelin-1 system activity contributes to cardiac maladaptive remodelling, including disturbances in  $Ca^{2+}$  and  $Na^+$  homeostasis in cardiac myocytes. At the age of 7 months, SHR exhibit enhanced endothelin-1 signalling and altered  $Ca^{2+}$  handling. Therefore, in the third part of the thesis we investigated the effect of endothelin-1 receptor blockage on blood pressure and expression and phosphorylation of  $Ca^{2+}$ -handling proteins, as well as the expression of proteins involved in endothelin-1 signalling in the atria of SHR.

The results revealed that the blockage of endothelin receptors by 8 weeks treatment with macitentan (novel dual endothelin A and endothelin B receptor antagonist) did not lower blood pressure in SHR. Expression and phosphorylation of major  $Ca^{2+}$ -handling proteins and endothelin-1 signalling proteins were both unaffected. Thus, the blockage of endothelin receptors did not cause any major changes in atrial  $Ca^{2+}$  remodelling in SHR.

## Zusammenfassung

Arterielle Hypertonie induziert die Entwicklung von hypertensiver Herzerkrankung. Die Aktivierung von neurohormonalen Systemen und ständiger, mechanischer Stress führen zu Änderungen in der Struktur und Funktion des Herzmuskels. Diese Umbauprozesse werden als „Remodelling“ bezeichnet. Das Remodelling ist am Anfang adaptiv, aber später werden diese Veränderungen pathologisch und beeinträchtigen die Herzfunktion. Umbauprozesse treten bei hypertensiver Herzerkrankung, Vorhofflimmern und Herzinsuffizienz auf. Diese Krankheiten teilen sich eine gemeinsame Pathogenese und begünstigen die gegenseitige Entwicklung und Aufrechterhaltung.

Während das ventrikuläre Remodelling bei hypertensiver Herzerkrankung vergleichsweise gut verstanden ist, bleiben die Mechanismen des atrialen Remodellings weitgehend unbekannt.

Natrium-Ionen ( $\text{Na}^+$ ) sind an vielen zellulären Prozessen im Myokard beteiligt, wie zum Beispiel der Bildung des Aktionspotenzials, der Regulation der intrazellulären  $\text{Ca}^{2+}$  Konzentration, dem pH, dem Zellmetabolismus und der Kontraktilität. Die Regulation der intrazellulären  $\text{Na}^+$ -Konzentration ( $[\text{Na}^+]_i$ ) ist für die normale Herzfunktion von großer Bedeutung.

In dem ersten Teil der Arbeit wurden die ionalen Aspekte ( $\text{Na}^+$ -Homöostase) und die funktionellen Aspekte (Kontraktilität) des atrialen Remodellings im Tiermodell der hypertensiven Herzerkrankung bei „spontan-hypertensiven Ratten“ (SHR) untersucht. Als Kontrolltiere wurden normotensive Wistar Kyoto Ratten (WKY) gewählt. Im frühen Stadium der Hypertonie wiesen die SHR erhöhte Blutdruckwerte und isolierte linksventrikuläre Hypertrophie auf. Die Vorhöfe waren nicht vergrößert. Die Kontraktilität der Vorhofmyozyten,  $[\text{Na}^+]_i$  und die Expression von  $\text{Na}^+$ -regulierenden Proteinen waren unverändert.

Im späten Stadium der hypertensiven Herzerkrankung zeigten die SHR linksventrikuläre Hypertrophie und Zeichen von Herzinsuffizienz. Die linken Vorhöfe der SHR waren vergrößert und die Kontraktilität der Vorhofmyozyten war vermindert.  $[\text{Na}^+]_i$  war signifikant verringert in Kombination mit der erhöhten Expression der

$\alpha$  1-Untereinheit der  $\text{Na}^+/\text{K}^+$ -Pumpe. Die Expression des  $\text{Na}^+/\text{H}^+$ -Austauschers im Vorhofmyokard der SHR war ebenfalls erhöht.

Beim Vergleich von SHR mit Herzinsuffizienz (mit erhöhtem Lungengewicht) mit den SHR ohne Herzinsuffizienz wurden die rechtventrikuläre Hypertrophie und die Progression der Vorhofhypertrophie in den Ratten mit Herzinsuffizienz detektiert. Darüber hinaus wurde auch eine Verminderung der Kontraktilität der Vorhofmyozyten festgestellt.  $[\text{Na}^+]_i$  und die Expression der wichtigsten  $\text{Na}^+$ -regulierenden Proteinen blieben während des Übergangs zur Herzinsuffizienz unverändert.

Zusätzlich zu den Untersuchungen am Vorhofmyokard wurden auch Messungen der  $[\text{Na}^+]_i$  und Kontraktilität in Ventrikelmiozyten durchgeführt. Im Gegensatz zu den Vorhöfen waren  $[\text{Na}^+]_i$  und Kontraktilität der Ventrikelmiozyten unverändert. Das zeigt, dass das untersuchte Remodelling Vorhof-spezifisch ist.

Zusammen genommen zeigen die präsentierten Ergebnisse das Fehlen eines atrialen Remodellings (im Bezug auf die Kontraktilität und  $\text{Na}^+$ -Homöostase) im frühen Stadium der Hypertonie. Im späteren Stadium der Hypertonie sind die funktionellen Umbauprozesse vorhofspezifisch und könnten den Übergang von der kompensierten linksventrikulären Hypertrophie in die Herzinsuffizienz begünstigen.

Remodelling der Ionen-Homöostase im Vorhof ist ein wichtiger Faktor für die Entwicklung und Aufrechterhaltung des Vorhofflimmerns. Die Rolle der intrazellulären  $\text{Na}^+$ -Homöostase dafür ist noch nicht klar. Im zweiten Teil der Dissertation wurde die Expression von  $\text{Na}^+$ -regulierenden Proteinen im rechten Vorhofgewebe von Patienten mit paroxysmalem und chronischem Vorhofflimmern, im Vergleich zu den Patienten mit Sinus-Rhythmus, untersucht. Die Befunde weisen auf die unveränderte Expression der meisten  $\text{Na}^+$ -regulierenden Proteine hin, einschließlich der spannungsabhängigen  $\text{Na}^+$ -Kanäle, des  $\text{Na}^+/\text{H}^+$ -Austauschers, verschiedener Isoformen der  $\alpha$ -Untereinheit der  $\text{Na}^+/\text{K}^+$ -Pumpe und Phospholemman. Die Expression der  $\beta$  1-Untereinheit der  $\text{Na}^+/\text{K}^+$ -Pumpe bei Patienten mit chronischem Vorhofflimmern war signifikant erniedrigt, obwohl die funktionelle Bedeutung dieser Änderung noch unklar bleibt.

Endothelin-1 spielt eine große Rolle für die Regulation des Blutdrucks und in der Herzphysiologie. Die erhöhte Aktivität des Endothelin-1-Systems trägt zu der Entwicklung des pathologischen Remodellings, einschließlich der Störung der  $\text{Ca}^{2+}$ - und  $\text{Na}^+$ -Homöostase in den Herzmuskelzellen, bei. In 7 Monate alten SHR ist die Aktivität

des Endothelin-1-Systems erhöht, gemeinsam mit einer veränderten  $\text{Ca}^{2+}$ -Homöostase. Daher wurde im dritten Teil der Dissertation der Effekt der Endothelin-1-Rezeptor-Blockade auf den Blutdruck, die Expression von  $\text{Ca}^{2+}$ -regulierenden Proteinen und den beteiligten Komponenten der Endothelin-1-Signaltransduktionskaskade im linken Vorhof der SHR untersucht.

Der Blutdruck wurde durch die Blockade der Endothelin-Rezeptoren durch eine Behandlung mit Macitentan, einem neuen Endothelin A- and Endothelin B-Rezeptorantagonisten, für die Dauer von 8 Wochen nicht erniedrigt. Die Expression und Phosphorylierung der meisten  $\text{Ca}^{2+}$ -regulierenden Proteine blieben unverändert. Die Expression von Proteinen des Endothelin-1-Signalwegs war ebenso unverändert. Zusammenfassend zeigt der dritte Teil der Arbeit, dass die Blockade von Endothelin-Rezeptoren keinen wesentlichen Einfluss auf das  $\text{Ca}^{2+}$ -abhängige Remodelling des Vorhofs der SHR hat.

## 3. Introduction

### 3.1. Arterial hypertension, heart failure and atrial fibrillation

#### 3.1.1. Hypertensive heart disease

Hypertensive heart disease is the most common cause of cardiac disease worldwide. According to European Society of Cardiology and European Society of Hypertension (ESC/ESH) guidelines, there are two types of hypertension: primary and secondary. Hypertension is defined as values exceeding 140 mmHg for systolic and 90 mmHg for diastolic blood pressure (Mancia et al. 2014).

**Primary or essential hypertension** - the cause of elevated blood pressure is unclear.

**Secondary hypertension** - the increased blood pressure is a consequence of another disease (pheochromocytoma, Cushing disease, renal diseases). Secondary hypertension is characterized by rapid progression and high blood pressure values. In most of the cases, it can be treated by therapeutic correction of the primary disease or surgical intervention.

Essential hypertension accounts for about 90% of all cases. Usually, mild or moderate elevation of blood pressure is observed and no reason for elevated blood pressure can be identified (Greene & Harris 2008). Since primary hypertension is the most common type of hypertension, the term “hypertension” will be used further in this thesis for the essential type of the disease.

Prolonged elevation in blood pressure may induce several pathological changes in myocardial structure, coronary vessels and the cardiac conduction system, collectively termed “hypertensive heart disease”. These pathological changes cause left ventricular hypertrophy, coronary artery disease, cardiac arrhythmias, and heart failure (McLenachan et al. 1987), (Levy et al. 1996), (Diamond & Phillips 2005). Hypertension can change cardiac structure and function directly via increased afterload and indirectly via activation of several neurohormonal mechanisms, such as activation of the renin-angiotensin-aldosterone and the sympathetic nervous system (Weber et al. 1991).

### **3.1.2. Left ventricular hypertrophy**

Elevated afterload together with activation of the renin-angiotensin-aldosterone and the sympathetic nervous system stimulates myocyte growth, fibroblast activation and collagen formation (Weber et al. 1991). These changes result in left ventricular structural remodelling with disproportionate elevation in fibrous tissue in the myocardium. This, in turn, leads to reduction of left ventricular compliance and, eventually, diastolic dysfunction. Coronary arteries are also structurally changed and, together with increased interstitial fibrosis and myocardial mass, vascular coronary flow decreases, predisposing to ischemic episodes. Moreover, in hypertrophic myocardium fibrosis disturbs normal electrical conduction (Kahan 1998), (Kahan & Bergfeldt 2005). Thus, left ventricular hypertrophy caused by hypertension is a risk factor for the development of myocardial infarction, heart failure and arrhythmias (Kahan & Bergfeldt 2005).

### **3.1.3. Heart failure**

The term “heart failure” describes not a single disease but rather a syndrome with many possible aetiologies, and it can be defined as a failure of the heart to sufficiently perfuse the body with blood (Greene & Harris 2008). Hypertension is one of the major risk factors for left ventricular dysfunction and hypertrophy. Left ventricular hypertrophy can be beneficial in the beginning since it increases or maintains cardiac output. When the disease is progressing, remodelling becomes detrimental and left ventricular structure and function change, e.g. chambers of the heart dilate (Drazner 2011). Functionally, further development of fibrosis causes impairment of contractility and, thus, pumping of the heart becomes less efficient. This results in global hypoperfusion. In addition, the amount of blood remaining in the ventricle is increased, so that left ventricular end diastolic pressure rises, causing elevation of pressure in the left atrium. As a result, the pressure in the lung capillaries also increases, eventually leading to lung oedema and dyspnoea as the clinical manifestation.

Left ventricular failure can also lead to right ventricular dysfunction. This type of dysfunction is characterized by increased pressure in the right ventricle and right atrium, which causes a rise in systemic venous pressure. Consequently, pressure is elevated in the liver, gastrointestinal tract, and low extremities, causing hepatomegaly and peripheral oedema (Kemp & Conte 2012).

Clinically, heart failure is classified as **compensated** and **decompensated** heart failure. Symptoms of compensated heart failure are stable, and the signs of fluid retention and lung oedema are absent (Millane et al. 2000). Decompensated heart failure, as defined by Felker et al., is a deterioration and progression of the compensated form and is characterized by the appearance of new or worsening of already existing symptoms of dyspnoe, fatigue and oedema (Felker et al. 2003).

Left ventricular dysfunction can be divided into two categories: **systolic** and **diastolic dysfunction**. Systolic dysfunction occurs when ventricular contraction and ejection fraction are reduced. This type occurs in 70% of patients with heart failure. Diastolic dysfunction is present in 30% of heart failure patients and is characterized by impaired ventricular relaxation and filling during diastole (Kemp & Conte 2012).

### 3.1.4. Atrial fibrillation

Atrial fibrillation is the most common pathological arrhythmia. The prevalence of atrial fibrillation is about 1-2% of the general population (Andrade et al. 2014). The prevalence increases with advancing age and is associated with the presence of other cardiovascular diseases, such as hypertension and heart failure. The electrocardiogram of fibrillating atria shows undulations of the baseline and the absence of P-waves (Figure 1B), which normally represent regular atrial depolarization. Ventricular rates in atrial fibrillation are slower than in the atria due to filtering of electrical conduction by the atrioventricular node. The QRS complexes, which show ventricular depolarization, are narrow and irregular (Katz 2010), (Wakili et al. 2011).

Figure 1 shows an ECG recording of normal sinus rhythm and atrial fibrillation.

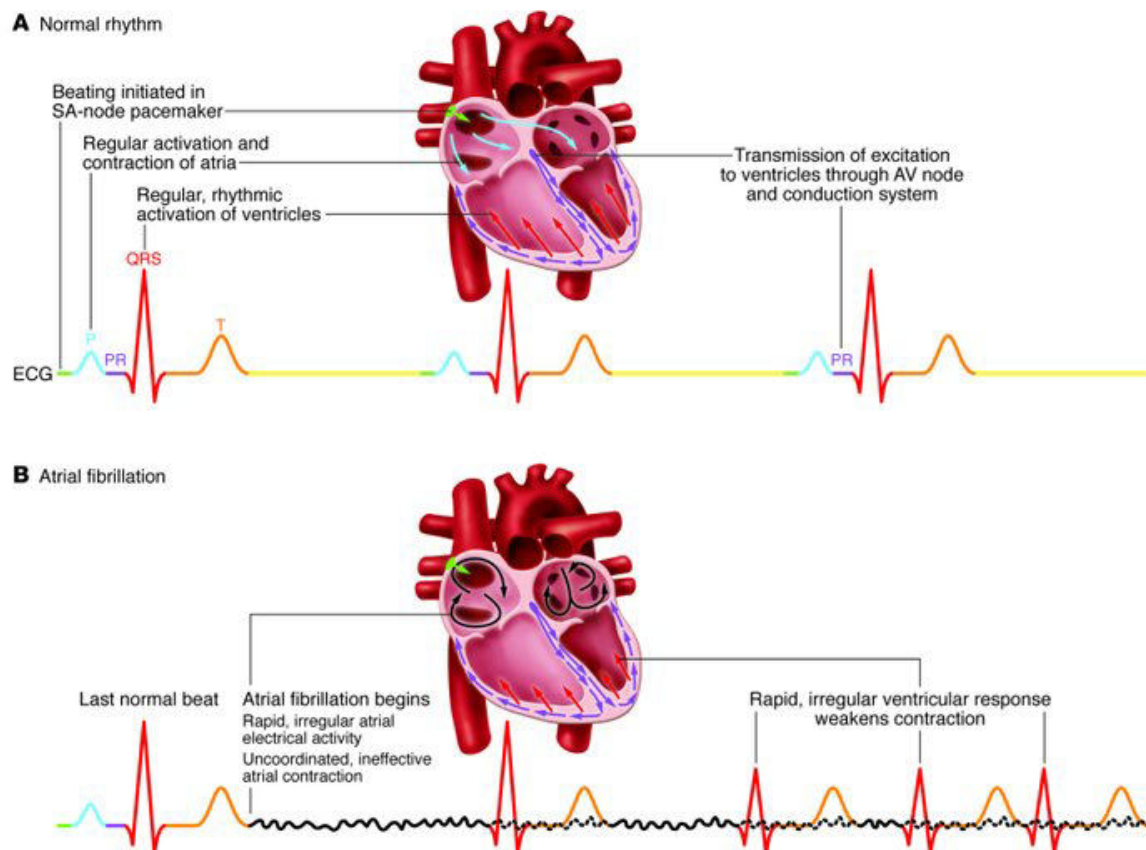


**Figure 1. Electrocardiographic recording of sinus rhythm and the onset of an atrial fibrillation episode.**

Figure is taken from (Wakili et al. 2011)



Due to impaired atrial contractility, blood in the atria (in particular in the left atrial appendage) stagnates and coagulates, causing the major life-threatening complication of atrial fibrillation: stroke (Schotten et al. 2011).

Clinically, atrial fibrillation is classified into paroxysmal, when the episodes of atrial fibrillation are short and selfterminating (Heijman et al. 2014), persistent, when the arrhythmic episode lasts seven days or more, and permanent (chronic), when the normal sinus rhythm can not be regained. Another form of atrial fibrillation is called “lone”. This type of arrhythmia is present in young patients without clinical evidence of hypertension or cardiopulmonary disease and with low risk of cardioembolic complications (Camm et al. 2012). The paroxysmal form can remain or progress further to permanent atrial fibrillation. Similarly, permanent atrial fibrillation is not necessarily a result of the progression of paroxysmal atrial fibrillation; it can develop with a first arrhythmic episode (Schotten et al. 2011).

Many cardiovascular diseases are associated with atrial fibrillation, such as hypertension, valvular heart disease (rheumatic heart disease), heart failure, congenital heart diseases and coronary artery disease. Among others, hypertension and heart failure are very common predictors of atrial fibrillation (Schotten et al. 2011).

Hypertension is responsible for 14% of all atrial fibrillation cases and, at the same time, found in 60-80% of atrial fibrillation patients (Andrade et al. 2014), (Schotten et al. 2011). Furthermore, hypertension is an independent predictor of the disease and contributes to disease progression (Schotten et al. 2011). As discussed above, hypertension induces left ventricular remodelling. Similar remodelling processes are also observed at the atrial level.

### **3.1.4.1. Atrial remodelling and arrhythmogenic mechanisms for atrial fibrillation**

The phenomenon of atrial remodelling has been extensively studied in atrial fibrillation. Atrial remodelling is a time-dependent adaptive regulation of atrial cardiac myocytes to maintain homeostasis and function. The strength and duration of exposure to the stress factors influence the type and extent of remodelling. Tachycardia with high rates of cell depolarization (for example, atrial fibrillation) and volume/pressure overload (mitral valve disease, hypertension and heart failure) belong to the most prominent stress factors for atrial myocytes. Atria respond to these factors by adaptive or maladaptive structural and functional changes. These changes include: myocyte growth and

hypertrophy, necrosis and apoptosis, alterations in the composition of extracellular matrix, alterations in the expression and function of ion channels, as well as in secretion of atrial hormones (Casaclang-Verzosa et al. 2008).

### **Structural remodelling**

Atrial dilation is the typical sign of structural remodelling. Upon normal physiological conditions, atria are expandable chambers with relatively low pressures inside. In the presence of pressure overload or injury, atria become more rigid and stiff. Myocyte hypertrophy and elevated interstitial fibrosis are found at the ultrastructural level (Casaclang-Verzosa et al. 2008). It is important to mention that fibrosis impairs the normal coupling between myocytes and, thus, electrical conduction (Burstein & Nattel 2008). In addition, signs of necrosis and changes in the mitochondrial structure are present in the atrial myocytes. All structural changes, in turn, contribute to the development of electrical remodelling (Casaclang-Verzosa et al. 2008).

### **Electrical remodelling**

A hallmark of atrial electrical remodelling is the shortening of action potential duration. Several studies revealed that changes in the expression and/or activity of ion channels are causing this phenomenon. The density of L-type  $\text{Ca}^{2+}$  current (which is responsible for the plateau phase of the action potential) and/or expression of L-type  $\text{Ca}^{2+}$  channel are reduced, as shown in many animal models of rapid atrial pacing and human atrial fibrillation (Schotten et al. 2011). Potassium repolarizing currents, especially transient outward current ( $I_{to}$ ), are also markedly decreased in atrial fibrillation, whereas inward rectifier potassium current ( $I_{K1}$ ) and the acetylcholine-activated potassium current ( $I_{K,ACh}$ ) are increased in atrial fibrillation. These changes contribute to the decrease in refractoriness of the atrial myocardium and, thus, to perpetuation of the arrhythmia (Bosch et al. 1999), (Schotten et al. 2011). Another important factor in electrical remodelling is disturbed  $\text{Ca}^{2+}$  homeostasis and, thus, impaired electrical excitation and contractile function (Casaclang-Verzosa et al. 2008) ( $\text{Ca}^{2+}$  homeostasis will be discussed in more detail below). Loss of atrial contractile function has the important clinical consequence of increasing the risk of thromboembolism (Schotten et al. 2011).

#### **3.1.4.2. Mechanisms of atrial fibrillation initiation**

For atrial fibrillation to occur and be maintained, ectopic electrical activity (trigger) and an obstacle for the conduction of an electrical impulse (substrate) should be present in

atrial myocardium. Focal ectopic/triggered activity is caused by early or delayed afterdepolarizations (Heijman et al. 2014). Early afterdepolarizations occur before the completion of repolarization of an action potential (Zeng & Rudy 1995) and are promoted by prolonged repolarization (Heijman et al. 2014) and  $\text{Ca}^{2+}$  handling abnormalities: changes in L-type  $\text{Ca}^{2+}$  channel activation and de-activation or spontaneous  $\text{Ca}^{2+}$  release from sarcoplasmic reticulum (Schotten et al. 2011). Delayed afterdepolarizations occur after complete repolarization of the action potential and mostly result from the spontaneous release of  $\text{Ca}^{2+}$  from sarcoplasmic reticulum during diastole (January & Fozzard 1988), (Dobrev & Nattel 2010).

There are two types of re-entry mechanisms: leading circle and spiral wave. Leading circle re-entry occurs when refractoriness of the atrial myocardium is short, or conduction is slow, so that continuous conduction in the re-entry zone can be initiated. Re-entry terminates if the refractoriness of the tissue is prolonged or conduction accelerates. In case of the spiral wave, a rapidly circulating rotor with a wavefront rotating around the core maintains re-entry. Reduction of the excitability or prolongation of refractoriness can terminate the spiral wave re-entry (Dobrev & Nattel 2010).

As discussed before, changes in atrial electrophysiology cause the shortening of refractoriness, which stimulates an initiation or maintenance of ectopic electrical activity. Structural remodelling (fibrosis and dilation of the atria) also creates a prolongation of electrical conduction and/or creates an anatomic obstacle in the atrial tissue, which favours initiation of the re-entry (Wakili et al. 2011). Thus, atrial structural (mainly fibrosis) and electrical remodelling both create an arrhythmogenic substrate.

Figure 2 illustrates the key mechanisms and role of atrial remodelling for atrial fibrillation initiation.

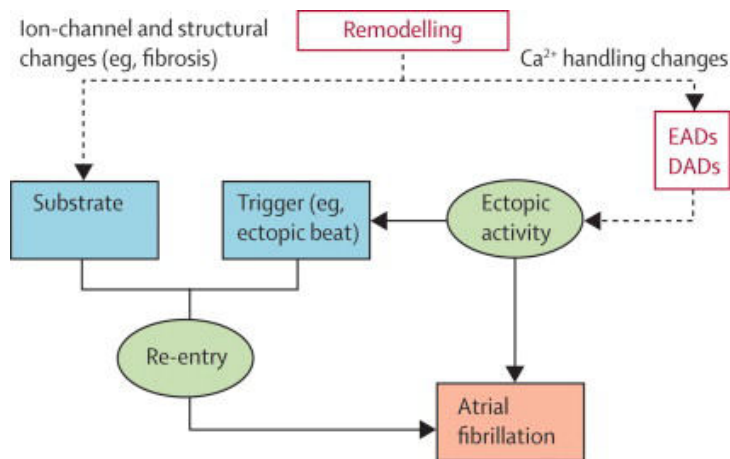


**Figure 2. Role of atrial remodelling in the initiation of atrial fibrillation**

Figure is reproduced from (Dobrev & Nattel 2010)

Atrial fibrillation is maintained by either re-entry or rapid and sustained ectopic activity. Development of re-entry depends on the presence of a vulnerable substrate and a trigger (ectopic beat), acting on this substrate. Atrial remodelling creates a substrate for re-entrant atrial fibrillation by changing ion channel function and/or inducing fibrosis.  $\text{Ca}^{2+}$  handling changes cause early (EADs) or delayed (DADs) afterdepolarizations, resulting in ectopic activity.

### 3.1.4.3. Interconnection between heart failure and atrial fibrillation

There is strong evidence for interconnection between heart failure and atrial fibrillation. Clinical data indicate that among heart failure patients the prevalence of atrial fibrillation is in the range of 13-41%, depending on the age and severity of heart failure (Wang et al. 2003), (Carson et al. 1993). On the other hand, among atrial fibrillation patients the prevalence of heart failure ranges from 30-65% (Patel et al. 2011). Atrial fibrillation and heart failure have common risk factors: ageing, hypertension, diabetes mellitus, valvular and coronary artery disease. Atrial fibrillation and heart failure often coexist, and this coexistence is worsening the prognosis (Ferreira & Santos 2015). Of note, echocardiographic characteristics of heart failure such as left atrial enlargement, increased left ventricular wall thickness and reduced left ventricular ejection fraction were found to predispose to atrial fibrillation development. This interconnection between heart failure and atrial fibrillation is termed “heart failure begets atrial fibrillation/atrial fibrillation begets heart failure” (Maisel & Stevenson 2003).

Heart failure and atrial fibrillation share a common pathophysiological background: hemodynamic and cellular changes, and neurohormonal dysbalance (Maisel & Stevenson 2003), (Ferreira & Santos 2015).

### **Hemodynamic background**

Left ventricular filling pressure is increased in heart failure and can be caused by systolic or diastolic dysfunction. This increase in pressure affects the left atrium by mechanical stress and activates several cellular and molecular mechanisms. In the presence of atrial fibrillation, resting heart rate is increased and subsequently left ventricular filling is decreased. In addition, loss of atrial contraction compromises diastolic function (Ferreira & Santos 2015). Due to irregular ventricular contractions, cardiac output decreases, left atrial pressure raises, causing an increase in pressure in the lung capillaries and symptoms of dyspnoe (Maisel & Stevenson 2003).

### **Neurohormonal dysbalance**

Activation of the renin-angiotensin-aldosterone system (RAAS) and the sympathetic nervous system are both present in heart failure. Moreover, atrial stretch itself also causes activation of RAAS. This leads to the activation of hypertrophic and profibrotic signalling pathways and, thus, remodelling and development of an arrhythmogenic substrate. The high adrenergic activity also causes changes in atrial electrophysiology by increasing early and delayed afterdepolarizations and, thus, arrhythmias (Ferreira & Santos 2015).

Figure 3 schematically presents the interconnection between heart failure and atrial fibrillation.

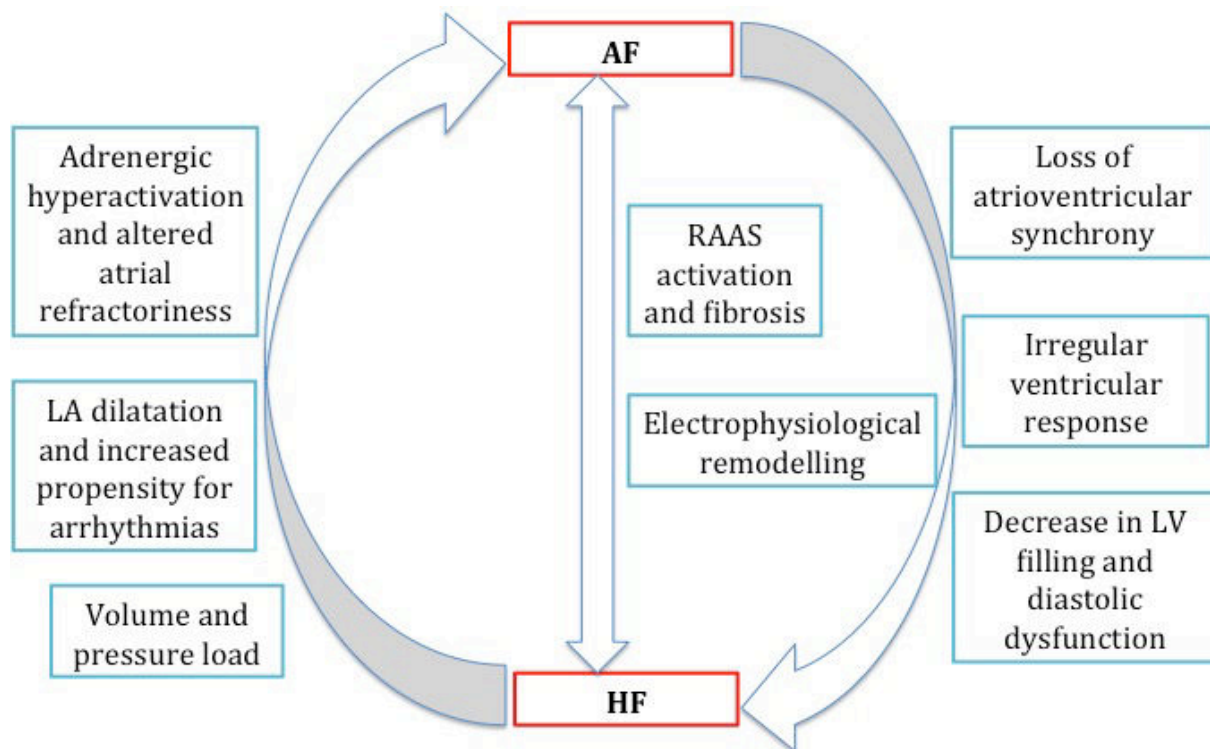


**Figure 3. Interconnection between heart failure and atrial fibrillation**

modified from (Maisel & Stevenson 2003) and (Ferreira & Santos 2015)

AF stands for atrial fibrillation; HF, heart failure; RAAS, renin-angiotensin-aldosterone system; LV, left ventricle; LA, left atrium.

Thus, heart failure and atrial fibrillation often coexist and induce development of one another.

### **3.1.5. Conclusions and role of hypertension for the maintenance and development of heart failure and atrial fibrillation**

As discussed above, hypertension causes left ventricular hypertrophy. Left ventricular hypertrophy is an important predictor for atrial fibrillation (Healey & Connolly 2003). Independent from that, left atrial enlargement (which is also an important prognostic factor for atrial fibrillation) can develop early in hypertension, even before any signs of ventricular hypertrophy. Additionally, hypertension often causes heart failure. Of note, not only atrial enlargement but also atrial functional remodelling is an independent risk factor for heart failure development and death. However, despite intensive research, the data on functional atrial remodelling in heart failure are still sparse (Shah & Lam 2014).

It is worth noting, that left ventricular hypertrophy and left atrial enlargement are independent risk factors for stroke (Benjamin et al. 1995). Thus, hypertension, heart failure and atrial fibrillation are tightly linked (Figure 4). However, not all mechanisms connecting these pathological conditions are fully understood.

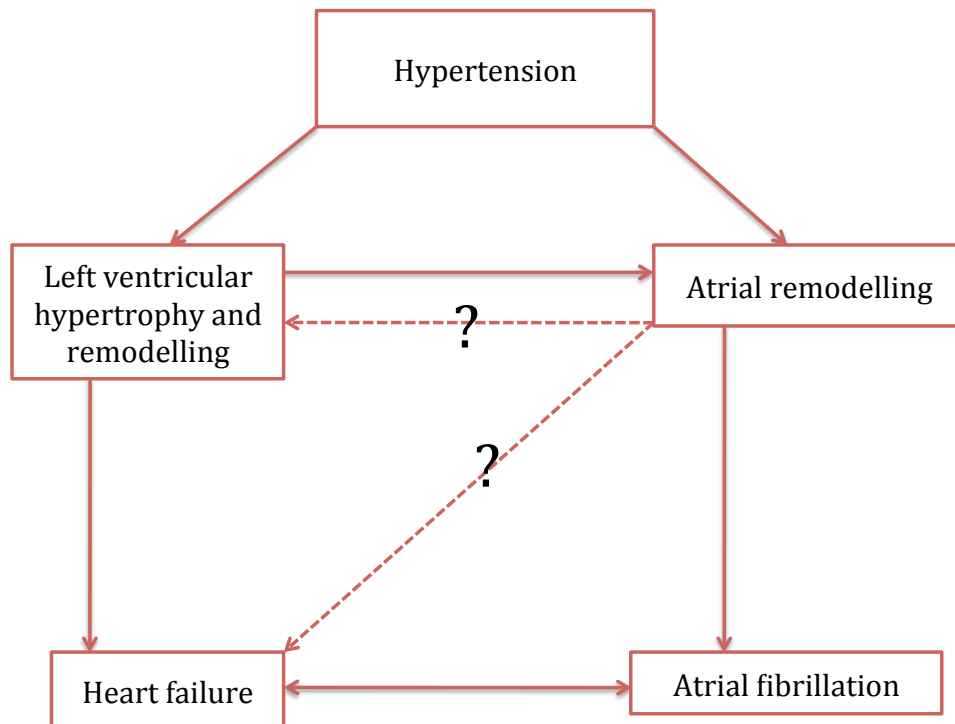


**Figure 4. Association and potential connections between hypertension, heart failure and atrial fibrillation**

## **3.2. Neurohormonal systems involved in the regulation of blood pressure and atrial remodelling**

### **3.2.1. Renin-angiotensin-aldosterone system (RAAS)**

RAAS is one of the fundamental systems, which regulates blood pressure, plasma volume, electrolyte balance and sympathetic nervous system activity. The RAAS hormonal cascade starts with the secretion of renin from the juxtaglomerular apparatus in the kidneys. In the plasma renin converts angiotensinogen produced by the liver into angiotensin I. Angiotensin I is further converted by the angiotensin-converting enzyme (ACE) into the active octapeptide angiotensin II. Angiotensin II exhibits several important effects on the cardiovascular system. Firstly, it is a potent vasoconstrictor, secondly, it activates sympathetic neuronal noradrenaline release, thirdly, it stimulates aldosterone secretion from adrenal cortex. Aldosterone, in turn, stimulates reabsorption of  $\text{Na}^+$  in the collecting duct and water retention. Thus, as a result of RAAS activation, the circulating plasma volume and blood pressure increase (Tsukamoto & Kitakaze 2013).

Hyperactivation of RAAS with increased angiotensin II production is one of the hallmarks of hypertensive heart disease and heart failure (Drazner 2011).

Angiotensin II exhibits not only systemic effects but can also be produced locally and is able to stimulate pathological cardiac tissue remodelling. In the heart, angiotensin II binds to the angiotensin type 1 receptor ( $\text{AT}_1$ ) and mediates proliferative, prohypertrophic and pro-inflammatory effects (Tsukamoto & Kitakaze 2013). The  $\text{AT}_1$  receptor belongs to the family of Gq-protein-coupled receptors. When agonist binds to the receptor, phospholipase  $\text{C}\beta$  ( $\text{PLC}\beta$ ) is activated and hydrolyzes phosphatidylinositol 4,5-bisphosphate ( $\text{PIP}_2$ ) into inositol 1,4,5-trisphosphate ( $\text{IP}_3$ ) and diacylglycerol (DAG). DAG stimulates protein kinase C (PKC). This kinase phosphorylates important targets in the myocytes, including  $\text{Ca}^{2+}$  handling proteins.  $\text{IP}_3$  activates  $\text{Ca}^{2+}$  release from the sarcoplasmic reticulum (SR) and  $\text{Ca}^{2+}$  transport into the nucleus, where  $\text{Ca}^{2+}$  is able to activate the prohypertrophic gene program (Heineke & Molkentin 2006). Increased activity of RAAS exerts arrhythmogenic effects and may trigger atrial fibrillation together with maladaptive atrial remodelling (Korantzopoulos et al. 2003), (Schotten et al. 2011).



### 3.2.2. Sympathetic nervous system

Activation of the sympathetic nervous system increases blood pressure and has among other important effects, positive inotropic effects on the myocardium. Epinephrine and norepinephrine are two catecholaminergic mediators of the sympathetic system, which bind to  $\beta$  and  $\alpha$  adrenergic receptors in the myocardium and blood vessels.

Human heart expresses  $\beta$  1/  $\beta$  2 adrenergic receptors in a 70 to 30% ratio. (Bylund et al. 1994), (Triposkiadis et al. 2009). The  $\beta$  1 adrenergic receptor is  $G_s$ -coupled and, when an agonist binds to this receptor, adenylate cyclases become active, inducing an increase in cAMP production and activation of protein kinase A (PKA). PKA mediates phosphorylation of  $Ca^{2+}$ -handling proteins, which results in the positive inotropic effect.  $\alpha$  1 receptors are  $G_q$ -coupled, and their stimulation activates the PLC $\beta$ /DAG/IP $_3$  signalling cascade, causing PKC activation, IP $_3$ -dependent  $Ca^{2+}$  release and positive inotropy.

Stimulation of vascular  $\alpha$  1 adrenergic receptors induces vasoconstriction, and activation of central  $\alpha$  2 adrenergic receptors results in a decrease in sympathetic outflow and blood pressure (Triposkiadis et al. 2009).

A marked increase in sympathetic activity is present in many cardiovascular diseases, such as hypertension and heart failure (Seravalle et al. 2014). The increased sympathetic activity is associated with atrial fibrillation in humans and in animal models of the disease (Chen et al. 2014), (Korantzopoulos et al. 2003).

### 3.2.3. Endothelin-1 system

Endothelin-1 belongs to the family of cyclic 21 amino acid peptides and was first isolated from porcine aortic endothelial cells (Yanagisawa et al. 1988). Endothelin-1 binds to either Endothelin A (ET $_A$ R) or Endothelin B (ET $_B$ R) receptors (Drawnel et al. 2013). In the atria, more endothelin binding sites are present than in the ventricles and the ET $_A$ R accounts for more than 80% of all endothelin binding sites in the heart (Horinouchi et al. 2013). Both receptors are G-protein coupled. The ET $_A$ R exhibits a higher affinity to endothelin-1 than the ET $_B$ R. ET $_A$ Rs are coupled to the G $_q$  subtype and stimulation of this receptor activates the PLC/DAG/IP $_3$  cascade (Drawnel et al. 2013). This, in the first place, results in the positive inotropic effect, however, increased IP $_3$  production stimulates spontaneous  $Ca^{2+}$  release from the sarcoplasmic reticulum, what can trigger arrhythmias. Moreover, stimulation of IP $_3$  receptors in the nuclear envelope

alters nuclear  $\text{Ca}^{2+}$  homeostasis and activates the transcription of prohypertrophic genes (Kockskämper, Zima, et al. 2008). Many studies have demonstrated that endothelin-1 can cause maladaptive cardiomyocyte remodelling and hypertrophy. Moreover, elevation in plasma endothelin-1 was found in heart failure, ageing, ischemia and atrial fibrillation. Thus, hyperactivity of the endothelin-1 system can contribute to both aetiology and pathology of these diseases (Drawnel et al. 2013), (Mayyas et al. 2010).

### **3.3. Regulation of intracellular $\text{Ca}^{2+}$ concentration in cardiac myocytes**

#### **3.3.1. Excitation-contraction coupling**

$\text{Ca}^{2+}$  is an important second messenger in all cell types. Alterations of the cellular  $\text{Ca}^{2+}$  concentration regulate many cellular processes: cell growth and cell death, release of hormones and neuromediators, energy production and many others (Bootman et al. 2006), (Berridge et al. 2003).

In the heart,  $\text{Ca}^{2+}$  is a crucial ion for cardiac myocyte contraction and relaxation (Bers et al. 2006). Excitation-contraction coupling (ECC) is the process of coupling depolarization of the plasma membrane with the contraction of the cell, and  $\text{Ca}^{2+}$  is the key mediator in this process.

During the depolarization of cardiac myocytes,  $\text{Ca}^{2+}$  enters the cell via sarcolemmal L-type  $\text{Ca}^{2+}$  channels creating an inward  $\text{Ca}^{2+}$  current ( $I_{\text{Ca}}$ ), which mediates the action potential plateau. The entering  $\text{Ca}^{2+}$  triggers  $\text{Ca}^{2+}$  release from the sarcoplasmic reticulum (SR) through ryanodine receptors (RyRs). This process is called  $\text{Ca}^{2+}$ -induced  $\text{Ca}^{2+}$  release (CICR). The increase in the free  $\text{Ca}^{2+}$  concentration allows it to bind to the myofilament protein troponin C (Bers 2002). The conformational change of the troponin complex changes the position of tropomyosin, which allows actin to interact with myosin, and so the contraction occurs (Katz 2010). To achieve relaxation,  $\text{Ca}^{2+}$  must be taken up into the sarcoplasmic reticulum by the sarcoplasmic  $\text{Ca}^{2+}$ -ATPase (SERCA), or transported out of the cell by the sarcolemmal  $\text{Na}^+/\text{Ca}^{2+}$  exchanger (NCX) or the sarcolemmal  $\text{Ca}^{2+}$ -ATPase and into the mitochondria by mitochondrial  $\text{Ca}^{2+}$  uniport (Bers 2002). In the SR lumen,  $\text{Ca}^{2+}$  is bound to calsequestrin (CSQ), which buffers the high  $\text{Ca}^{2+}$  concentration in the SR (Bootman et al. 2011). Figure 5 schematically presents excitation-contraction coupling in ventricular myocytes (from (Bers 2002)).

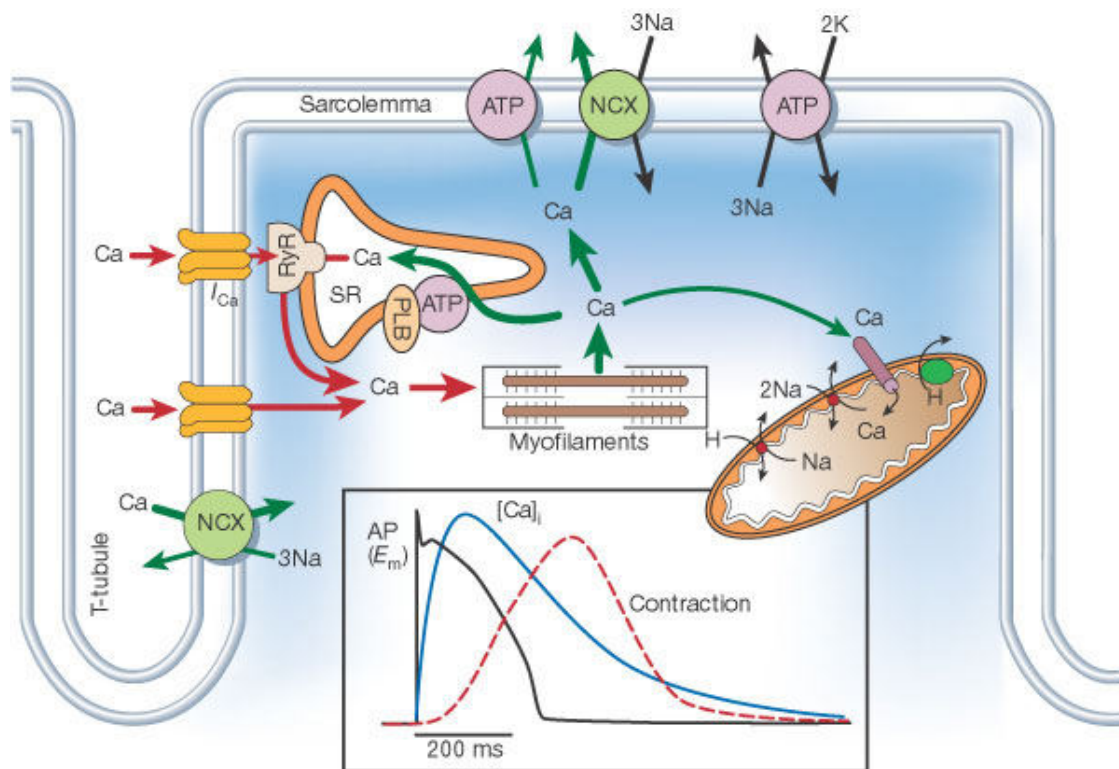


**Figure 5. Excitation-contraction coupling in ventricular myocyte**

reproduced from (Bers 2002)

During the AP  $Ca^{2+}$  enters the cells via L-type  $Ca^{2+}$  channels ( $I_{Ca}$ ), triggering the  $Ca^{2+}$  release from the SR via RyR (red arrows).  $Ca^{2+}$  binds to the myofilaments, allowing the contraction of the myocyte.  $Ca^{2+}$  is then transported out of the cytosol by four extrusion paths (green arrows): 1) to SR via SERCA, out of the cell by 2) SERCA and 3) NCX and 4) into the mitochondria via mitochondrial  $Ca^{2+}$  uniporter. Inset illustrates the time course of AP,  $Ca^{2+}$  transient and contraction, measured in rabbit ventricular myocytes.

AP, action potential; SR, sarcoplasmic reticulum; RyR, ryanodine receptor; NCX,  $Na^+/Ca^{2+}$  exchanger; SERCA, sarcoplasmic  $Ca^{2+}$ -ATPase; PLB, phospholamban

### 3.3.2. $Ca^{2+}$ handling in atrial myocytes

There are, however, some differences in excitation-contraction coupling between atrial and ventricular myocytes. Ventricular myocytes express sarcolemmal invaginations, called T-tubules, which go perpendicular deep inside the myocyte. L-type  $Ca^{2+}$  channels are located on the T-tubular plasma membrane in close proximity to RyRs, which are

located in the membrane of sarcoplasmic reticulum. Thus, when the plasma membrane depolarizes, CICR is activated simultaneously throughout the ventricular myocyte, making the  $\text{Ca}^{2+}$  increase homogenous and contraction of ventricular myocardium coordinated (Smyrniak et al. 2010), (Blatter et al. 2003). In contrast to ventricular myocytes, atrial myocytes do not express T-tubules (Blatter et al. 2003), (Bootman et al. 2006). Hence, an important functional difference exists regarding localization of L-type  $\text{Ca}^{2+}$  channels and RyRs in atrial myocytes. L-type  $\text{Ca}^{2+}$  channels are present only at the plasma membrane of atrial myocyte. Thus, during electrical excitation, only junctional RyRs (located in close proximity to the plasma membrane) get activated by  $\text{Ca}^{2+}$  entry via L-type  $\text{Ca}^{2+}$  channels, and then the  $\text{Ca}^{2+}$  wave distributes further inside the atrial myocyte via non-junctional RyRs (Kockskämper et al. 2001). As a consequence of this functional difference, propagation of the  $\text{Ca}^{2+}$  signal is more heterogeneous in atrial myocytes (Blatter et al. 2003), (Bootman et al. 2011).

### **3.4. Intracellular $\text{Na}^+$ regulation and its role in cardiac myocytes**

Intracellular  $\text{Na}^+$  is crucial for the physiology of cardiac myocytes. There is a large  $\text{Na}^+$  gradient across the membrane: extracellular  $\text{Na}^+$  concentration is about 140 mM and intracellular concentration ( $[\text{Na}^+]_i$ ) is normally from 4 to 14 mM (Bers & Despa 2009). However,  $[\text{Na}^+]_i$  varies in a species-dependent manner: it is kept relatively low in most mammals, whereas in rat and mouse  $[\text{Na}^+]_i$  is higher. The reason for that can be species-related differences in excitation-contraction coupling (Pieske & Houser 2003). In excitable cells, the energy stored in the sodium concentration gradient is the basis for action potential upstroke and propagation and energetically unfavourable transmembrane transport of glucose, amino acids and neurotransmitters (Bers & Despa 2009).

It was shown in many studies that  $\text{Na}^+$  is a major determinant of the intracellular  $\text{Ca}^{2+}$  concentration and, thus, excitation-contraction coupling and contractility. Moreover,  $\text{Na}^+$  is involved in the transport of  $\text{H}^+$  and, correspondingly, regulates pH in cardiac myocytes (Aronsen et al. 2013). Another important role of  $\text{Na}^+$  is the modulation of mitochondrial  $\text{Ca}^{2+}$  and thus cardiac metabolism (Coppini et al. 2013).

### 3.4.1. Na<sup>+</sup> and excitation contraction coupling

[Na<sup>+</sup>]<sub>i</sub> is the balance between Na<sup>+</sup> influx and Na<sup>+</sup> efflux, generated by a number of channels and transporters. The influx of Na<sup>+</sup> occurs via voltage-dependent Na<sup>+</sup> channels, Na<sup>+</sup>/Ca<sup>2+</sup> exchanger (NCX) and Na<sup>+</sup>/H<sup>+</sup> exchanger (NHE). The efflux of Na<sup>+</sup> is primarily regulated by Na<sup>+</sup>/K<sup>+</sup>-ATPase (NKA) and /or by NCX acting in “reverse mode”, when pumping Na<sup>+</sup> out of the cell and bringing Ca<sup>2+</sup> ions into the cell (Coppini et al. 2013).

The upstroke of the action potential (AP) is triggered by opening of voltage-dependent Na<sup>+</sup> channels. Within a few milliseconds, the channels inactivate. That process brings in a small amount of Na<sup>+</sup>: around 6-15 μmol/L. During the AP, L-type Ca<sup>2+</sup> channels open and activate Ca<sup>2+</sup>-induced Ca<sup>2+</sup> release from the SR. This excess of Ca<sup>2+</sup> is then brought back into the SR by SERCA and is taken out by NCX. Ca<sup>2+</sup> extrusion via NCX brings in around 32 μmol/L of Na<sup>+</sup>. Under physiological conditions, NHE exchanger extrudes protons at a slower rate and carries 2 μmol/l of Na<sup>+</sup> into the cell. The excess of Na<sup>+</sup> influx, resulting from each heart beat (40-45 μmol/L) beat is pumped out of the cell via NKA (Bers & Despa 2009).

Figure 6 illustrates Na<sup>+</sup> fluxes in a cardiac myocyte during excitation-contraction coupling.

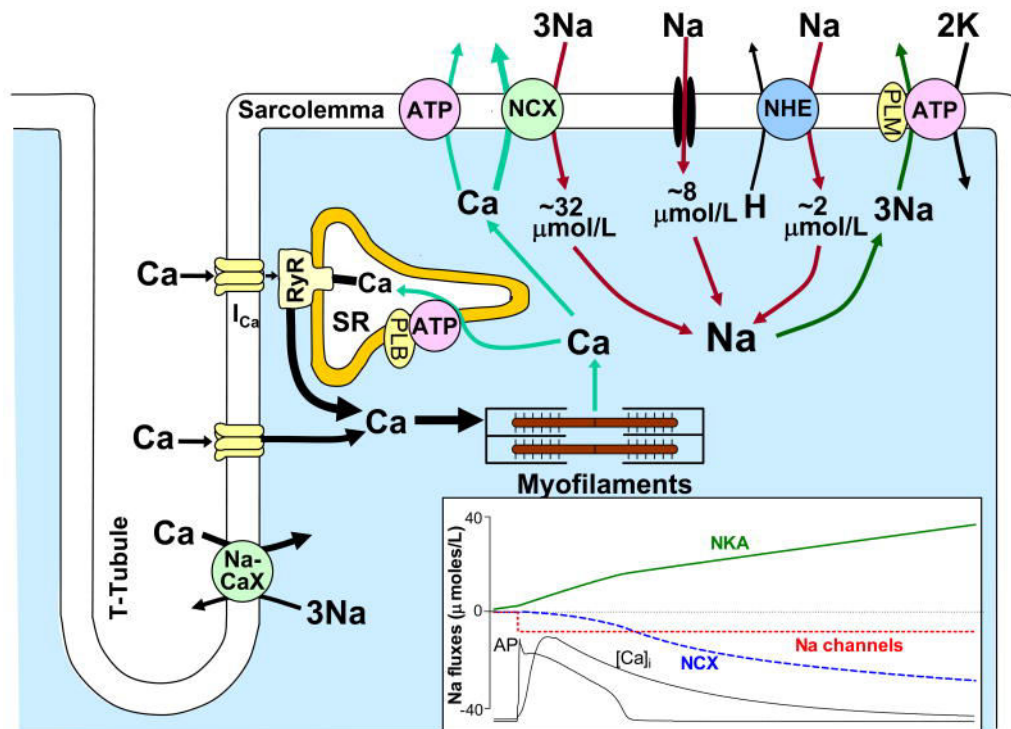


**Figure 6. Na<sup>+</sup> involvement in excitation-contraction coupling in ventricular myocyte**

reproduced from (Bers & Despa 2009)

During electrical excitation of the heart, Na<sup>+</sup> enters the myocyte through voltage-gated Na<sup>+</sup> channels, triggering the AP. NCX extrudes the resulting increase in Ca<sup>2+</sup> after the contraction and brings Na<sup>+</sup> into the myocyte. NHE extrudes protons and brings in Na<sup>+</sup>. NKA pumps the resulting excess of Na<sup>+</sup> out of the cell. Na<sup>+</sup> influx is shown by red and Na<sup>+</sup> efflux by dark-green arrows.

Inset shows Na<sup>+</sup> fluxes through voltage-gated Na<sup>+</sup> channels, NCX and NKA during an AP. The action potential and the corresponding Ca<sup>2+</sup> are also shown.

AP, action potential; NCX, Na<sup>+</sup>/Ca<sup>2+</sup> exchanger; NHE, Na<sup>+</sup>/H<sup>+</sup> exchanger, NKA, Na<sup>+</sup>/K<sup>+</sup>-ATPase; PLM, phospholemman.

### 3.4.2. Na<sup>+</sup> current, action potential formation, late Na<sup>+</sup> current

Fast upstroke of the action potential is generated by voltage-gated Na<sup>+</sup> channels, which inactivate rapidly and bring in a small amount of Na<sup>+</sup> during each activation. The voltage-gated Na<sup>+</sup> channel is composed of a pore-forming  $\alpha$  subunit with one or two auxiliary  $\beta$  subunits (Kaufmann et al. 2013). The most highly expressed isoform of Na<sup>+</sup> channel is Na<sub>v</sub>1.5 (encoded by the SCN5 gene) (Coppini et al. 2013). Some other

neuronal isoforms, however, have also been identified in the human atrium. The contribution of such channels to the total sodium current is substantial (around 27%), and their function is necessary for maximal contractility (Kaufmann et al. 2013).

As mentioned before, most of the Na<sup>+</sup> channels inactivate rapidly. However, another component of Na<sup>+</sup> current, the so-called late Na<sup>+</sup> current, was also identified. This current follows the peak Na<sup>+</sup> current and, under normal physiological conditions, is very small and does not affect action potential duration or total Na<sup>+</sup> influx (Coppini et al. 2013). The mechanisms for late Na<sup>+</sup> current initiation are not yet completely understood (Chen-Izu et al. 2015). In some cardiac diseases or due to mutations in the SCN5 gene, late Na<sup>+</sup> current is elevated and brings a significant amount of Na<sup>+</sup> into the cell, due to the longer duration of this current in comparison to peak Na<sup>+</sup> current. This results in a prolongation of action potential duration and disturbances in Ca<sup>2+</sup> homeostasis (Coppini et al. 2013).

### **3.4.3. Na<sup>+</sup> and Ca<sup>2+</sup> regulation**

Na<sup>+</sup> and Ca<sup>2+</sup> homeostasis are tightly linked via NCX, which exchanges 3 Na<sup>+</sup> for 1 Ca<sup>2+</sup> and is the primary Ca<sup>2+</sup> extrusion path (Despa & Bers 2013). The NCX1 isoform is the only isoform expressed in the heart (Despa & Bers 2013). It has a large cytoplasmic loop with two Ca<sup>2+</sup>-binding sites. When intracellular Ca<sup>2+</sup> rises, Ca<sup>2+</sup> binds to these domains and activates NCX. The exact mechanism of how [Na<sup>+</sup>]<sub>i</sub> modulates NCX function is unclear (Shattock et al. 2015).

The rate and transport mode of the exchanger depends on the intra- and extracellular concentrations of both Na<sup>+</sup> and Ca<sup>2+</sup> and on the membrane potential. Most of the Ca<sup>2+</sup> extrusion occurs at negative resting potentials, and the electrochemical gradient favours the so-called “forward” mode of the NCX: Ca<sup>2+</sup> efflux and Na<sup>+</sup> inflow (Coppini et al. 2013). NCX can also function in a “reverse” mode (Ca<sup>2+</sup> influx and Na<sup>+</sup> efflux) (Baartscheer & van Borren 2008). This mode is favoured by increased [Na<sup>+</sup>]<sub>i</sub> and membrane depolarization. When intracellular Na<sup>+</sup> rises, NCX switches to a “reverse mode” and correspondingly brings an excess of Ca<sup>2+</sup> into the myocyte and simultaneously increases SR Ca<sup>2+</sup> content. Eventually, Ca<sup>2+</sup> transients become bigger and contractile force increases (Despa & Bers 2013). However, increased SR Ca<sup>2+</sup> load may also trigger spontaneous Ca<sup>2+</sup> release and thus arrhythmias (Wakili et al. 2011).



#### 3.4.4. Na<sup>+</sup> and pH regulation

Na<sup>+</sup> modulates proton transport in cardiac myocytes via Na<sup>+</sup>/H<sup>+</sup> exchanger (NHE). The major function of NHE is pH maintenance in cardiac myocytes. NHE1 is the primary isoform expressed in cardiac myocytes. NHE functions as a proton extruder in 1 Na<sup>+</sup> to 1 H<sup>+</sup> stoichiometry. NHE activity is allosterically regulated by protons and by phosphorylation of its intracellular C-terminus by kinases and interaction with a variety of regulatory proteins. NHE1 is also involved in cell volume regulation, cell growth and differentiation (Lee, B.L. et al. 2012). Mechanical stretch and a wide range of hormones (ET-1, AT-II, catecholamines) and oxidative stress also stimulate NHE (Vaughan-Jones et al. 2009).

Under ischemic conditions, pH is reduced, the activity of NHE increases and it is extruding protons from the cytosol to normalize pH (Coppini et al. 2013). This process leads to a subsequent increase in intracellular Na<sup>+</sup> concentration and, as a result, NCX extrudes Na<sup>+</sup> from the cell and brings in excessive Ca<sup>2+</sup>. At the same time, under ischemic conditions, there is an energy starvation present and, thus, ATP is depleted, so that the NKA function decreases, contributing to an additional rise in [Na<sup>+</sup>]<sub>i</sub>. Ca<sup>2+</sup> overload triggers arrhythmias and is able to activate hypertrophic pathways and cell death. This phenomenon is called ischemia-induced injury (Avkiran 2003), (Lee, B.L. et al. 2012). Moreover, NHE activation is involved in the development of cardiac hypertrophy and heart failure via activation of prohypertrophic pathways (Wakabayashi et al. 2013), (Hisamitsu et al. 2012).

#### 3.4.5. Na<sup>+</sup>/K<sup>+</sup>-ATPase (NKA)

The NKA is the major Na<sup>+</sup> extrusion mechanism in cardiac myocytes. It utilizes energy derived from ATP hydrolysis and extrudes 3 Na<sup>+</sup> in exchange for 2 K<sup>+</sup>. The major NKA function is the maintenance of electrochemical Na<sup>+</sup> and K<sup>+</sup> gradients, which is crucial for transport and electrogenic processes (Shattock et al. 2015). The NKA is composed of three subunits: the catalytic  $\alpha$  subunit, the auxiliary  $\beta$  subunit and the regulatory  $\gamma$  subunit (phospholemman). The  $\alpha$  subunit contains Na<sup>+</sup>, K<sup>+</sup>, ATP and cardiac glycoside binding sites. The  $\beta$  subunit is responsible for trafficking and insertion of the enzyme into the plasma membrane (Despa & Bers 2013). In the heart  $\alpha$  1,  $\alpha$  2 and  $\alpha$  3 isoforms are expressed and the  $\beta$  1 isoform.  $\alpha$  1 is quantitatively the dominant isoform (Shattock et al. 2015).

NKA activity is regulated by phospholemman (PLM). Unphosphorylated PLM inhibits NKA activity, and, when phosphorylated by PKA and PKC, it dissociates from NKA and relieves the inhibition. During intensive adrenergic stimulation  $[Na^+]_i$  increases due to enhanced extrusion of  $Ca^{2+}$  and subsequent  $Na^+$  influx via NCX. Elevated  $[Na^+]_i$  (which can be deleterious as described above) is attenuated by stimulation of NKA. Thus, PLM regulation of NKA is a physiological protective mechanism preventing  $Na^+$  and  $Ca^{2+}$  overload and, thus, arrhythmias (Despa & Bers 2013).

#### **3.4.6. $Na^+$ and regulation of cardiac metabolism**

At high workload, adrenergic stimulation increases cytoplasmic  $Ca^{2+}$  transients and mitochondrial  $Ca^{2+}$  uptake via the  $Ca^{2+}$  uniporter (Despa & Bers 2013). High mitochondrial  $Ca^{2+}$  concentrations regulate several dehydrogenases involved in the tricarboxylic acid cycle, stimulate NADH and NADPH regeneration and, thus, ATP production.  $Na^+$  controls mitochondrial  $Ca^{2+}$  concentration via the mitochondrial  $Na^+/Ca^{2+}$  exchanger, which extrudes mitochondrial  $Ca^{2+}$  and brings  $Na^+$  into the mitochondrion. This exchanger functions with a similar stoichiometry as the sarcolemmal NCX: it exchanges 3  $Na^+$  for 1  $Ca^{2+}$ . Its activity is very sensitive to  $[Na^+]_i$ . When  $[Na^+]_i$  is elevated, mitochondrial NCX decreases mitochondrial  $Ca^{2+}$  concentration and, subsequently, ATP production (Kohlhaas et al. 2010).

### 3.4.7. Intracellular Na<sup>+</sup> homeostasis in cardiac disease

Numerous studies report increased [Na<sup>+</sup>]<sub>i</sub> in ventricular cardiomyocytes in hypertrophy, heart failure and ischemia (Pogwizd 2003), (Despa & Bers 2013), (Pieske & Houser 2003), (Clancy et al. 2015).

Elevated [Na<sup>+</sup>]<sub>i</sub> occurs under the following conditions: increased rates of depolarization, mechanical stretch, hormonal and neuroendocrine activation (Angiotensin II, Endothelin-1) (Pieske & Houser 2003) (Aiello et al. 2005). For example, in ischemia-reperfusion injury, NHE activity is increased, and Na<sup>+</sup> efflux is blunted, due to the blockage of NKA function, increasing the [Na<sup>+</sup>]<sub>i</sub>.

In hypertrophy and heart failure, there are several mechanisms responsible for elevated [Na<sup>+</sup>]<sub>i</sub>: increased late Na<sup>+</sup> current, “reverse” mode of NCX function (Ca<sup>2+</sup> extrusion and Na<sup>+</sup> influx) and/or reduction in NKA function and/or expression. However, there is certain controversy regarding the expression and function of NKA in different species and disease models (Despa & Bers 2013). Elevated [Na<sup>+</sup>]<sub>i</sub> in hypertrophy and heart failure increases Ca<sup>2+</sup> influx via NCX what stimulates spontaneous Ca<sup>2+</sup> release from the SR and generation of delayed afterdepolarizations (Pogwizd 2003). However, the detailed mechanisms of increased [Na<sup>+</sup>]<sub>i</sub> in ventricular myocytes are still under investigation.

### 3.4.8. Intracellular Na<sup>+</sup> homeostasis in atrial fibrillation and remodelling

Current knowledge about Na<sup>+</sup> homeostasis in atrial myocytes is very limited. However, some aspects of it were studied in the context of atrial fibrillation. In human atrial fibrillation, there is evidence for increased NCX expression and current, together with unchanged NKA function (Schotten et al. 2010), (Voigt et al. 2012). Another study found a decrease in peak Na<sup>+</sup> current together with an increase in the late Na<sup>+</sup> current (Sossalla et al. 2010). Moreover, authors of this study also found that the expression of different Na<sup>+</sup> channel isoforms was shifted towards the increase in neuronal isoform expression and a decrease in the cardiac specific Na<sub>v</sub> 1.5 type expression (Sossalla et al. 2010). A recent study has also shown that there is an interconnection between increased late Na<sup>+</sup> current and SR Ca<sup>2+</sup> leak, providing an important link between Na<sup>+</sup> and Ca<sup>2+</sup> homeostasis in atrial fibrillation (Fischer et al. 2015).

Interestingly, another study found decreased  $[\text{Na}^+]_i$  in an animal model of rapid atrial pacing together with reduced NKA function and unchanged NKA expression (Greiser et al. 2014). To conclude, the data on intracellular  $\text{Na}^+$  homeostasis in atrial remodelling and atrial fibrillation are very scarce and contradictory.

### **3.5. Spontaneously hypertensive rats (SHR) as a model for hypertensive heart disease**

Spontaneously hypertensive rats (SHR) represent a well-established model for essential hypertension and hypertensive heart disease.

The SHR strain was generated by Okamoto and Aoki in 1963 in Kyoto, Japan, by breeding a hypertensive male Wistar rat with a female Wistar rat with slightly elevated blood pressure (Okamoto & Aoki 1963). Starting from 1968, this strain was further developed in the USA. SHR are normotensive for the first 6-8 weeks of life; afterwards, they develop hypertension. The Wistar Kyoto rats (WKY) were established in 1971 as a normotensive control group as an inbred of the Wistar Kyoto colony by brother x sister mating (Doggrell & Brown 1998).

Hypertension in SHR and humans has some common aspects, making these rats a suitable model for studying of hypertension-related diseases. These aspects include:

Progression of hypertension follows that in human: first comes the pre-hypertensive period, followed by sustaining of elevated blood pressure. These phases are lasting for months, mimicking long lasting development of hypertension in human (Doggrell & Brown 1998).

Hypertension in SHR leads to the compensated left ventricular hypertrophy and then progresses from stable hypertrophy to heart failure (Chan et al. 2011).

More rapid and severe development in male rats in comparison to female SHR (Chan et al. 2011).

Specific genes responsible for the development of hypertension have not been identified in SHR. The same is true for human primary hypertension (Doggrell & Brown 1998).

The exact reasons for elevated blood pressure in SHR remain unclear. However, it was demonstrated that transplantation of kidneys from SHR to normotensive rats increased the blood pressure in them and SHR receiving kidneys from normotensive donors had reduced blood pressure (Bianchi et al. 1974). Another study has also revealed impaired kidney function in SHR even in the prehypertensive stage (Vanecková 2002). Moreover, there is evidence that SHR exhibit increased activity of RAAS and the stress axis (Kodavanti et al. 2000), (Shanks & Herring 2013). Some investigations revealed several changes in genes responsible for hypertension development in these rats (Doggrell &

Brown 1998). However, the link between these observed changes and hypertension is still unclear.

### 3.5.1. Pathophysiological changes induced by hypertension in SHR

SHR are extensively used for studies of hypertension-induced changes in cardiac function, since SHR mimic many aspects of hypertensive heart disease in humans (Trippodo & Frohlich 1981). As described above, hypertension causes left ventricular hypertrophy in humans. SHR also develop left ventricular hypertrophy (Doggrell & Brown 1998) and heart failure (Houser et al. 2012). A comprehensive study by Chan et al. characterized cardiovascular parameters of SHR during the whole lifespan, including also age-induced changes. Since the rats used for this thesis were all male, the following findings of this study, listed below, are restricted to male SHR.

Survival rate and life expectancy are lower in SHR than in WKY.

- Elevated blood pressure causes left ventricular hypertrophy and fibrosis.
- SHR develop signs of heart failure at around 15-18 months of age, including systolic and diastolic dysfunction, and left ventricular dilatation.
- Action potential duration is prolonged in SHR, making them more susceptible to arrhythmias (Chan et al. 2011).

Figure 7 presents onsets of different cardiovascular changes in SHR during the whole lifespan.

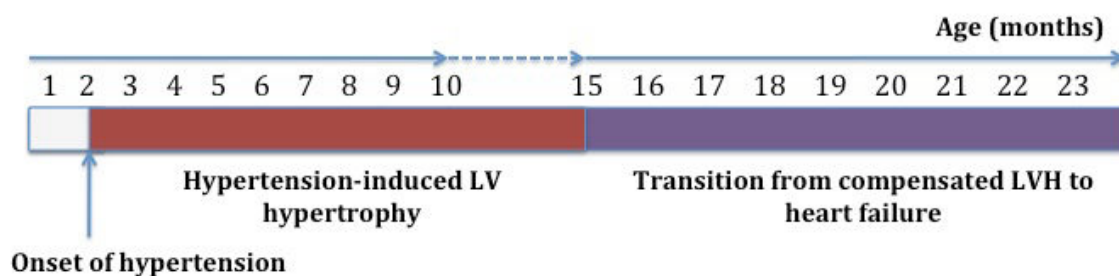


**Figure 7. The onsets of cardiovascular changes during the lifespan of SHR**

As in humans, the exact mechanisms of progression from stable hypertrophy to heart failure in these rats are not completely understood. SHR are a suitable model to study the transition from compensated left ventricular hypertrophy to heart failure, since this progression is, as in humans, associated with aging (Bing et al. 2002).

In the context of atrial remodelling and arrhythmias SHR were also found to be a suitable model. The electrocardiographic study by Dunn et al. revealed bi-peak notching

of a P-wave in the SHR, indicating atrial enlargement (Dunn et al. 1978). Another study found increased incidence and duration of atrial arrhythmias in SHR together with fibrotic and electrophysiological changes (Choisy et al. 2007). Moreover, as demonstrated by Scridon et al., SHR are also prone to unprovoked atrial tachyarrhythmias (Scridon et al. 2012). A more recent study by Lau et al. observed increased interstitial fibrosis and bi-atrial enlargement together with heterogeneous conduction in the atria, which resulted in increased arrhythmia inducibility. In other words, some signs of structural and electrical remodelling are present in the atria of SHR (Lau et al. 2013).

However, data on hypertension-induced functional changes in the atria are still lacking. Exact mechanisms underlying atrial remodelling in SHR are not completely understood, and atrial remodelling during the transition from compensated left ventricular hypertrophy to heart failure is unknown.

### 3.6. Aims of the study

Arterial hypertension is associated with high morbidity and mortality worldwide. It develops gradually and causes many cardiovascular diseases, e.g. left ventricular hypertrophy, heart failure and atrial fibrillation. These diseases are tightly linked and contribute to the development of one another. Remodelling is an adaptive regulation of cardiac myocytes to stress factors, such as elevated blood pressure, and includes structural and functional changes of the myocytes. While ventricular remodelling has been intensively studied, much less is known about atrial remodelling in hypertension, left ventricular hypertrophy and heart failure.

Intracellular Na<sup>+</sup> homeostasis is essential for the physiology of cardiac myocytes: it regulates Ca<sup>2+</sup> homeostasis, intracellular pH, cardiac metabolism and contractility. However, the available data on Na<sup>+</sup> homeostasis in the atria are scarce.

We hypothesized that long-standing hypertension may cause atrial remodelling in terms of impaired contractility and Na<sup>+</sup> homeostasis. Thus, the first and major part of this study was to characterize atrial remodelling in hypertensive heart disease with particular focus on contractility and Na<sup>+</sup> homeostasis. To this end, we used spontaneously hypertensive rats (SHR), a well-established animal model for human essential hypertension. Wistar Kyoto rats (WKY) were chosen as a normotensive control. Hypertensive heart disease develops gradually in these rats. Therefore, we have chosen 3 time points to investigate hypertension-induced changes in the atria of SHR:

- 3 months old, shortly after the development of hypertension,
- 7 months old, when sustained hypertension has caused compensated left ventricular hypertrophy
- 15-23 months of age, when there is a transition from compensated left ventricular hypertrophy to heart failure.

The atrial remodelling in SHR was studied in terms of:

- Cardiovascular changes (blood pressure, heart rate, cardiac hypertrophy)
- Contractility of atrial myocytes
- Intracellular Na<sup>+</sup> concentration in atrial myocytes
- Expression of Na<sup>+</sup>-handling proteins in the atria of SHR.



Hypertension is one of the major predictors for atrial fibrillation. Atrial fibrillation causes atrial remodelling and, vice versa, atrial remodelling contributes to the development of atrial fibrillation. Various aspects of atrial remodelling in this arrhythmia have been intensively investigated, however, the role of Na<sup>+</sup> homeostasis is not yet completely understood. Therefore, the second aim of this thesis was to analyze the expression of Na<sup>+</sup> handling proteins in atrial tissue from patients suffering from paroxysmal and chronic atrial fibrillation.

Endothelin-1 is a vasoactive peptide involved in the regulation of blood pressure. Overactivation of the endothelin-1 system causes atrial remodelling, including alterations in Ca<sup>2+</sup> handling and development of pro-arrhythmogenic events. Thus, the third aim of the study was to test the effect of endothelin receptor blockade on blood pressure, expression of Ca<sup>2+</sup>-handling proteins and proteins involved in Endothelin-1 signalling in the atria of SHR.

## 4. Materials and methods

### 4.1. Animals

All animal experiments were approved by local authorities (Regierungspräsidium Gießen, experimental project V 54 - 19 c 20 15 (1) MR 20/29 Nr. A 21/2010 and AK-9-2014-Kockskämper, approved by animal welfare officer, University of Marburg). Animal experiments conducted in Magdeburg were approved by the council on local animal care committee (Halle, Saxony Anhalt, approval: 42502-2-1259 UniMD). Male SHR and WKY rats were obtained from Janvier-labs (Saint Berthevin, France) or Charles River (Köln, Germany). Rats were kept in the local animal housing facilities with standard chow and water *ad libitum* in 12 hours light/dark conditions. Animal handling procedures were in accordance with the German Animal Welfare Act (Tierschutzgesetz).

### 4.2. Non-invasive blood pressure and heart rate measurements in rats

Blood pressure and heart rate measurements were performed on conscious rats by using the CODA™ system (Kent Scientific Corporation, Torrington, Connecticut, USA). The experimental setup is shown in Figure 8.

The non-invasive blood pressure method uses a tail-cuff (4) placed on the tail to occlude the blood flow. Upon deflation, a volume pressure recording (VPR) cuff (5) is used as a sensor for blood pressure measurements. This sensor is placed distal to the occlusion tail-cuff. The occlusion tail-cuff is inflated to impede the blood flow to the tail. Then the occlusion cuff is slowly deflated and the VPR cuff measures the physiological characteristics of the returning blood flow. As the blood returns to the tail, when the tail-cuff is deflated, the VPR sensor cuff measures the tail swelling as a result of the arterial pulsations from the blood flow. Systolic blood pressure is automatically measured at the time point when a tail begins to swell. Diastolic blood pressure is automatically calculated when the increasing rate of swelling is fading away in the tail (Malkoff 2005). The following average cardiovascular characteristics are considered to be normal for the

rat: systolic/diastolic blood pressure (mean values):  $\approx 120/80$  mmHg, heart rate:  $\approx 350/450$  beats per minute (bpm) (Sharp & Villano 2012).

In this study the rats were put inside the rodent holder (2) on the warming platform (3). This platform was previously heated to 34°C in order to reduce the animal's stress and increase the blood flow in the tail. After the rat had recovered from stress, the occlusion cuff was placed on the base of the tail and the VPR cuff was placed distal to the occlusion cuff. The measurements were performed after the rat had acclimated to the holder and the cuffs. The systolic and diastolic blood pressure values were taken for the analysis only when the heart rate did not exceed 450 bpm, which indicated that the rat was under stress.

Figure 8 shows the CODA system.

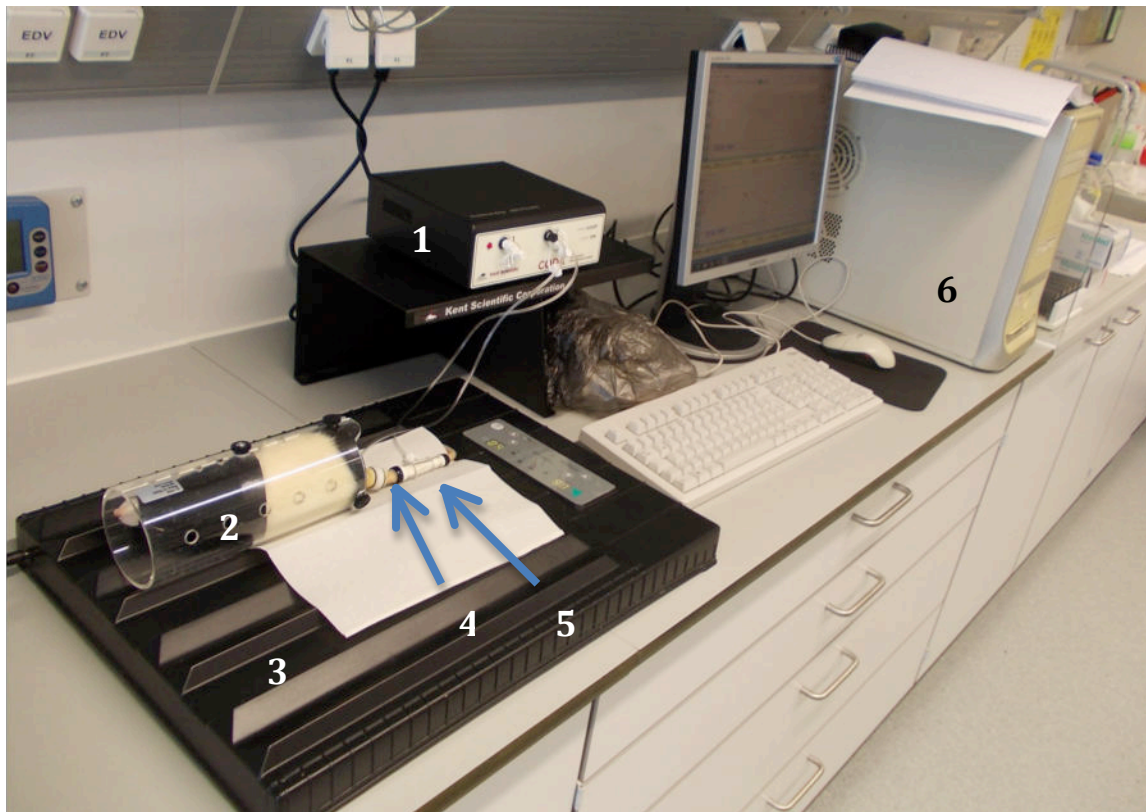


**Figure 8. CODA system for measurements of blood pressure and heart rate.**

1-Coda controller, 2-rat holder, 3-warming platform, 4-occlusion cuff, 5-VPR cuff, 6-computer.

VPR, volume-pressure recording

### 4.3. Isolation of rat atrial myocytes

#### 4.3.1. Chemicals and reagents

All standard chemicals were purchased from Roth (Karsruhe, Germany) or Sigma-Aldrich (München, Germany), if not mentioned otherwise. All solutions and buffers were prepared using demineralised, ultrapure water (ddH<sub>2</sub>O), prepared with the Milli-Q Reference A+ system (Merck Millipore, Darmstadt, Germany).

#### 4.3.2. Solutions for atrial myocyte isolation

The basic Tyrode's solution (without Ca<sup>2+</sup>) was prepared one day prior to the cell isolation procedure (Table 1). All the other solutions were made from Tyrode's solution at the day of cell isolation. These solutions are listed below.

**Table 1. Basic Tyrode's solution (without Ca<sup>2+</sup>) 1l, pH 7.4**

Substance	Concentration
NaCl	130 mM
KCl	5.4 mM
MgCl <sub>2</sub>	0.5 mM
NaH <sub>2</sub> PO <sub>4</sub> x 2H <sub>2</sub> O	0.33 mM
Glucose x H <sub>2</sub> O	22 mM
HEPES	25 mM
1 M NaOH	q.s. for pH adjustment

**Table 2. Cardioplegic solution**

Basic Tyrode's solution	147 ml	Final concentration
1 M KCl	3 ml	20 mM

**Table 3. Cannulation solution**

Basic Tyrode's solution	250 ml	Final concentration
1 M CaCl <sub>2</sub>	37.5 µl	150 µM

Heparin-Na <sup>+</sup> 5000 U/ml	100 $\mu$ l	2 U/ml
-----------------------------------	-------------	--------

**Table 4. Ca<sup>2+</sup> - free solution**

Basic Tyrode's solution	50 ml	Final concentration
100 mM EGTA-Na <sup>+</sup> solution	200 $\mu$ l	20 mM
Heparin-Na <sup>+</sup> 5000 U/ml	20 $\mu$ l	2 U/ml
BDM	50 mg	10 mM

**Table 5. Enzyme solution**

Basic Tyrode's solution	50 ml	Final concentration
Collagenase (Worthington, Collagenase type 2) 255 U/mg	40 mg	204 U/ml
Protease XIV	2.5 mg	0.05 mg/ml
BDM	50 mg	10 mM
1 M CaCl <sub>2</sub>	10 $\mu$ l	0.2 mM

**Table 6. Stop solution (0.5 mM Ca<sup>2+</sup>)**

Basic Tyrode's solution	15 ml	Final concentration
1 M CaCl <sub>2</sub>	7.5 $\mu$ l	0.5 mM
BDM	15 mg	10 mM
BSA	30 mg	2 mg/ml

**Table 7. 1 mM Ca<sup>2+</sup> solution**

Basic Tyrode's solution	15 ml	Final concentration
BSA	30 mg	2 mg/ml
1 M CaCl <sub>2</sub>	15 $\mu$ l	1 mM

**Table 8. 1.5 mM Ca<sup>2+</sup> solution**

Basic Tyrode's solution	100 ml	Final concentration
1 M CaCl <sub>2</sub>	150 $\mu$ l	1.5 mM

**Table 9. 2 mM Ca<sup>2+</sup> solution**

1.5 mM Ca <sup>2+</sup> solution	10 ml	Final concentration
1 M CaCl <sub>2</sub>	5 µl	2 mM

### 4.3.3. Isolation procedure

The rats were anesthetized with isoflurane, weighed and decapitated. Heparin-Na<sup>+</sup> solution (1000 U/kg) was injected in the apex of the heart to prevent thrombi formation. The heart was quickly removed and transferred into a beaker with the oxygenated ice-cold cardioplegic solution. Then, the heart was cannulated via the ascending aorta and perfused with cannulation solution. When the chambers of the heart began to contract, and blood was washed out from the coronary arteries, the cannula with the heart was mounted on the Langendorff apparatus (Figure 9) (FMI Föhr Medical instruments, Seeheim-Jugenheim, Germany), previously heated to 37°C. Perfusion with the oxygenated Ca<sup>2+</sup>-free solution was immediately started. When the heart stopped contracting, which indicates that calcium ions are washed out, the perfusion was switched to the enzyme solution. When the atria started to look flaccid and pale, digestion was stopped, and atria were separated from the heart and placed into 0.5 ml of the enzyme solution (0.2 mM Ca<sup>2+</sup>) without collagenase and protease. Beakers with left and right atria were placed on a rocking platform to allow cell dissociation from the tissue.



**Figure 9. Langendorff system for isolation of cardiac myocytes.**

1-Circulating waterbath, 2-peristaltic pump, 3-perfusate reservoir, 4-thermal chamber, 5-heart.

In order to restore physiological  $\text{Ca}^{2+}$  concentration, we used several solutions with increasing  $\text{Ca}^{2+}$  concentration (Tables 6-9).  $\text{Ca}^{2+}$  concentration was increased gradually. This allows the cells to return to normal intracellular  $\text{Ca}^{2+}$  concentration without becoming  $\text{Ca}^{2+}$  overloaded and depolarized, which may cause cell damage (Louch et al. 2011). Solutions with increasing  $\text{Ca}^{2+}$  concentration were added gradually every 2 minutes according to the scheme in Table 10.

**Table 10. Scheme of atrial myocytes adaptation to physiological  $\text{Ca}^{2+}$  concentration**

<b>Stop solution (0.5 mM <math>\text{Ca}^{2+}</math>)</b>	5 x 0.1 ml
<b>1 mM <math>\text{Ca}^{2+}</math> solution</b>	4 x 0.1 ml
	3 x 0.2 ml
<b>1.5 mM <math>\text{Ca}^{2+}</math> solution</b>	5 x 0.2 ml
<b>Final solution for adaptation of atrial myocytes (2 mM <math>\text{Ca}^{2+}</math>)</b>	4 x 0.1 ml
	3 x 0.2 ml

After the adaptation procedure, the remaining atrial tissue was dispersed with fine forceps and left for 10 minutes without rocking. Then, 2 ml of the supernatant were aspirated and the remaining tissue removed. The solution on the bottom of the beaker contained isolated atrial myocytes.

#### **4.3.4. Plating of isolated atrial myocytes**

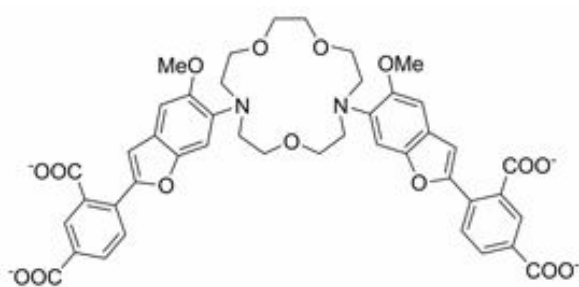
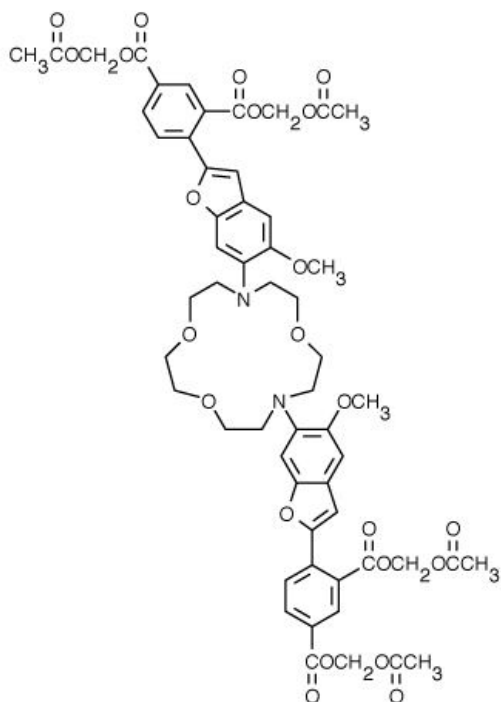
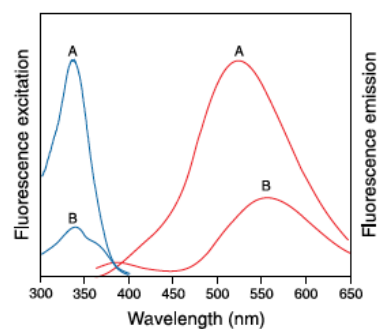
Glass coverslips were covered with 50 µg/ml laminin (Sigma-Aldrich, München, Germany) dissolved in the Tyrode's solution for at least 1 hour at room temperature. The leftover of laminin was aspirated by pipette and coverslips were left to dry. Afterwards, the solution with atrial myocytes was seeded on the coverslips, and the myocytes were left to attach to the bottom of the coverslips for about 20 minutes before conducting of recordings.

#### **4.4. Measurements of intracellular Na<sup>+</sup> concentration and contractility of atrial myocytes**

For the intracellular Na<sup>+</sup> measurements, we used the fluorescent dye SBFI (Sodium-binding benzofuran isophthalate). This dye is a crown ether linked via its nitrogen atoms to the fluorophore groups. In this molecule fluorophores are the benzofurans bound to the isophthalate groups (Minta & Tsien 1989). Since the SBFI molecule is negatively charged, it cannot enter the cell (Figure 11 A). Because of that, the SBFI molecule is modified to the acetoxymethyl ester (SBFI-AM), so that the non-charged molecule of the dye can enter the cell (Figure 11 B). Unspecific intracellular esterases release the polyanionic form of the indicator, which is trapped inside the cell (Johnson & Spence 2010). When Na<sup>+</sup> binds to SBFI the indicator's fluorescence increases, its excitation peak narrows and the emission maximum shifts to shorter wavelengths (Figure 11 C) (Johnson & Spence 2010). The SBFI molecule is excited at two wavelengths: 340 and 380 nm and emits fluorescence at ≈500-600 nm with a maximum at 550 nm.

The fluorescence spectrum of SBFI is shifted in vivo. In rat ventricular myocytes it was shown by Donoso et al. that an increase in [Na<sup>+</sup>]<sub>i</sub> decreased fluorescence intensity at 380 nm and had no effect at 340 nm (Donoso, et al. 1992). The ratio 340 nm/380 nm is used as a measure of [Na<sup>+</sup>]<sub>i</sub>.



**A****B****C**

**Figure 11. SBFI molecule and the fluorescent spectrum of SBFI**

**A:** SBFI molecule, **B:** SBFI-AM molecule, **C:** Fluorescence excitation (detected at 505 nm) and emission (excited at 340 nm) spectra of SBFI in pH 7.9 buffer containing 135 mM (A) or zero (B) Na<sup>+</sup>

(Figures are taken from: [www.teflabs.com](http://www.teflabs.com), [www.lifetechnologies.com](http://www.lifetechnologies.com), (Johnson & Spence 2010), respectively).

The advantage of using ratiometric fluorescence indicators, such as SBFI, is the elimination of data distortions caused by photobleaching (destruction of the excited fluorophore due to a photosensitized generation of reactive oxygen species), leakage of the indicator out of the cell, movement artifacts or its nonuniform distribution and illumination instability.

The dissociation constant ( $K_d$ ) of an indicator depends on several factors, such as pH, temperature, ionic strength, concentrations of other ions and dye-protein interactions (Johnson & Spence 2010). Due to these factors, the  $K_d$  determined in aqueous solutions differs from the values obtained in living cells. The  $K_d$  of SBFI is 11.3 mM in the presence of  $K^+$  in a solution with a combined  $Na^+$  and  $K^+$  concentration of 135 mM, which approximates physiological ionic strength. In several studies different  $K_d$  ( $Na^+$ ) values in living cells were detected in the range of  $\approx 20$ -30 mM (Diarra et al. 2001), (David et al. 1997), (Ito et al. 1997), (Donoso et al. 1992).

SBFI is approximately 18-fold more selective for  $Na^+$  than for  $K^+$  (Johnson & Spence 2010). Since the intracellular  $K^+$  concentration is about 150 mM and is not changing under physiological conditions, so the intracellular  $Na^+$  measurements are not affected by  $K^+$  concentration. Another important factor is the intracellular pH. Diarra et al. showed that acidification results in an apparent decrease and alkalinization in an apparent increase in  $[Na^+]_i$  values. However the  $K_d$  of SBFI for  $Na^+$  was relatively insensitive to changes in pH in the range of 6.8–7.8 (Diarra et al. 2001).

Due to the big differences in  $K_d$  values obtained in various cell types and because of high compartmentalization of the dye, an *in situ* calibration of the fluorescent signal must be performed (Donoso et al. 1992). Several studies (Harootunian et al. 1989), (Donoso et al. 1992), (Levi et al. 1994) have revealed that the following conditions must be fulfilled in order to perform the calibration of the SBFI signal:

- 1) Intracellular and extracellular  $Na^+$  must be equilibrated.
- 2) Calibration solutions with different  $Na^+$  concentrations should be divalent-free. This allows  $Na^+$  ions to enter through  $Ca^{2+}$  channels.
- 3) The pore-forming antibiotic gramicidin D should be present in the calibration solutions to permeabilize the membrane for  $Na^+$ .
- 4)  $Na^+$  efflux via the  $Na^+/K^+$ -ATPase should be inhibited by the presence of a cardiac glycoside.

#### 4.4.1. Loading the atrial myocytes with SBFI-AM

First, the 1 mM stock solution of SBFI-AM was prepared. Pluronic F-127 was dissolved in DMSO (at 37°C) to get a 20% concentration. Then, 50 µg of SBFI-AM were dissolved in 44 µl of that solution. Pluronic acid is a nonionic, surfactant polyol, which was shown to facilitate the solubilization of water-insoluble dyes in physiological media (Johnson & Spence 2010). On the day of measurements, 6 µl of 1 mM SBFI-AM stock solution were dissolved in 600 µl of recording solution (Table 11) to get a final SBFI concentration of 10 µM.

Atrial myocytes were incubated with 95 µl of 10 µM SBFI-AM solution in 20% Pluronic in DMSO for 90 minutes at room temperature in the dark. Afterwards, an equal amount of recording solution was added, and cells were allowed to de-esterify at least 20 minutes.

**Table 11. Recording solution, pH 7.4**

Substance	Concentration
NaCl	140 mM
KCl	4 mM
MgCl <sub>2</sub>	1 mM
CaCl <sub>2</sub>	1 mM
HEPES	10 mM
Glucose	10 mM
1 M Tris base	q.s. for pH adjustment

#### 4.4.2. Intracellular SBFI calibration and intracellular Na<sup>+</sup> measurements

In this study, the three-point calibration of SBFI was used (Despa 2002). At the end of each experiment, cells were superfused with calibration solutions with various Na<sup>+</sup> concentrations: 0, 10 and 20 mM. They were prepared by mixing of two solutions: A and B in different proportions (Tables 12 and 13).

**Table 12. Solution A for SBFI calibration (145 mM Na<sup>+</sup>), pH 7.2**

Substance	Concentration
NaCl	30 mM
Sodium gluconate	115 mM
HEPES	10 mM
EGTA	2 mM
Glucose	10 mM
1 M Tris base	q.s. for pH adjustment

**Table 13. Solution B for SBFI calibration (145 mM K<sup>+</sup>), pH 7.2**

Substance	Concentration
KCl	30 mM
Potassium gluconate	115 mM
HEPES	10 mM
EGTA	2 mM
Glucose	10 mM
1 M Tris base	q.s. for pH adjustment

To equilibrate the extracellular and intracellular [Na<sup>+</sup>], 10 μM of gramicidin D were added, and the Na<sup>+</sup>/K<sup>+</sup>-ATPase was blocked with 100 μM of ouabain. A stock solution of 10 mM gramicidin D was prepared in DMSO. Since the calibration solutions are aggressive due to the absence of Ca<sup>2+</sup>, the permeabilization of the membrane with gramicidin, the presence of DMSO and ouabain, some cells were dying at the beginning of the calibration. To avoid this, we applied solution B (which has no Na<sup>+</sup> and Ca<sup>2+</sup>) with 10 μM DMSO (the final concentration of gramicidin solved in DMSO). Cells, which did not die during the perfusion with this solution, were subjected to calibration.

#### 4.4.3. Ion Optix setup and atrial myocyte $\text{Na}^+$ and contractility measurements

Intracellular  $\text{Na}^+$  concentration and contractility measurements were conducted on the Ion Optix setup (Ion Optix Limited, Dublin, Ireland).

##### 4.4.3.1. The Ion Optix setup

The Ion Optix setup allows simultaneous measurements of sarcomere shortening (as a measure of contractile function of cardiac myocytes) and fluorescence signals. Figure 12 shows the setup.

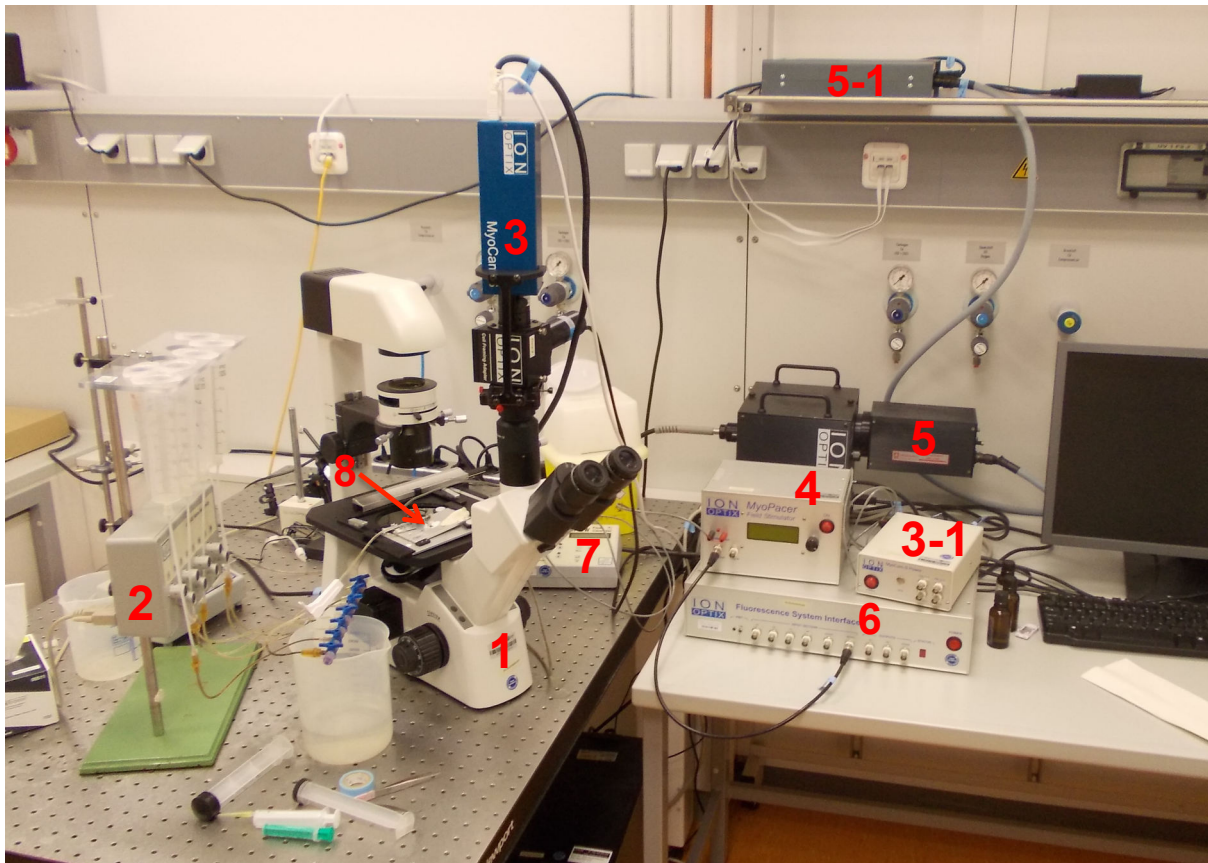


**Figure 12 Setup for  $[\text{Na}^+]$  and contractility measurements**

1-Inverted epifluorescence microscope, 2-Perfusion system (Flow control system), 3-Myo-Cam-S camera, 3-1-Myo-Cam-S power supply, 4-MyoPacer Cell Stimulator, 5-Hyper Switch Light Source (contains Xenon Arc lamp), 5-1 Power supply, 6-Fluorescence System Interface, 7-Mini pump variable flow, 8-Chamber.

The Ion Optix setup was built around an inverted epifluorescence microscope (Figure 12, 1). A coverslip with atrial myocytes was placed into a chamber (Figure 12, 8) on the stage of the microscope. The chamber is shown in Figure 13. This chamber was equipped with two platinum stimulation wires (Figure 13, 1) connected to the cell Stimulator (Figure 12, 4). The optimal level of the solution in the chamber and exchange of the solution was reached via a balance between inflow and outflow (Figure 13, 2 and 3) controlled by the flow control system (Figure 12, 2) and the mini pump variable flow (Figure 12, 7), respectively.

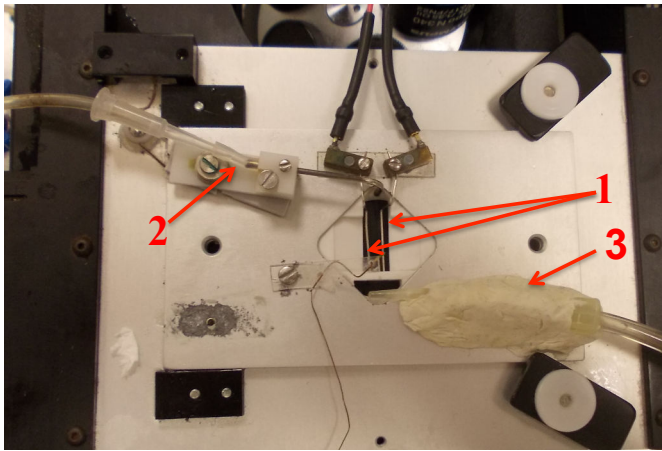


**Figure 13. Chamber system**

1-Platinum stimulation wires, 2-inflow, 3-outflow.

#### 4.4.3.2. Recording protocols and analysis of the data

Cells were chosen for recordings on the basis of the following criteria:

- Rod-shaped
- Regular and stable contractions during electrical stimulation
- Defined and regular striations.

#### 4.4.3.3. Contractility measurements

Atrial myocytes were field stimulated at 1 Hz in the recording solution (Table 11) for about 1 minute. Average sarcomere length shortening was measured in a user-defined region of interest (Figure 14).

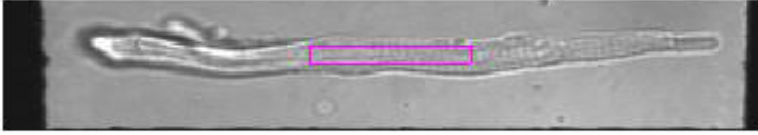


**Figure 14. Video image of an atrial myocyte with region of interest for measurement of sarcomere shortening.**

The user-defined region of interest is enclosed in the pink rectangular.

#### 4.4.3.4. Intracellular Na<sup>+</sup> measurements

Intracellular Na<sup>+</sup> was recorded by the inverted epifluorescent microscope, connected to the Ion Optix Setup (Ion Optix Limited, Dublin, Ireland). SBF1 was excited alternately (2 Hz) at 340 and 380 nm and fluorescence emission was collected at wavelength >515 nm. The cells loaded with SBF1 were stimulated at 1 Hz for about 5 minutes to record a fluorescence signal under steady-state stimulation. Afterwards, the stimulation was switched off for another 5 minutes until a new steady-state under resting conditions was reached. After a brief perfusion (3 minutes) with solution B (0 Na<sup>+</sup>, 0 Ca<sup>2+</sup> with 10 μM DMSO), *in situ* calibration in each cell was performed by applying solutions containing 0, 10 and 20 mM Na<sup>+</sup> in the presence of 100 μM ouabain and 10 μM gramicidin.

#### 4.4.3.5. Data analysis

Acquisition and data analysis were done with Ion Wizard (Ion Optix Limited, Dublin, Ireland) software and Microsoft Excel (Microsoft, Redmond, USA).

For the analysis of sarcomere shortening the following parameters were determined:

- Diastolic sarcomere length (μm) shows the length of the sarcomere at diastole.
- Fractional shortening (%) indicates the percent change of sarcomere length during a twitch.

Kinetic parameters of sarcomere shortening:

- Time to peak 90% (s) (characterizes the time for the sarcomere to reach 90% of maximum contraction).
- Time to baseline 50% (s) (represents the time for the sarcomere to reach 50% of the diastolic sarcomere length).

- Time to baseline 90% (s) (shows the time for the sarcomere to reach 90% of the diastolic sarcomere length).

Figure 15 depicts a representative contractility transient and characteristics used for the analysis of contractility.

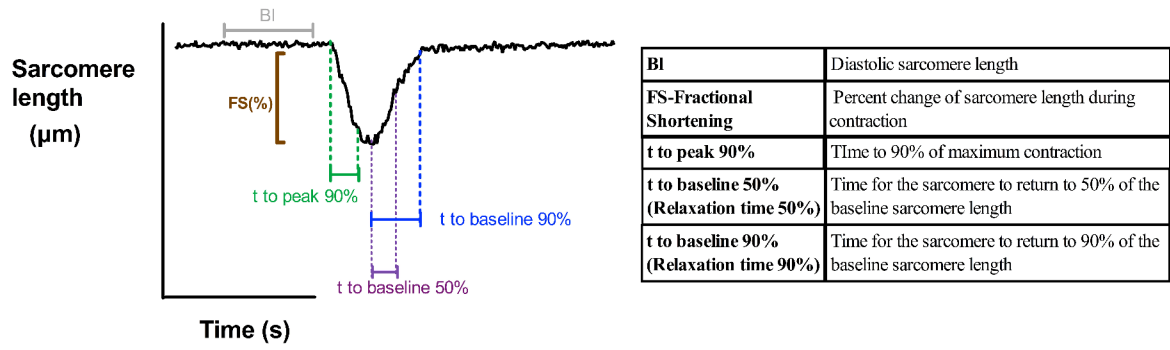


Figure 15. Analysis of twitch



## **4.5. Analysis of protein expression**

### **4.5.1. Tissue collection**

Rats were anesthetized with isoflurane and sacrificed by decapitation. Hearts were quickly removed and collected in the ice-cold cardioplegic solution. Hearts were cut into the four chambers, weighed, and, afterwards, tissue was immediately frozen in liquid nitrogen. Dr. Florentina-Cornelia Pluteanu collected rat tissue for western blot analysis. Human atrial tissue was provided by Prof.Dr. Ursula Ravens (Dresden University of Technology). Experimental protocols were approved by the ethic committee of Dresden University of Technology (EK790799). Each patient gave written informed consent. Right atrial appendages were collected during open-heart surgery for either coronary artery bypass grafting and/or valve replacement. All tissue samples were collected in Dresden and then sent to our laboratory.

### **4.5.2. Homogenization**

All homogenization steps were performed on ice. Frozen atrial tissue was placed into the Micro tissue grinder (Wheaton UK Limited, Rochdale, United Kingdom) and 100 µl of the ice-cold homogenization buffer (Table 14) were added. Then the tissue was manually homogenized with pestle until the solution became slightly red. 100 µl of this fraction was centrifuged for 3 minutes at 3000 revolutions per minute (rpm) and then transferred into an Eppendorf tube. Another 50 µl of the lysis buffer were added to the rest of the tissue and homogenized till the tissue became flaccid and pale. The same centrifugation step (3 minutes at 3000 rpm) was repeated, and 50 µl of the supernatant were transferred into the Eppendorf tube with 100 µl of the first homogenization fraction. Afterwards, 150 µl of homogenate was centrifuged for 3 minutes at 13000 rpm and supernatant was transferred into another Eppendorf tube, rapidly frozen in liquid nitrogen and stored at -80°C.

**Table 14. Homogenization (lysis) buffer**

Component	Concentration
NP-40 (Igepal)	1%
Glycerol	10%
NaCl	137 mM
Tris HCL (pH 7.4)	20 mM
Beta-glycerol phosphate	50 mM
EDTA (pH 8)	10 mM
EGTA (pH 7)	1 mM
Sodium pyrophosphate	1 mM
NaF	20 mM
PMSF	1 mM
Na <sub>3</sub> VO <sub>4</sub>	1 mM
Aprotinin	4 µg/ml
Leupeptin	4 µg/ml
PepstatinA	4 µg/ml

#### 4.5.3. Quantification of protein amount

To determine the protein concentration in atrial tissue homogenates the bicinchoninic acid assay (BCA) was performed. This assay relies on two steps: first Cu<sup>2+</sup> ions are reduced to Cu<sup>+</sup> by peptide bonds in proteins at alkaline pH; during the second step two BCA molecules bind to the cuprous ion, resulting in a chelating complex of intense purple color. This complex is water-soluble and exhibits a strong linear absorbance at 562 nm with increasing protein concentrations (Walker 1994).

First atrial homogenates were 50 times diluted in lysis buffer. The Pierce BCA Protein assay kit (Thermo Fisher Scientific, Schwerte, Germany) was used for the spectrophotometric determination of protein concentration. According to the manufacturer's instructions, working reagent (contained BCA) was prepared by mixing 50 parts of reagent A with 1 part of reagent B. Then 200 µl of working reagent were mixed with 5 µl of 1:50 diluted homogenate and 20 µl of dH<sub>2</sub>O. Afterwards, this mixture was incubated at 37°C for 30 minutes. Absorbance was measured at 562 nm by a

spectrophotometer (GENESYS™ 10S UV-Vis, Thermo Fisher Scientific, Schwerte, Germany). In order to calculate the protein amount in each sample a standard curve containing 0-1 mg/ml standard bovine serum albumin (Thermo Fisher Scientific, Schwerte, Germany) was used.

#### 4.5.4. Western blot analysis

Sodium dodecyl sulfate (SDS) electrophoresis is an analytical method used for separation of proteins according to their molecular weight in the electrical field. For analysis of major Na<sup>+</sup>- and Ca<sup>2+</sup>-handling proteins Glycine-SDS-PAGE electrophoresis was used. In order to improve separation of small proteins, such as PLB and PLM, Tricine-SDS-PAGE was performed. This electrophoretic system is preferentially used for the resolution of proteins smaller than 30 kDa (Schägger 2006).

##### 4.5.4.1. Gel preparation

8%-Glycine-SDS-PAGE gel and tricine-SDS-PAGE gels were prepared using the Bio-Rad gel casting system (Bio-Rad, München, Germany). They were composed of a 4% stacking gel (Table 16) and, subsequently, an 8%, 14% or 16% running gel (Tables 15,20). 4-20% gradient gels were from Bio-Rad (Bio-Rad, München, Germany).

**Table 15. Composition of 8% running gel for SDS-PAGE (10 ml)**

	8 %
ddH <sub>2</sub> O	4.7 ml
PAA/BIS 30%	2.7 ml
1.5 M Tris 8.8	2.5 ml
20% SDS	0.05 ml
TEMED	5 µl
10% APS	50 µl

**Table 16. Composition of 4% stacking gel for SDS-PAGE (5 ml)**

	4%
ddH <sub>2</sub> O	3.08 ml
PAA/BIS 30%	0.67 ml
1.5 M Tris 6.8	1.25 ml
20% SDS	250 µl
TEMED	10 µl
10% APS	25 µl

**Table 17. 10% Ammoniumpersulphate (APS)**

Ammoniumpersulfat	0.1 g
ddH <sub>2</sub> O	1 ml

**Table 18. 1.5 M Tris-HCL, pH 8.8**

Tris Base	27.23 g
ddH <sub>2</sub> O	150 ml
5 M HCl	q.s. for pH adjustment

**Table 19. 0.5 M Tris-HCL, pH 6.8**

Tris Base	6 g
ddH <sub>2</sub> O	100 ml
5 M HCl	q.s. for pH adjustment

**Table 20. Composition of 16% and 14% Tris-tricine running gel (12 ml)**

	16% Tris-tricine gel	14% Tris-tricine gel
ddH <sub>2</sub> O	1.5 ml	1.75 ml
PAA/BIS 30%	6.4 ml	4.2 ml
3M Tris-HCL/SDS (3x)	4 ml	6 ml
TEMED	10 µl	10 µl
10% APS	50 µl	100 µl

**Table 21. 3 M Tris HCl/SDS (3x), pH 8.45**

Tris Base	182 g
ddH <sub>2</sub> O	300 ml
5 M HCl	q.s. for pH adjustment
ddH <sub>2</sub> O	Add to 500 ml
SDS	1.5 g

#### 4.5.4.2. Sample preparation

4x Lämmli buffer (Table 22) containing 5%  $\beta$ -mercaptoethanol (the corresponding amount of  $\beta$ -mercaptoethanol was added on the day of experiment), lysis buffer and atrial homogenate corresponding to 20 or 35  $\mu$ g of total protein were mixed prior to loading on the gel. To identify the molecular weight of investigated proteins 5  $\mu$ l of PageRuler™ Plus Prestained Protein Ladder (Thermo Fisher Scientific, Schwerte, Germany) or Precision Plus Protein Prestained Standard Dual Color (Bio-Rad, München, Germany) were loaded next to the samples.

**Table 22. Lämmli buffer 4x, pH 6.8**

EGTA	16 mM
SDS	4%
Tris HCL (pH 6.8)	40 mM
Dithiothreitol (DTT)	16 mM
Glycerol	47%
Br-Ph Blue	0.05%

#### 4.5.4.3. Gel electrophoresis

Mini Trans-Blot Electrophoretic Transfer Cell (Bio-Rad, München Germany) was filled with the corresponding buffers (Tables 23,24,25), and gel electrophoresis was performed first at 90 V for 1 hour and then at 120 or 70 V for Glycine-SDS-PAGE or Tricine-SDS-PAGE, respectively, until optimal separation was reached.

**Table 23. Running buffer for Glycine-SDS-PAGE**

TRIS base	25 mM
Glycine	192 mM
SDS	0.1%

**Table 24. Cathode buffer for Tricine-SDS-PAGE, pH 8.25**

Tris Base	100 mM
Tricine	100 mM
SDS 20%	0.1%

**Table 25. Anode buffer for Tricine-SDS-PAGE, pH 8.9**

Tris Base	200 mM
5 M HCl	q.s. for pH adjustment

**4.5.4.4. Blotting**

Separated proteins were transferred from the gel onto a nitrocellulose membrane. First, the membrane was incubated in ddH<sub>2</sub>O for 5 minutes and then in the transfer buffer containing 20% methanol (Table 26). At the same time, gel, filter papers and sponges were also incubated in the transfer buffer for 15 minutes. After assembling the “blotting sandwich,” blotting was performed in a Mini Trans-Blot Electrophoretic Transfer Cell (Bio-Rad, München, Germany) for 2 hours at 150 mA per gel (for blotting of proteins with molecular weight > 250 kDa) and then at 30 mA per gel overnight at 4°C.

**Table 26. 10x Transfer buffer 1l**

Tris base	39.4 g	0.33 M
Glycine	144 g	1.92 M
ddH <sub>2</sub> O	Ad to 1l	

**4.5.4.5. Blocking and immunostaining**

The next day, the membrane was stained with Ponceau S to check the protein abundance on the membrane, then washed 3 times for 10 minutes with TBST buffer (Table 27) and afterwards blocked with 5% milk blocking buffer (prepared by diluting the corresponding amount of skimmed milk powder in TBST buffer) for 1 hour at room

temperature (RT). After that, the membrane was washed 3 times for 10 minutes with TBST. Next, the primary antibodies, diluted in 0.5% milk blocking buffer, were put on the membrane and incubated either for 2 hours at RT or overnight at 4°C (Table 28). After the incubation with primary antibody, the membrane was washed 3 times for 10 minutes with TBST buffer and then HRP-conjugated secondary antibody, diluted in 0.5% milk blocking buffer (Table 29) were added to the membrane and incubated for 1 hour at RT. Afterwards, the membrane was washed 3 times for 10 minutes with TBST buffer. Thereafter, the membrane was covered with a chemiluminescent substrate solution HRP-Juice (PJK, Kleinblittersdorf, Germany) and after 2 minutes the chemiluminescent signal was detected by the Chemidoc-XRS Imaging System (Bio-Rad, München, Germany). For the detection of pCaMKII, a more sensitive chemiluminescent substrate solution: SuperSignal West Femto Maximum Sensitivity Substrate (Thermo Fischer Scientific, Schwerte, Germany) was used. GAPDH or actin served as loading controls. Quantification of the signal was done with ImageJ (NIH, Bethesda, Maryland, USA).

**Table 27. 20x TBS buffer pH 7.5**

NaCl	198.2g	1.7 M
Tris Base	24.2g	0.1 M
5 M HCl	q.s. for pH adjustment	
ddH <sub>2</sub> O	Ad to 1l	

In order to prepare TBST buffer Tween 20 was added to 1 l 1xTBS buffer after the pH adjustment to get final 0.1% concentration



**Table 28. Investigated proteins and primary antibodies**

<b>Protein (molecular weight, kDa)</b>	<b>Primary antibodies</b>	<b>Company and catalogue number</b>	<b>Species</b>	<b>Dilution</b>	<b>Gel</b>
pan Na <sup>+</sup> channel 250	Anti-Pan Na <sub>v</sub>	Alomone labs, ASC- 003	rabbit	1:500	4-20% gradient gel
NCX 120	Sodium/Calcium Exchanger 1 Antibody (6H2)	Thermo Scientific, MA1-4672	mouse	1:1000	4-20% gradient gel
NHE 100	Mouse Anti - Na <sup>+</sup> /H <sup>+</sup> Exchanger isoform NHE 1 monoclonal antibody	Chemicon International, MAB3140	mouse	1:1000	4-20% gradient gel
α 1 subunit of NKA 100	Anti-α 1 Sodium Potassium ATPase antibody	Abcam, ab2872	mouse	1:1000	4-20% gradient gel
α 2 subunit of NKA 100	Rabbit anti- sodium pump α 2 polyclonal antibody	Chemicon International, AB9094	rabbit	1:500	4-20% gradient gel
α 3 subunit of NKA 100	Anti-α 3 Sodium Potassium ATPase antibody	Abcam, ab2826	mouse	1:1000	4-20% gradient gel
β 1 subunit of NKA 35	Anti-β 1 Sodium Potassium ATPase antibody	Abcam, ab8344	mouse	1:5000	4-20% gradient gel
PLM 10	Anti FXYD1 antibody	Abcam, ab76597	rabbit	1:1000	16% tris- tricine gel
GAPDH 34	Anti- Glyceraldehyde -3-Phosphate Dehydrogenase antibody (Clone: 6C5)	Calbiochem, CB1001	mouse	1:50 000	

Actin 44	Mouse Anti-Actin, Monoclonal (Clone: C4)	MP LLC. #69100Biomedicals,	mouse	1:50 000	
RyR 565	Ryanodine receptor antibody (C3- 33)	Thermo Scientific, MA3-916	rabbit	1:5000	4-20% gradient gel
RyR pSer2808	Ryanodine receptor 2 (RYR2) (pSer2808) pAb	Badrilla, A010-30	rabbit	1:5000	4-20% gradient gel
RyR pSer2814	Ryanodine Receptor 2 (RYR2) (pSer2814) pAb	Badrilla, A010-31	rabbit	1:5000	4-20% gradient gel
PLB 25	Phospholamba n A1 Antibody	Badrilla, A010-14	mouse	1:5000	14% tris- tricine gel
PLB pS16	Phospholamba n Phospho Serin1-16 Anti- Serum	Badrilla, A010-12	rabbit	1:5000	14% tris- tricine gel
PLB pT17	Phospholamba n Phospho Threonine-17 Anti-Serum	Badrilla, A010-13	rabbit	1:5000	14% tris- tricine gel
PLB pS10	Phospholamba n Phospho Serine-10 Affinity Purified Antibody	Badrilla, A010-10AP	rabbit	1:1000	14% tris- tricine gel
CSQ 55	Anti- Calsequestrin Polyclonal Antibody	Thermo Scientific,PA1-913	rabbit	1:2500	4-20% gradient gel
SERCA 100	Anti-SERCA2a Antibody	Badrilla, A010-20	rabbit	1:5000	4-20% gradient gel
LTCC 250	Anti Cav 1.2a (cardiac type $\alpha$ 1c)	Alomone Labs	rabbit	1:200	8% glycine SDS- PAGE

ET <sub>AR</sub> 70	Anti-Endothelin Receptor A	Alomone Labs, AER-001	rabbit	1:500	8% glycine SDS-PAGE
PLC $\beta$ 1 150	PLC $\beta$ 1 (G-12): sc-205	Santa Cruz Biotechnology, sc-205	rabbit	1:1000	4-20% gradient gel
PLC $\beta$ 3 150	PLC $\beta$ 3 (C-20): sc-403	Santa Cruz Biotechnology, sc-403	rabbit	1:1000	4-20% gradient gel
CaMKII 50	CaMKII $\delta$	Badrilla, A010-55AP	rabbit	1:5000	4-20% gradient gel
pCaMKII pT286	Anti-CaMKII (phospho T286)	Abcam, ab32678	rabbit	1:1000	4-20% gradient gel
IP <sub>3</sub> R2 313	Anti-ITPR2	Abcam, ab77838	rabbit	1:1000	4-20% gradient gel
$\alpha$ 1 adrenoreceptor or 57	Anti- $\alpha$ 1 adrenergic receptor antibody	Abcam, ab166925	goat	1:750	4-20% gradient gel

**Table 29. Secondary antibodies**

Secondary antibodies	Company and a catalogue number	Dilution
Immunopure Goat Anti-Mouse IgG, (H+L), Peroxidase Conjugated	Thermo Scientific, 31430	1:5000
Immunopure Goat Anti-Rabbit IgG, (H+L), Peroxidase Conjugated	Thermo Scientific, 31460	1:5000
Donkey Anti-Goat IgG H&L (HRP) preadsorbed	Abcam, 97120	1:10 000

**4.5.4.6. Stripping**

Some membranes were incubated for 7 minutes with stripping buffer (Table 30) to remove bound primary and secondary antibodies and then washed twice with TBST buffer and afterwards reblocked in blocking buffer and reprobbed with different antibodies.

**Table 30. Stripping buffer, pH 2.2.**

Glycine	200 mM
SDS	1%
Tween 20	0.1%
5 M HCl	q.s. for pH adjustment

#### **4.6. Statistical analysis**

Statistical analysis was performed using GraphPad Prism (GraphPad Software, Inc., San Diego, USA). All data are presented as mean  $\pm$  the standard error of the mean (SEM). Statistical comparison between two groups was performed by using Student's t-test. When multiple groups were compared, analysis of variance ANOVA, Dunnett's multiple comparison test or Bonferroni's post hoc test was done. Levels of significance are indicated by asterisks (\*  $p < 0.05$ ; \*\*  $p < 0.01$ ) and/or by a hash sign (#  $p < 0.05$ ; ##  $p < 0.01$ ).

## 5. Results

### 5.1. Characterization of atrial remodelling in early hypertension

The onset of hypertension in SHR occurs starting with 6 weeks of age and hypertension is present during the remaining lifespan of these rats. The animals used for this study were in the age of 12-14 weeks and in the age of 6-8 months, further referred to 3 and 7 months old rats, respectively. We performed blood pressure measurements, estimation of cardiac hypertrophy and contractile function of atrial myocytes, measurements of intracellular sodium concentration ( $[Na^+]_i$ ) and western blot analysis of major  $Na^+$ -regulating proteins in the atria of WKY and SHR.

#### 5.1.1. Blood pressure and heart rate measurements, gravimetric assessment of hypertrophy

Dr. Florentina-Cornelia Pluteanu performed gravimetric assessment of hypertrophy. Hearts had been removed from the chest, cut into the four chambers and then weighed. Lung weight (LW) served as an indicator of fluid retention in the lungs and, thus, a sign of heart failure. All gravimetric parameters were normalized to tibia length (TL).

At the age of 3 months, SHR exhibited significant increases in diastolic, systolic, mean arterial pressure and heart rate (Figure 16A). Gravimetric assessment revealed no changes in lung weight but significant elevation of left ventricular weight, indicating an early onset of left ventricular hypertrophy. However, no significant changes were observed in right ventricular weight. Interestingly, the weight of both left and right atria was significantly reduced in SHR (Figure 16B).

As illustrated in Figure 16A, at the age of 7 months, SHR showed similar blood pressure and heart rate values. We observed a significant progression of left ventricular hypertrophy but no changes in right ventricular weight (Figure 16Ba and b, respectively). Left and right atrial hypotrophy was still present in the 7 months old SHR (Figure 16Bc and d, respectively). However, there was a significant increase in left atrial weight of SHR rats during aging (Figure 16Bc). Lung weight was not changed in 7 months old SHR (Figure 16Be).

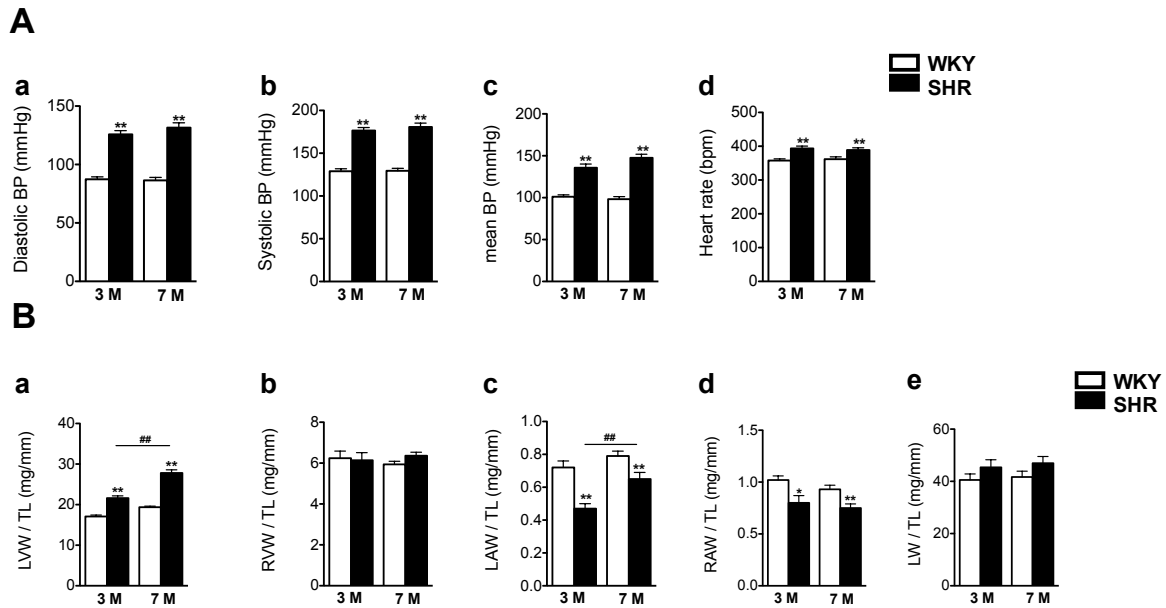


**Figure 16. Cardiovascular characteristics of 3 and 7 months old rats**

**A:** Blood pressure parameters: **a**-diastolic blood pressure, **b**- systolic blood pressure **c**-mean blood pressure **d**-heart rate. **B:** Gravimetric parameters normalized to tibia length (TL): **a**-left ventricular weight (LVW), **b**-right ventricular weight (RVW), **c**-left atrial weight (LAW), **d**-right atrial weight (RAW), **e**-lung weight (LW). N= number of rats per group for blood pressure measurements and gravimetric assessment, respectively: 3 months old animals: WKY N=24, 7; SHR N=24, 7; 7 months old animals: WKY N=30; 14-15 rats per group, SHR N=29; 14-15 rats per group. \* $p < 0.05$ , \*\* $p < 0.01$  WKY vs. SHR, Student's unpaired t-test, ## $p < 0.01$  3 months old vs. 7 months old, two-way ANOVA followed by Bonferroni post-test.

### 5.1.2. Measurements of contractility

Since atrial contractility is an important determinant of cardiac output and the loss of atrial contractility is one of the most frequently observed phenomena in atrial fibrillation, our next step was to characterize the contractile properties of atrial myocytes from SHR and WKY.

At the age of 3 months atrial myocytes from SHR did not show any major changes in  $Ca^{2+}$  handling (Pluteanu et al. 2015) and no changes in  $[Na^+]_i$ , as will be shown below. Because of this, we assumed that at 3 months of age no changes in contractility are

expected and began measurements at 7 months of age when first subcellular alterations in  $\text{Ca}^{2+}$  handling were observed (Pluteanu et al. 2015).

Figure 17 demonstrates representative contractility traces (A) and analysis of contractile parameters (B) from 7 months old WKY and SHR. Diastolic sarcomere length was almost equal between WKY and SHR (Figure 17Ba). Fractional shortening was also similar:  $12.0 \pm 1.0\%$  in WKY vs  $11.0 \pm 1.4\%$  in SHR (Figure 17Bb). Kinetic parameters of sarcomere shortening were not different between WKY and SHR (Figure 17Bc). Parameters characterizing relaxation were also similar between WKY and SHR, as can be estimated from Figure 17Bd and e. Thus, there were no changes in contractility in atrial myocytes from SHR compared to WKY at 7 months of age.

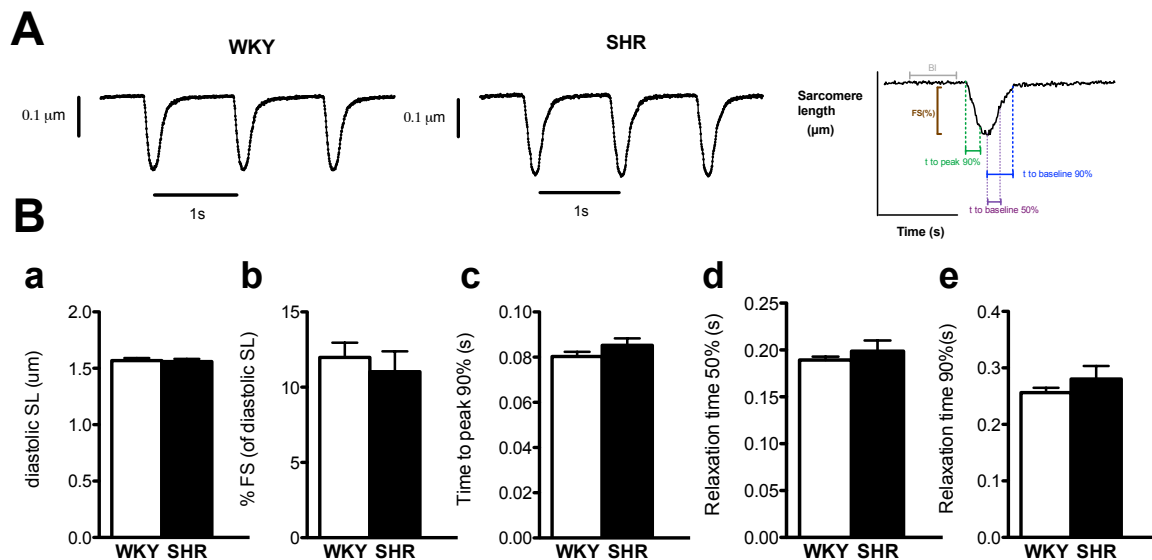


**Figure 17. Contractility of atrial myocytes in 7 months old rats**

**A:** Representative sarcomere length (SL) shortening traces in WKY and SHR atrial myocytes. **B:** Analyzed contractile parameters: **a**-diastolic sarcomere length, **b**-fractional shortening, **c**-time to peak 90%, **d**-relaxation time 50%, **e**-relaxation time 90%. (n/N=number of cells/number of animals: 36/5 for WKY and 25/7 for SHR). Data were analyzed by Student's unpaired t-test.

We also compared contractile parameters of left and right atrial myocytes in WKY and SHR. Figure 18 illustrates this comparison. Left and right atrial myocytes from WKY exhibited very similar diastolic sarcomere length (Figure 18Aa) and fractional shortening values (Figure 18Ab). Kinetic parameters were almost identical between left



and right atrial myocytes (Figure 18Ac-e). When left and right atrial myocytes from SHR were compared, we also did not observe any significant changes in diastolic sarcomere shortening (Figure 18Ba), fractional shortening (Figure 18Bb) or kinetic properties of contraction (Figure 18Bc-e). To conclude, left and right atrial myocytes from WKY and SHR at 7 months of age exhibited similar contractility.

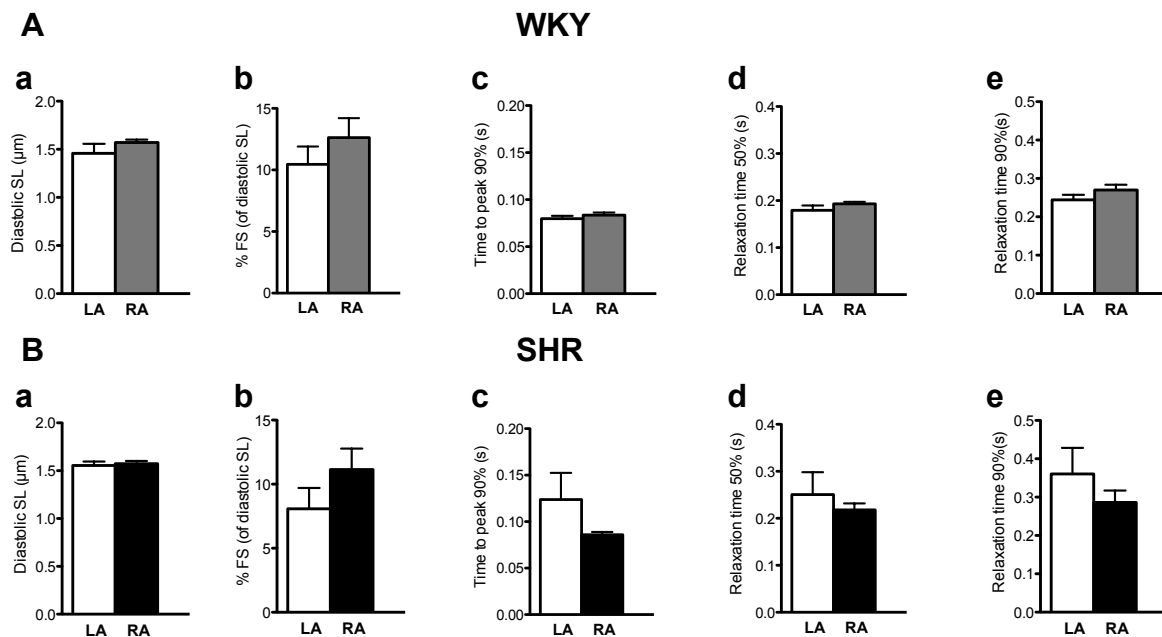


**Figure 18. Comparison of left and right atrial myocyte contractility in 7 months old rats**

**A:** Analyzed contractile parameters of WKY left (LA) and right (RA) atrial myocytes: **a**-diastolic sarcomere length, **b**-fractional shortening, **c**-time to peak 90%, **d**-time to baseline (relaxation time) 50%, **e**-time to baseline (relaxation time) 90%. **B:** (**a-e**) Same contractility parameters for the SHR left (LA) and right (RA) atrial myocytes (n/N=number of cells/number of animals: WKY rats: 16/5 and 16/4 for left and right atrial myocytes, respectively. SHR: 10/3 and 17/3 for left and right atrial myocytes, respectively. Data were analyzed by Student's unpaired t-test.

### 5.1.3. Intracellular Na<sup>+</sup> measurements

In order to characterize Na<sup>+</sup> homeostasis, we performed intracellular Na<sup>+</sup> measurements in atrial myocytes from SHR and WKY by using the fluorescent dye SBFI-AM.

Figure 19Aa illustrates the experimental protocol for [Na<sup>+</sup>]<sub>i</sub> measurements. An atrial myocyte was stimulated at 1 Hz until the fluorescent signal reached steady-state.

Afterwards, the stimulation was switched off, and the fluorescent signal was recorded at the resting state until it also reached steady-state. After a short perfusion with  $0\text{Na}^+/0\text{Ca}^{2+}$  solution, the three-point *in situ* calibration was performed (Figure 19A). The calibration curve, derived in this cell (Figure 19Aba), was used to calculate  $[\text{Na}^+]_i$  at 1 Hz stimulation and at the resting state. The average  $[\text{Na}^+]_i$  is presented in Figure 19B. Stimulation-dependent change in  $[\text{Na}^+]_i$  was calculated as the difference in  $[\text{Na}^+]_i$  between 1 Hz stimulation and resting conditions (Figure 19C).

In agreement with previous observations from ventricular myocytes (Bers & Despa 2009),  $[\text{Na}^+]_i$  was higher at 1 Hz in comparison to the resting state. The average  $[\text{Na}^+]_i$ , at 1 Hz stimulation, as shown in Figure 19B, was not different between WKY or SHR at 3 months ( $10.7 \pm 1.8$  mM in WKY vs.  $9.8 \pm 1.1$  mM in SHR) or 7 months of age ( $11.8 \pm 1.2$  mM in WKY vs.  $9.5 \pm 1.0$  mM in SHR). At the resting conditions,  $[\text{Na}^+]_i$  was also not changed in SHR compared to WKY at 3 months ( $7.7 \pm 1.8$  mM in WKY vs.  $7.5 \pm 1.3$  mM in SHR) or 7 months of age ( $9.6 \pm 0.9$  mM in WKY vs.  $8.5 \pm 1.3$  mM in SHR). Stimulation-dependent change in  $[\text{Na}^+]_i$  was not significantly different between WKY and SHR neither at 3 months nor at 7 months of age (Figure 19C).

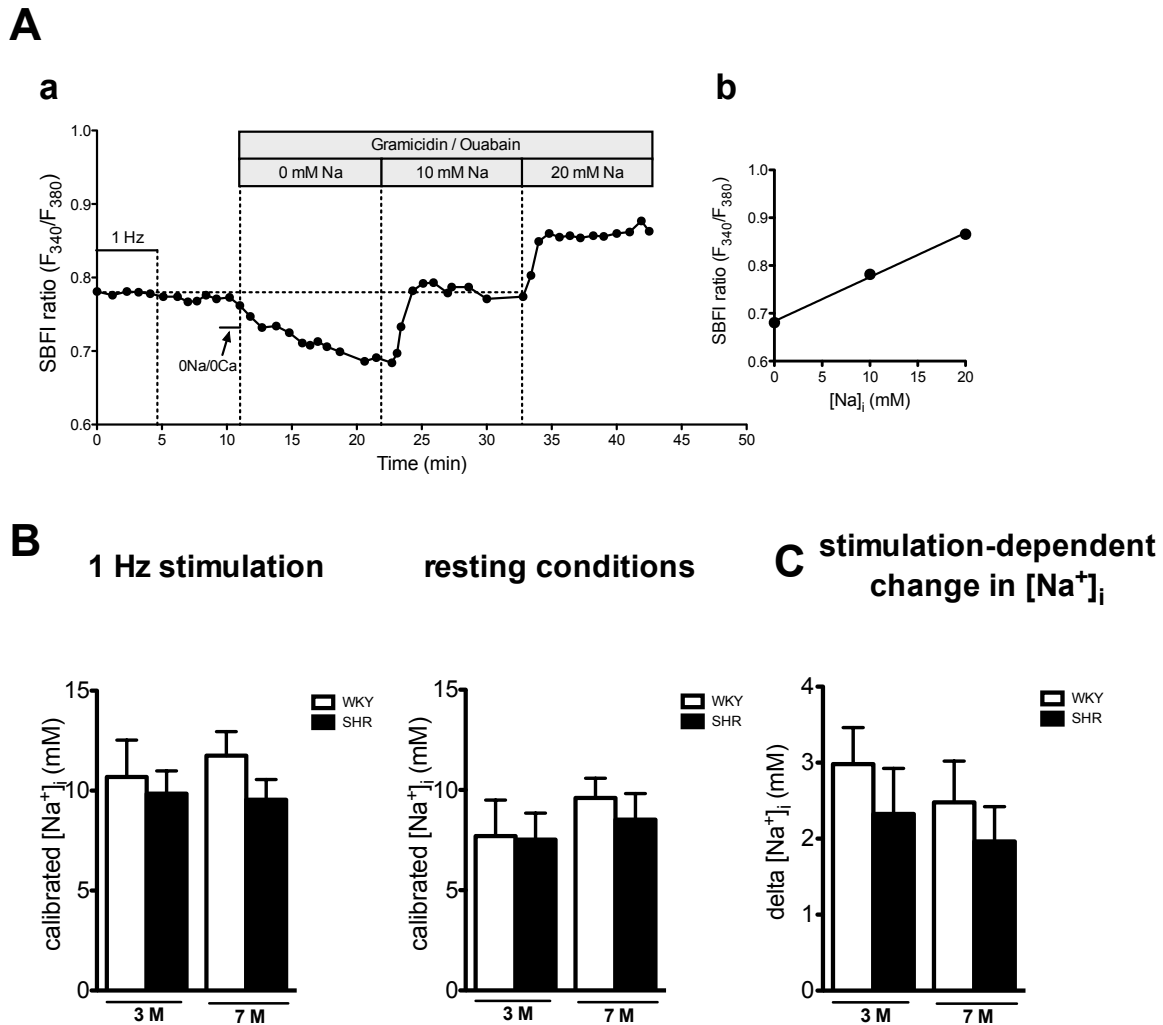


**Figure 19.  $[Na^+]_i$  in 3 and 7 months old animals**

**A:** Experimental protocol for  $Na^+$ -measurements in an atrial myocyte. A cell was stimulated at 1 Hz for 5 minutes. Stimulation was switched off until the SBFI ratio reached steady state.  $Na^+$ - and  $Ca^{2+}$ -free ( $0Na^+/0Ca^{2+}$ ) solution was applied for 3 minutes, before exposure to calibration solutions containing gramicidin and ouabain. **b**-SBFI-ratio as a function of  $[Na^+]_i$ . Line was obtained by linear regression analysis,  $r^2 > 0.99$ . **B:** Average  $[Na^+]_i$  in atrial myocytes under 1 Hz stimulation and resting conditions. **C:** Stimulation-dependent change in  $[Na^+]_i$  was calculated as the difference:  $[Na^+]_i$  at 1 Hz minus resting  $[Na^+]_i$ . All data presented as mean $\pm$ SEM; 3 months old animals n/N: WKY 7/5, SHR 7/4; 7 months old rats n/N: WKY 15/7, SHR 11/7. Data were analyzed by Student's unpaired t-test.

We also compared  $[Na^+]_i$  in left and right atrial myocytes in 7 months old WKY and SHR. Data are given in Figure 20. There were no significant difference in  $[Na^+]_i$  between left

and right atrial myocytes neither in WKY nor in SHR. Due to the limited number of left atrial myocytes measured in 3 months old SHR, we could not perform the comparison between left and right myocytes for this age.

In conclusion, atrial myocyte  $[Na^+]_i$  was not different between WKY and SHR in early hypertension.

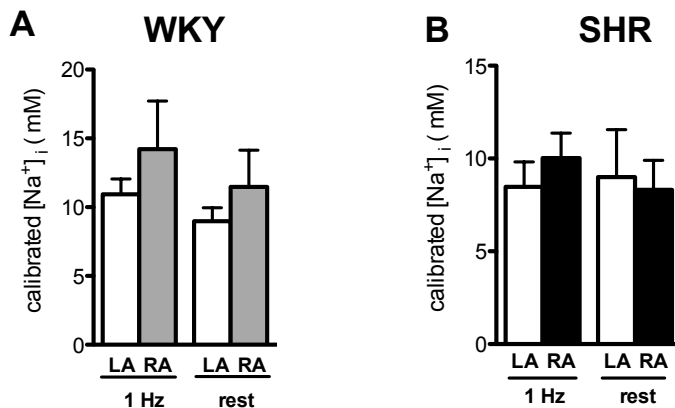


**Figure 20. Comparison of  $[Na^+]_i$  between left and right atrial myocytes in 7 months old animals**

**A:** Average  $[Na^+]_i$  in left (LA) and right (RA) atrial myocytes from WKY under 1 Hz stimulation (1Hz) and resting conditions (rest). **B:** Average  $[Na^+]_i$  in left (LA) and right (RA) atrial myocytes from SHR under 1 Hz stimulation (1Hz) and resting conditions (rest). n/N=number of cells/number of animals: WKY: 12/6 and 4/2 for left and right atrial myocytes, respectively; SHR: 4/4 and 9/6 for left and right atrial myocytes, respectively. Data were analyzed by Student's unpaired t-test.

#### 5.1.4. Expression of $Na^+$ regulating proteins in left and right atria from SHR and WKY rats

Next, we performed western blot analysis of major  $Na^+$ -handling proteins in left and right atria from WKY and SHR. Intracellular  $Na^+$  homeostasis is balanced by  $Na^+$  influx and  $Na^+$  efflux processes. As mentioned earlier, voltage-dependent  $Na^+$  channels,  $Na^+/Ca^{2+}$  exchanger (NCX) and  $Na^+/H^+$  exchanger (NHE) belong to the  $Na^+$  import proteins.  $Na^+$  efflux occurs by  $Na^+/K^+$ -ATPase (NKA), consisting of  $\alpha$  and  $\beta$  subunits.  $\alpha$  1,

$\alpha 2$  and  $\alpha 3$  are  $\alpha$  isoforms expressed in the heart.  $\beta 1$  is the only  $\beta$  cardiac isoform. NKA function is regulated by phospholemman (PLM).

Figure 21 shows original western blots of  $\text{Na}^+$  influx proteins in the left (A) and in the right (B) atrium of 3 months old rats and averaged data on protein expression (a for the left and b for the right atrium). Expression of  $\text{Na}^+$  import transporters was not significantly changed in the left atrium of SHR, compared to WKY (Figure 21a). However, in the right atrium expression of  $\text{Na}^+$  channels and NCX was significantly increased in the SHR, as evident from Figure 21b.

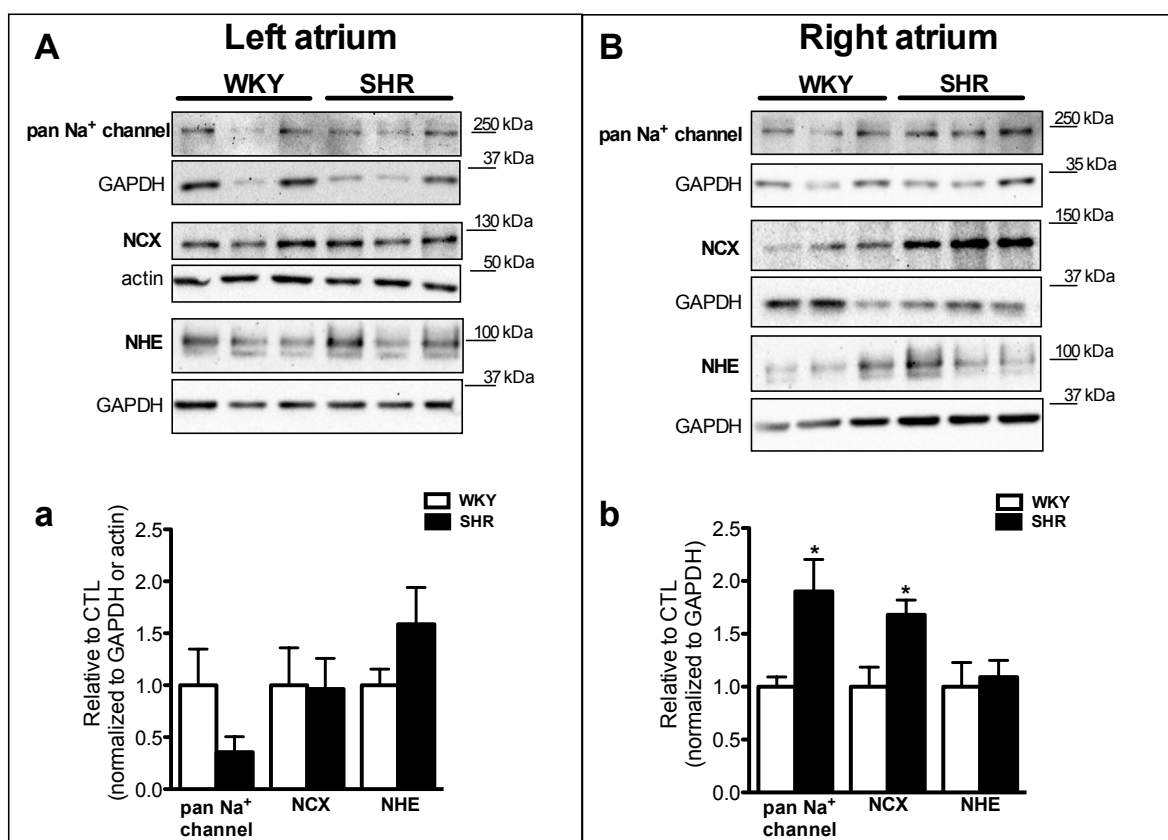


**Figure 21. Expression of  $\text{Na}^+$  influx proteins in left and right atrium from 3 months old rats**

**A, B:** Original western blots of pan  $\text{Na}^+$  channel, NCX and NHE proteins in left (A) and right (B) atrium from WKY and SHR; **a,b** – averaged data of  $\text{Na}^+$ -influx proteins expression in left (a) and right (b) atrium, normalized to GAPDH or actin. N=6-7 in each group. \*p < 0.05 Student's unpaired t-test.

Western blot analysis of NKA subunits and PLM is presented in Figure 22. In the left atrium (Figure 22A) no significant changes in the expression of different  $\alpha$  subunits and the  $\beta$  1 subunit of NKA were found. PLM expression was also unchanged. In order to estimate NKA function, we also calculated the ratio of  $\alpha$  1 to PLM expression ( $\alpha$  1/PLM). This ratio was unaffected in the left atrium of the SHR.

Expression of the  $\alpha$  1 and  $\beta$  1 subunit in the right atrium (Figure 22Bb) tended to be lower in SHR ( $p=0.06$  and  $p=0.08$ , respectively), however, expression of other  $\alpha$  subunits was unchanged. PLM expression and the  $\alpha$  1/PLM ratio were unaltered.

Overall, no significant changes in NKA and PLM expression in both atria were observed, suggesting unaffected atrial  $\text{Na}^+$  export in 3 months old SHR.

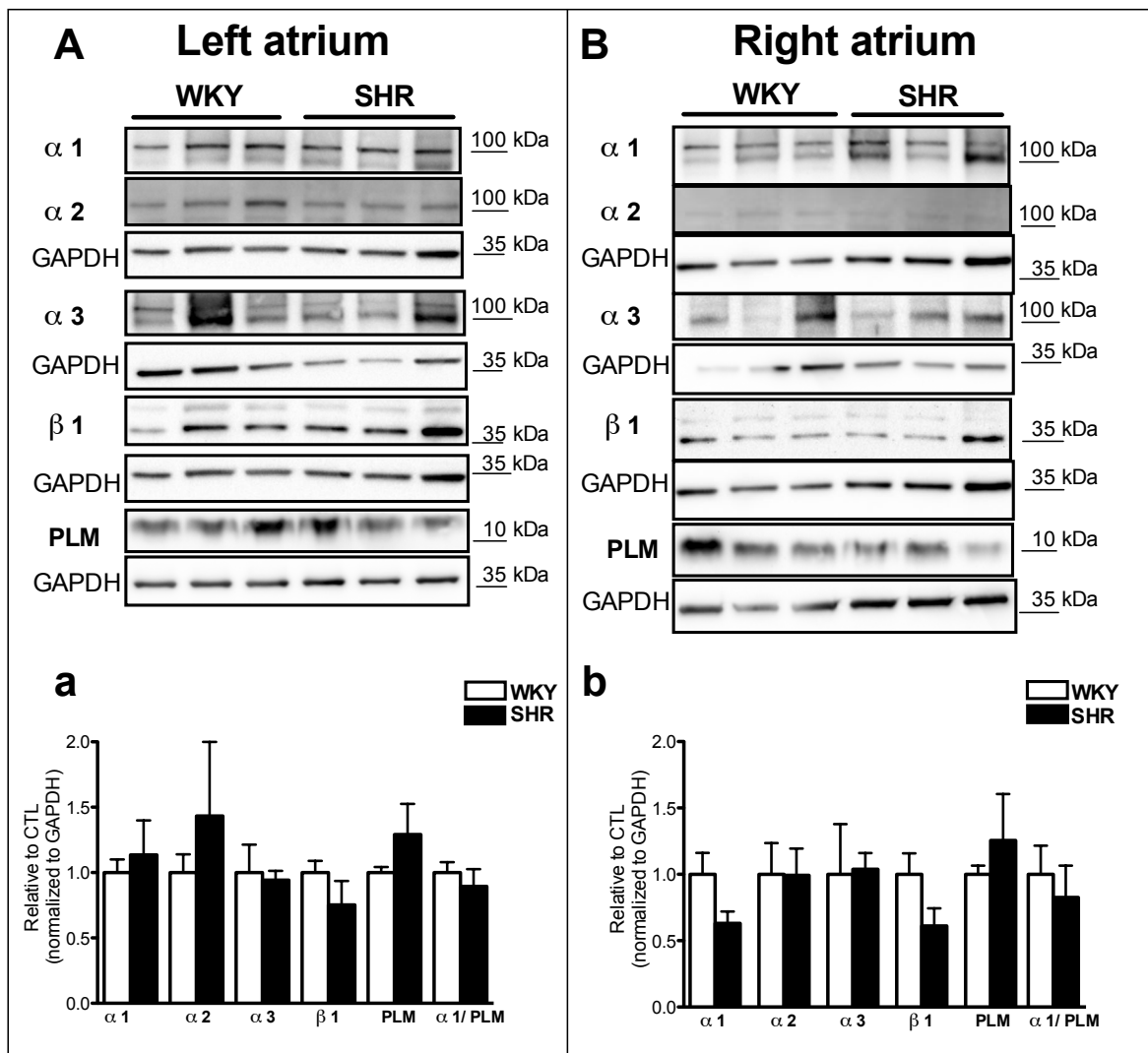


**Figure 22. Expression of Na<sup>+</sup> efflux proteins in left and right atrium from 3 months old rats**

**A, B:** Original western blots of Na<sup>+</sup>/K<sup>+</sup>-ATPase subunits and phospholemman in the left (A) and right (B) atrium from WKY and SHR rats. Note that GAPDH is identical for  $\alpha 1$ ,  $\alpha 2$ , and  $\beta 1$ , since they were stained on the same membrane. **a,b** – averaged data of Na<sup>+</sup> efflux protein expression in the left (a) and right (b) atrium, normalized to GAPDH. N=7 in each group. Data were analyzed by Student's unpaired t-test.

At the age of 7 months, expression of Na<sup>+</sup> influx transporters in the left atrium (Figure 23Aa) did not differ between WKY and SHR. Western blot analysis of Na<sup>+</sup> influx proteins in the right atrium also did not reveal any significant changes in the expression of Na<sup>+</sup>

import proteins (Figure 23 Bb). To conclude, at the age of 7 months, Na<sup>+</sup> influx was unaltered in SHR.

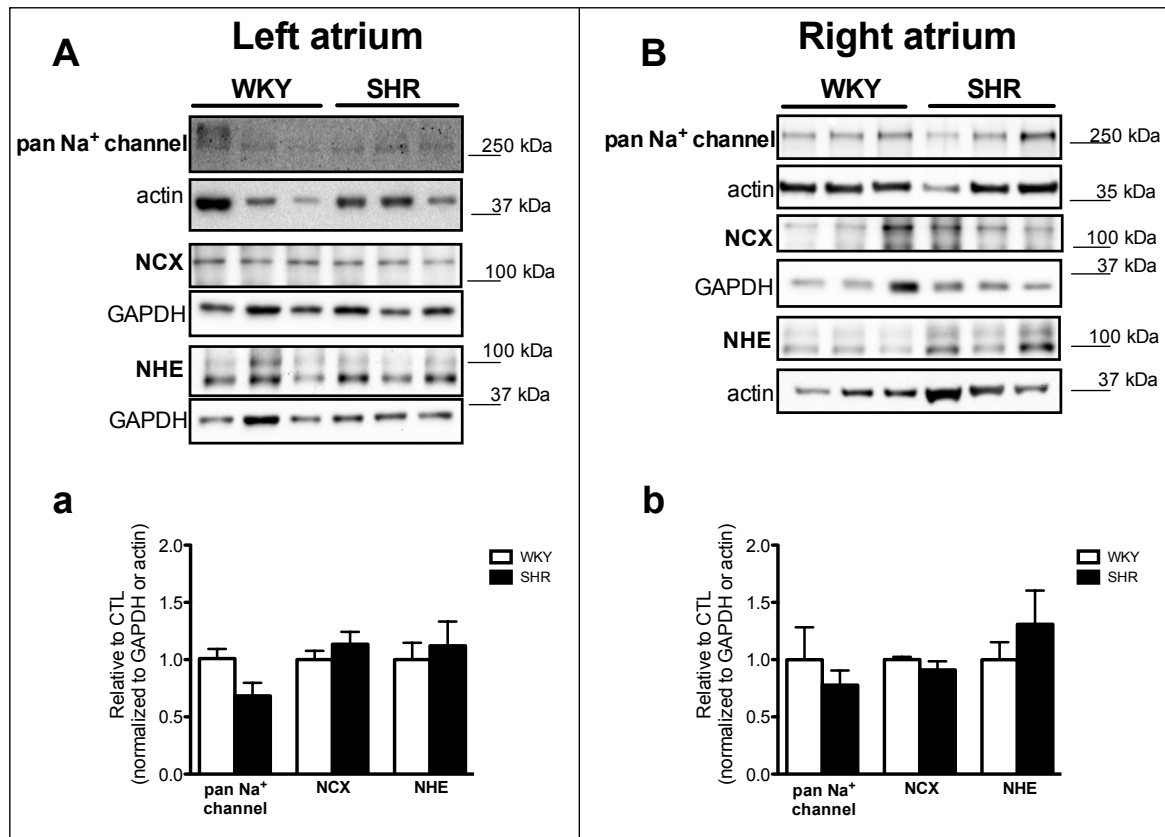


**Figure 23. Expression of Na<sup>+</sup> influx proteins in left and right atrium from 7 months old rats**

**A,B:** Original western blots of Na<sup>+</sup> influx proteins in left (A) and right (B) atria from WKY and SHR. **a,b:** averaged data of proteins expression in the left (a) and right (b) atrium, normalized to GAPDH or actin. N=7-9 in each group. Data were analyzed by Student's unpaired t-test.

Analysis of NKA expression revealed a significant decrease in the expression of the  $\alpha$  1 subunit in the left atrium of SHR compared to WKY (Figure 24Aa). Expression of other NKA subunits was unchanged in SHR. PLM expression and the  $\alpha$  1/PLM ratio were not different between WKY and SHR.

In the right atrium, we did not observe any major changes in the expression of different  $\alpha$  subunits of NKA (Figure 24Bb).  $\beta$  1 and PLM were almost equally expressed in the



right atrium of SHR compared to WKY. In addition to that,  $\alpha$  1/PLM ratio was not different between the strains.

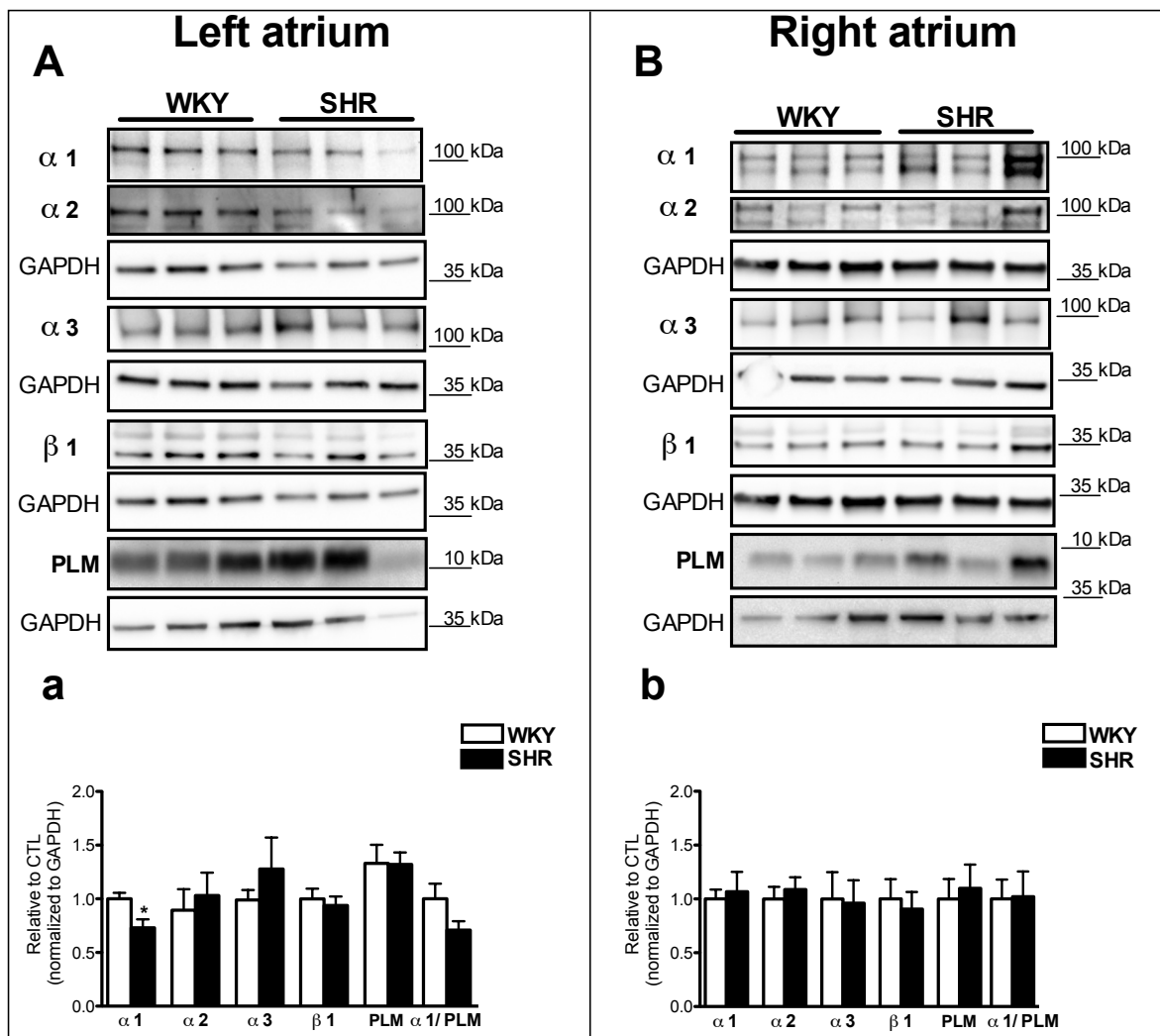


**Figure 24. Expression of Na<sup>+</sup> efflux proteins in left and right atrium from 7 months old rats**

**A, B:** Original western blots of Na<sup>+</sup> efflux proteins in the left (A) and right (B) atrium from WKY and SHR rats. Note that GAPDH is identical for  $\alpha$  1,  $\alpha$  2 and  $\beta$  1, since they were stained on the same membrane. **a,b:** averaged data on Na<sup>+</sup> influx protein expression in the left (a) and right (b) atrium, normalized to GAPDH. N=7-9 in each group \**p*< 0.05, Student's unpaired t-test.

Taken together, the presented results indicate that:

At the age of 3 months, SHR exhibited left ventricular hypertrophy and left and right atrial hypotrophy.  $[Na^+]_i$  was unchanged. Na<sup>+</sup> handling protein expression was unaltered

in the left atrium. In the right atrium, a significant increase in the expression of Na<sup>+</sup> channels and NCX was found.

At the age of 7 months, SHR exhibited a further increase in left ventricular hypertrophy. Left and right atrial hypertrophy was still present. Contractility of atrial myocytes and [Na<sup>+</sup>]<sub>i</sub> were unaltered. Expression of Na<sup>+</sup>-handling proteins was largely unchanged, except for a significant reduction in  $\alpha$  1 expression in the left atrium.

Thus, at the early hypertension stage, contractility and [Na<sup>+</sup>]<sub>i</sub> remained unaltered in atrial myocytes from SHR, despite occasional changes in the expression of Na<sup>+</sup>-handling proteins.

## **5.2. Characterization of atrial remodelling in advanced hypertension**

The majority of SHR rats, as mentioned earlier, develop signs of heart failure starting with 15-18 months of age (Chan et al. 2011). However, little is known about the factors causing the transition to heart failure, as well as about atrial remodelling processes accompanying this transition, especially in terms of contractility and Na<sup>+</sup> handling. Thus, the next step in this project was to characterize cardiovascular parameters, contractility, [Na<sup>+</sup>]<sub>i</sub>, and expression of key Na<sup>+</sup>-handling proteins in atria of old SHR and WKY.

### **5.2.1. Blood pressure and heart rate measurements; gravimetric assessment of hypertrophy**

For this part of the study, we used 15-23 months old animals. Blood pressure measurements revealed elevated systolic, diastolic, mean arterial pressure and heart rate values in SHR compared to WKY (Figure 25Aa-d).

Dr. Florentina-Cornelia Pluteanu performed gravimetric assessment of hypertrophy in our laboratory. SHR exhibited left and right ventricular hypertrophy (Figure 25Ba and b) together with left atrial hypertrophy (Figure 25Bc). Right atrial weight, however, was not different between SHR and WKY (Figure 25Bd). Lung weight in old SHR was significantly increased (Figure 25Be), indicating lung congestion and, thus, manifestation of heart failure.

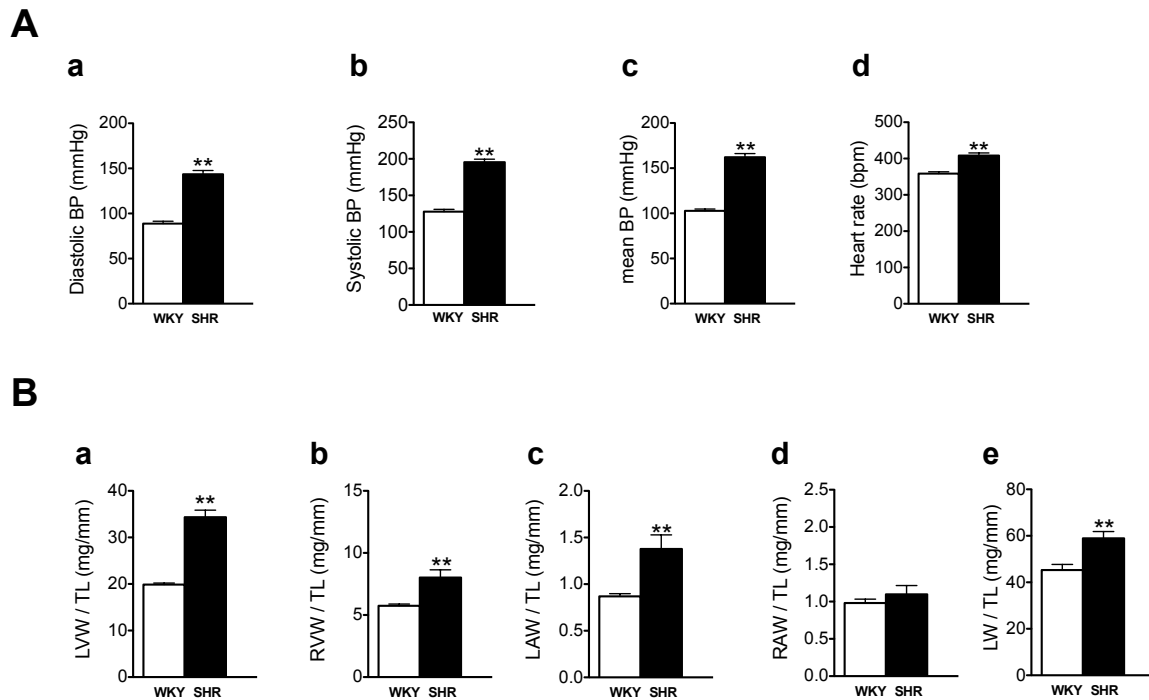


**Figure 25. Cardiovascular characteristics of 15-23 months old WKY and SHR**

**A:** Blood pressure parameters: **a**-diastolic blood pressure, **b**-systolic blood pressure, **c**-mean blood pressure, **d**-heart rate. N=number of animals: WKY: N=38, SHR: N=37 **B:** Gravimetric parameters normalized to tibia length (TL): **a**-left ventricular weight (LVW), **b**-right ventricular weight (RVW), **c**-left atrial weight (LAW), **d**-right atrial weight (RAW), **e**-lung weight (LW). WKY: N=17, SHR: N=18. \*\*p<0.01, Student's unpaired t-test

It should be noted, that many SHR developed difficulties breathing, weight loss and decreased activity. However, not all of the SHR developed these signs of heart failure. Therefore, SHR were subdivided into two groups based on the presence or absence of elevated lung weight. First, we calculated the mean value of lung weight, normalized to tibia length (LW/TL), in WKY. The resulting value was 50 mg/mm. SHR with LW/TL lower than this threshold were defined as the non-failing group (SHR-NF), whereas SHR with LW/TL equal to or higher than this value were defined as SHR with heart failure (SHR-HF). When non-failing SHR were compared with failing animals, we observed a small increase in diastolic blood pressure (Figure 26Aa) but no changes in systolic and mean blood pressure and heart rate (Figure 26Ab-d). Gravimetric assessment of hypertrophy revealed a significant increase in lung weight, right ventricular, right and left atrial mass in failing SHR, as shown in Figure 26Bb-e.

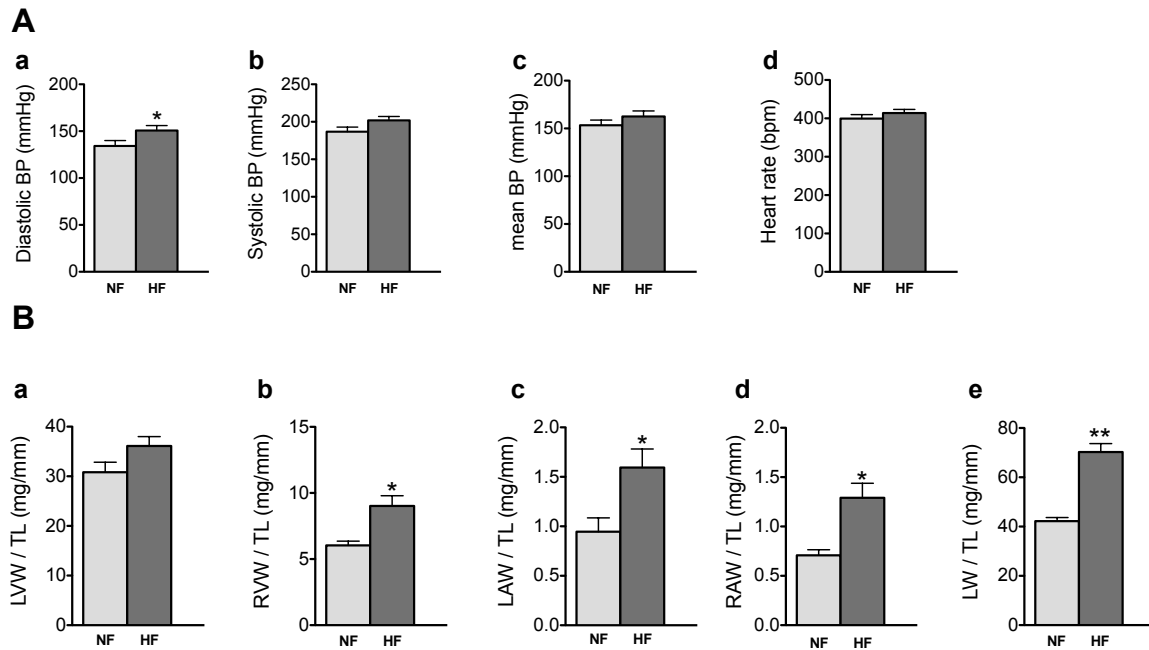


**Figure 26. Cardiovascular characteristics of SHR-NF and SHR-HF**

**A:** Blood pressure parameters: **a**-diastolic blood pressure, **b**-systolic blood pressure, **c**-mean blood pressure, **d**-heart rate. N=number of animals: SHR-NF: N=16, SHR-HF: N=21.

**B:** Gravimetric parameters normalized to tibia length (TL): **a**-left ventricular weight (LVW), **b**-right ventricular weight (RVW), **c**-left atrial weight (LAW), **d**-right atrial weight (RAW), **e**-lung weight (LW). SHR-NF: N=6, SHR-HF N=12. \* $p < 0.05$ , \*\* $p < 0.01$ , Student's unpaired t-test.

Taken together, these data indicate that old SHR developed the whole heart hypertrophy and some of them signs of heart failure between 15 and 23 months of age. Furthermore, right and left atrial hypertrophy, as well as right ventricular hypertrophy accompanied transition from compensated left ventricular hypertrophy to heart failure.

### 5.2.2. Contractility measurements

The next aim was to characterize contractility of atrial myocytes from WKY, non-failing SHR (SHR-NF) and failing rats (SHR-HF). Data are given in Figure 27.

Original contractility traces of atrial myocytes from WKY, SHR-NF and SHR-HF, are presented in Figure 27A. Figure 27B compares contractile properties of WKY and SHR. Diastolic sarcomere length was almost equal in WKY and SHR (Figure 27Ba). SHR exhibited a significant decrease in fractional shortening:  $8.9 \pm 0.5\%$  in WKY vs.  $5.8 \pm 0.5\%$

in SHR, as can be seen from Figure 27Bb. Kinetic parameters of contraction were unchanged in atrial myocytes from SHR (Figure 27Bc-e).

Figure 27C illustrates comparison of contractile parameters between SHR-NF and SHR-HF. During the transition from compensated left ventricular hypertrophy to heart failure diastolic sarcomere length remained unchanged (Figure 27Ca). Interestingly, we observed a significant reduction of fractional shortening:  $7.4 \pm 1\%$  in SHR-NF and  $5.1 \pm 0.6\%$  in SHR-HF, as shown in Figure 27Cb. None of the kinetic parameters were significantly different between SHR-NF and SHR-HF (Figure 27Cc-e).

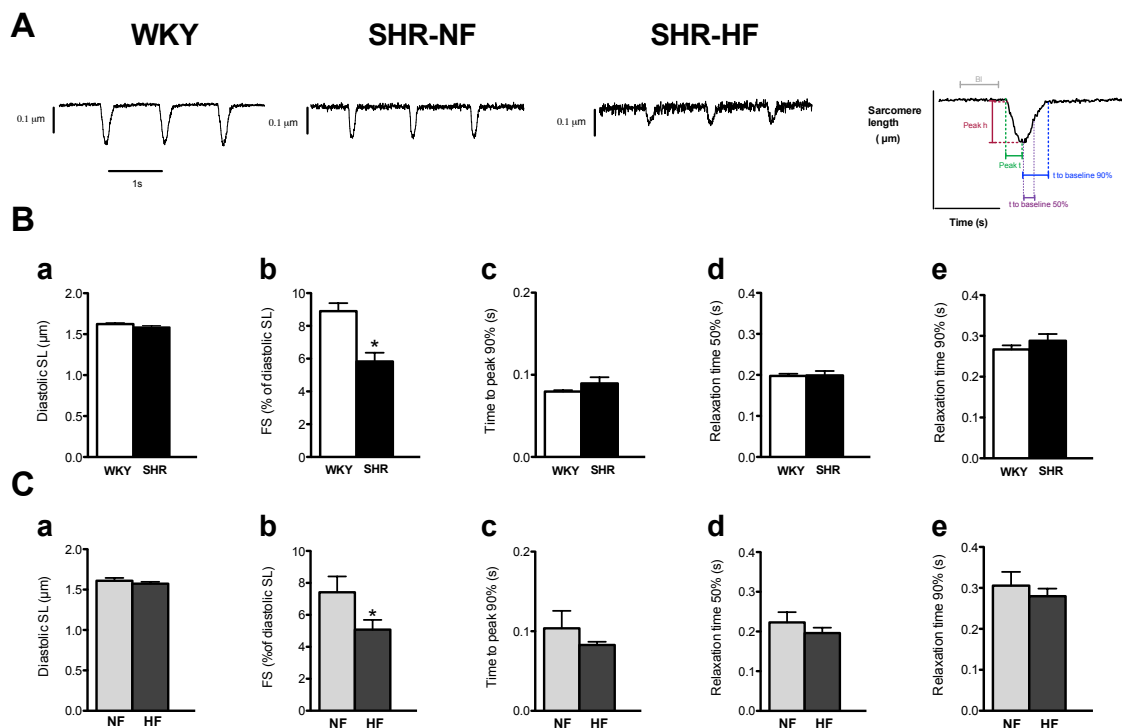


**Figure 27 Sarcomere length (SL) shortening in atrial myocytes from WKY, SHR-NF and SHR-HF**

**A:** Original SL shortening traces of electrically stimulated atrial myocytes from WKY, SHR-NF and SHR-HF. **B (a-e):** Average values of SL parameters in atrial myocytes from WKY (n/N=101/16) and SHR (n/N=50/16); **a**-diastolic SL, **b**-fractional shortening (FS), **c**-time to peak (90%), **d**-time to 50% of relaxation, **e**-time to 90% of relaxation. **C (a-e):** Comparison of the same SL shortening parameters between SHR-NF (n/N=16/5) and SHR-HF (n/N=34/11).

\*  $p < 0.05$ , Student's unpaired t-test.

Thus, atrial myocytes from SHR displayed a significant reduction in contractility compared to WKY. During the transition from compensated left ventricular hypertrophy to heart failure there was a further reduction in the contractile function.

We also compared contractile properties of left and right atrial myocytes in WKY and SHR to take into consideration possible differences between left and right atrial myocytes. Data are presented in Figure 28. Left and right atrial myocytes from WKY revealed very similar values for all of the contractile parameters analyzed, as evident from Figure 28Aa-e. When we performed comparison between left and right atrial myocytes in SHR, similar diastolic sarcomere length and fractional shortening were observed (Figure 28Ba and b, respectively). Interestingly, we found a significant reduction in time to peak 90% (Figure 28Bc) and relaxation time 50% (Figure 28Bd), suggesting faster kinetic of contraction and relaxation in right atrial myocytes in SHR. Relaxation time 90% was, however, not significantly different (Figure 28Be).

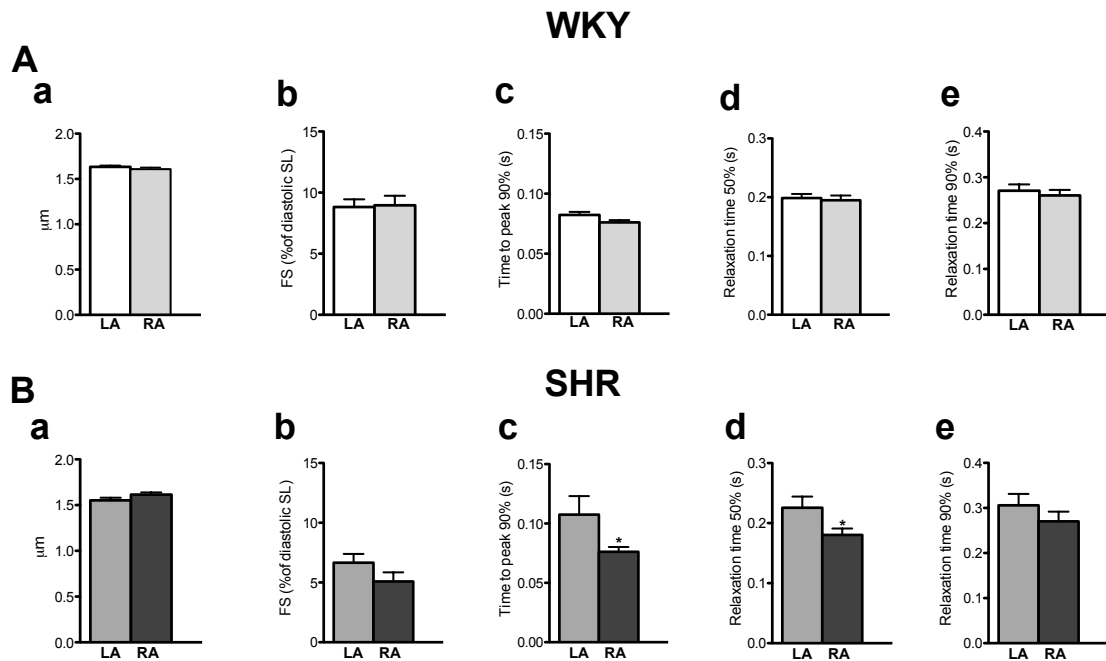


**Figure 28. Comparison of left and right atrial myocyte contractility in 15-23 months old WKY and SHR**

**A:** Analyzed contractility parameters of WKY left (LA) and right (RA) atrial myocytes: **a**-diastolic sarcomere length, **b**-fractional shortening, **c**-time to peak 90%, **d**-time to baseline (relaxation time) 50%, **e**-time to baseline (relaxation time) 90%. **B: (a-e)** same contractility parameters for SHR left (LA) and right (RA) atrial myocytes. n/N=number of cells/number of animals: WKY rats: 48/11 and 52/13 for left and right atrial myocytes, respectively. SHR: 22/8 and 28/11 for left and right atrial myocytes, respectively. \*  $p < 0.05$ , Student's unpaired t-test

Figure 29 presents comparison of contractility between left and right atrial myocytes from SHR-NF (A) and SHR-HF (B). Left and right atrial myocytes from SHR-NF exhibited similar diastolic sarcomere length (Figure 29Aa). Fractional shortening was also not significantly different between left and right atrial myocytes (Figure 29 Ab). Kinetic parameters of left and right atrial myocytes were not markedly different (Figure 29 Ace).

Diastolic sarcomere length of left and right atrial myocytes from failing SHR was almost equal, as can be estimated from Figure 29Ba. Fractional shortening and kinetic parameters of contraction were also not significantly different between left and right atrial myocytes (Figure 29Bb-e).



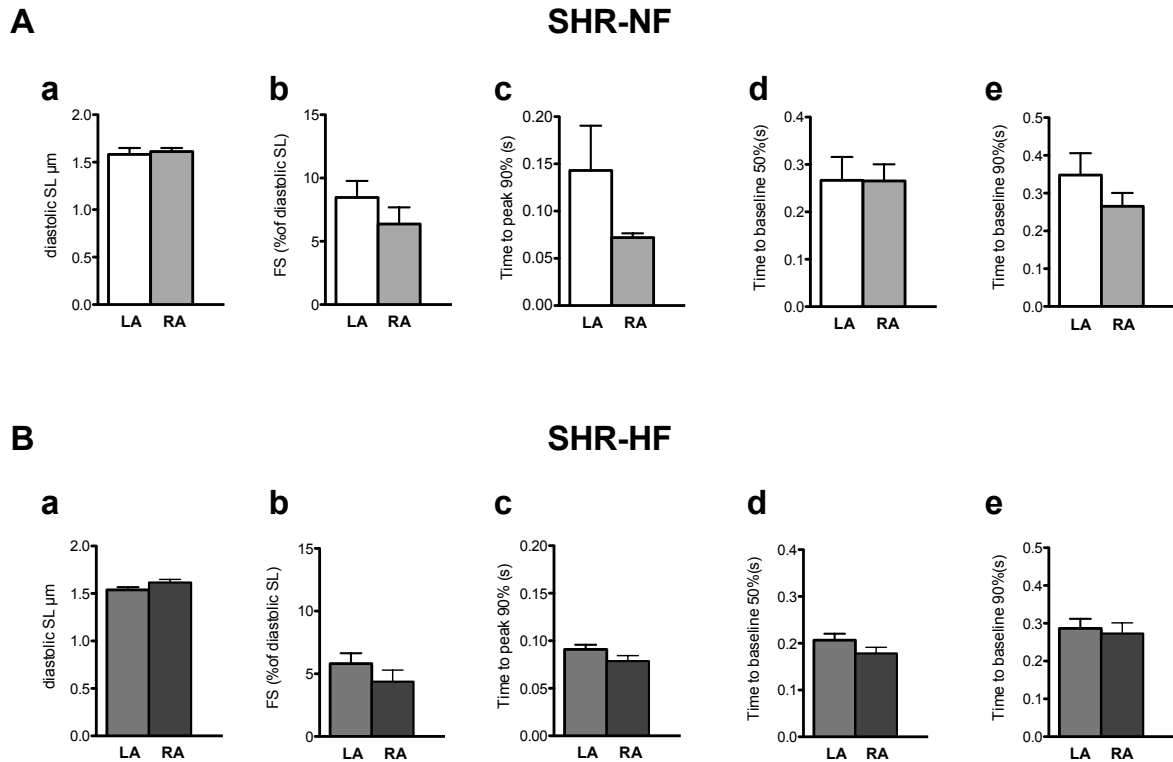


**Figure 29. Comparison of left and right atrial myocyte contractility in SHR-NF and SHR-HF**

**A:** Analyzed contractility parameters for left (LA) and right (RA) atrial myocytes from SHR-NF: **a**-diastolic sarcomere length, **b**-fractional shortening, **c**-time to peak 90%, **d**-time to baseline (relaxation time) 50%, **e**-time to baseline (relaxation time) 90%. **B: (a-e)** same contractility parameters for left (LA) and right (RA) atrial myocytes from SHR-HF (HF). n/N=number of cells from left (LA) or right (RA) atrium/number of animals: SHR-NF: 7/3 (LA) and 10/3 (RA); for SHR-heart failure: 15/5 (LA) and 18/6 (RA). Data were analyzed by Student's unpaired t-test

Thus, there were no significant differences in the contractile parameters between left and right atrial myocytes in WKY or SHR.

We were also interested in the contractility of ventricular myocytes. Data are given in Figure 30. Representative contractility traces of ventricular myocytes from WKY, non-failing and failing SHR are presented in panel A. Comparison between WKY and SHR is illustrated in panel B. Diastolic sarcomere length and fractional shortening of ventricular myocytes were very similar between old WKY ( $11.6 \pm 0.5\%$ ) and SHR ( $12.2 \pm 0.4\%$ ), as can be seen in Figure 30Ba and b. Kinetics of contraction were also unaffected in ventricular myocytes from SHR, as can be seen from Figure 30B(c-e).

Figure 30C illustrates comparison of the contractile parameters between ventricular myocytes from non-failing and failing SHR. During the transition from compensated left ventricular hypertrophy to heart failure ventricular myocytes from non-failing and failing SHR exhibited similar diastolic sarcomere length (Figure 30Ca). Fractional shortening was also unaffected:  $12.4 \pm 0.1\%$  in SHR-NF vs.  $12.1 \pm 0.5\%$  in SHR-HF, as can be estimated from Figure 30Cb. Time to peak 90% was not significantly different between SHR-NF and SHR-HF (Figure 30Cc). However, ventricular myocytes from failing SHR exhibited slight but significant prolongation of the relaxation time 50% ( $0.32 \pm 0.01$  s in SHR-NF vs.  $0.37 \pm 0.01$  s in SHR-HF) and 90% ( $0.39 \pm 0.02$  s in SHR-NF vs.  $0.43 \pm 0.01$  s in SHR-HF), as evident from Figure 30Cd and e, respectively.

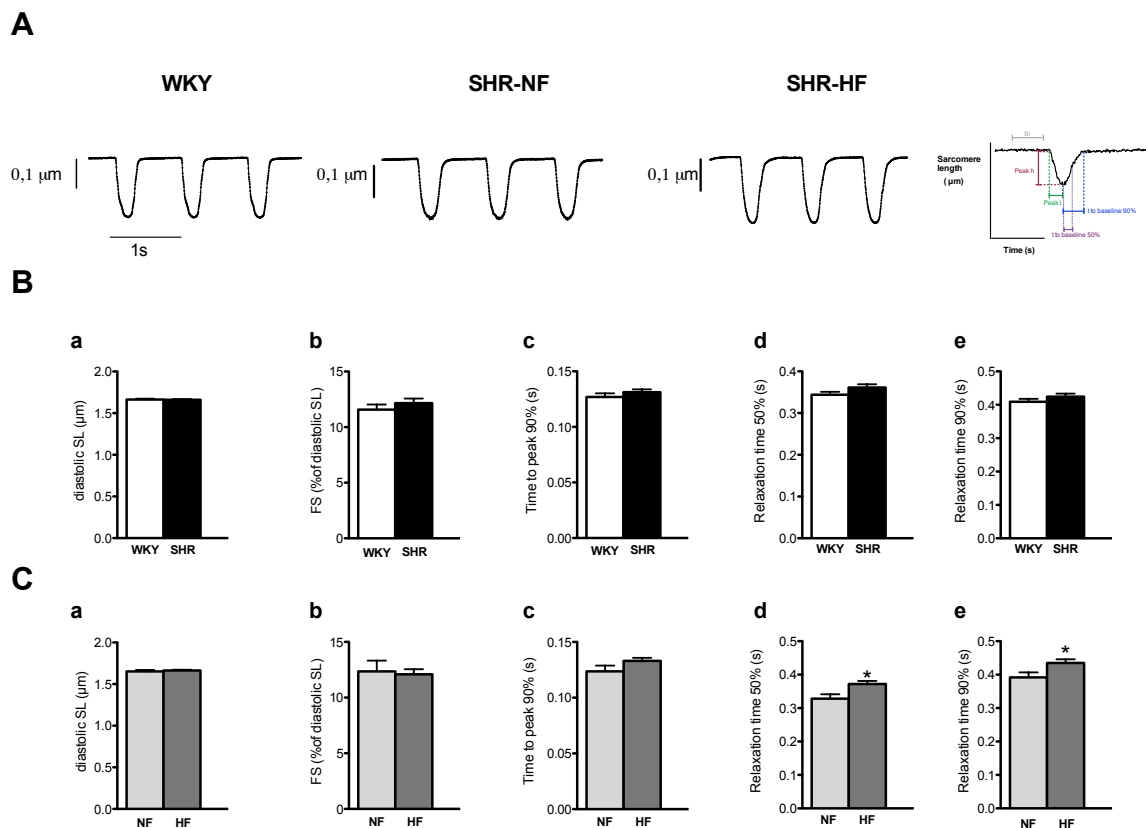


**Figure 30. Sarcomere length (SL) shortening in ventricular myocytes from WKY, SHR-NF and SHR-HF**

**A:** Original SL shortening traces of electrically stimulated ventricular myocytes from WKY, SHR-NF and SHR-HF **B:** Average values of SL parameters in ventricular myocytes from WKY (n/N=71/12) and SHR (n/N=87/15); from left to right: diastolic SL, fractional shortening (FS), time-to-peak (90%) shortening, and time to 50% and 90%, respectively, of relaxation. **C:** Comparison of the same SL shortening parameters between SHR-NF (n/N=20/4) and SHR-HF (n/N=63/11). \*  $p < 0.05$ , Student's unpaired t-test.

To conclude, atrial myocytes from old SHR exhibited significant reduction in contractility when compared to WKY and further impairment in the contractile function during the transition to heart failure. In contrast to these observations, contractile function of ventricular myocytes from SHR was not affected. Moreover, during the transition from compensated left ventricular hypertrophy to heart failure the fractional

shortening of ventricular myocytes remained unchanged, indicating that atria undergo specific remodelling of the contractile function.

### 5.2.3. Intracellular Na<sup>+</sup> measurements

Measurements of [Na<sup>+</sup>]<sub>i</sub> in atrial myocytes from old WKY and SHR are presented in Figure 31. Figure 31A shows a recording from an SHR-HF left atrial myocyte and calibration of the fluorescent signal (a). Panel b presents the calibration curve derived from the recording in panel a. Figure 31B, left panel, compares [Na<sup>+</sup>]<sub>i</sub> between old WKY and SHR at 1 Hz stimulation and at the resting conditions (Figure 31C, left panel). We observed a significant reduction in [Na<sup>+</sup>]<sub>i</sub> in atrial myocytes from SHR at 1 Hz stimulation (13.5±1.2 mM in WKY vs. 10.7±0.7 mM in SHR) and at the resting conditions (10.0±0.7 mM in WKY vs. 8.0±0.6 mM in SHR).

During the transition from compensated left ventricular hypertrophy to heart failure, no further changes in [Na<sup>+</sup>]<sub>i</sub> were found (Figure 31B and C, right panels). Stimulation-dependent change in [Na<sup>+</sup>]<sub>i</sub> was not significantly different between WKY and SHR (Figure 31D, left panel), as well as between non-failing and failing animals (Figure 31D, right panel).

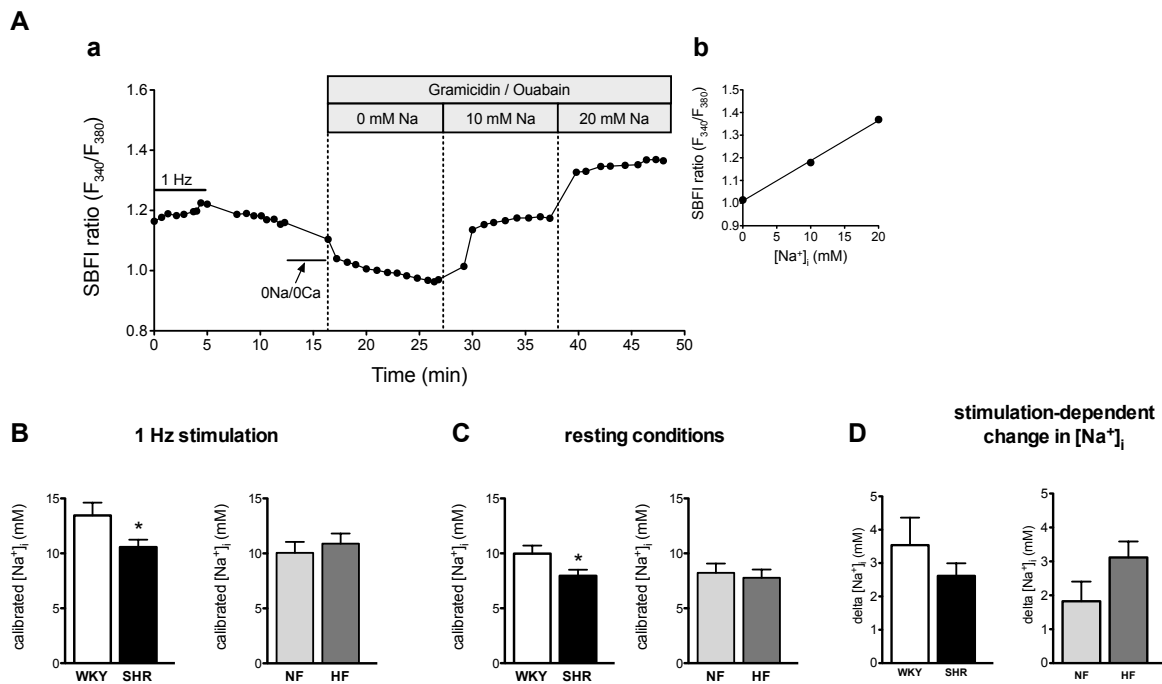


**Figure 31. [Na<sup>+</sup>]<sub>i</sub> in atrial myocytes from WKY, SHR-NF and SHR-HF**

Recording (**Aa**) and calibration of SBFI fluorescence in an SHR-HF left atrial myocyte. Cell was stimulated at 1 Hz. Stimulation was switched off and Na<sup>+</sup>- and Ca<sup>2+</sup>-free (0Na<sup>+</sup>/0Ca<sup>2+</sup>) solution was applied, before exposure to calibration solutions containing gramicidin and ouabain. (**Ab**) SBFI calibration curve derived from recording in (**Aa**). Average values of [Na<sup>+</sup>]<sub>i</sub> at 1 Hz stimulation (**B**) and under resting conditions (**C**). **D**: delta [Na<sup>+</sup>]<sub>i</sub> ([Na<sup>+</sup>]<sub>i</sub> at 1Hz – resting [Na<sup>+</sup>]<sub>i</sub>). For comparison between WKY and SHR: n/N=29/15, n/N=31/17, respectively (presented in left panels). For comparison between SHR-NF: n/N=12/6 and SHR-HF: n/N=19/11 (shown in right panels). \*p<0.05, Student's unpaired t-test.

[Na<sup>+</sup>]<sub>i</sub> did not differ between left and right atrial myocytes neither in WKY nor in SHR, as shown in Figure 32A and B, respectively. Comparison of [Na<sup>+</sup>]<sub>i</sub> between left and right atrial myocytes from non-failing SHR revealed no significant changes (Figure 32C). Left and right atrial myocytes from failing SHR also exhibited similar [Na<sup>+</sup>]<sub>i</sub>, as shown in Figure 32D.

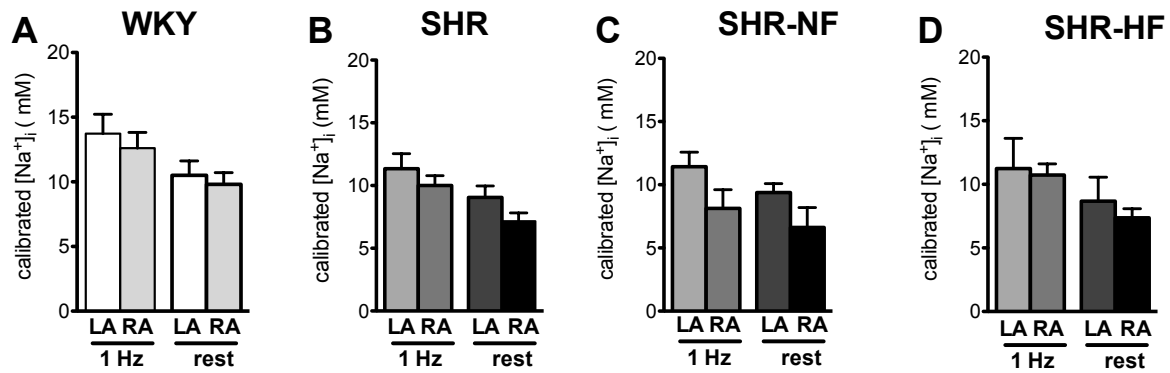


**Figure 32. Comparison of intracellular  $Na^+$  concentration between left and right atrial myocytes in WKY, SHR-NF and SHR-HF rats**

**A:** Average  $[Na^+]_i$  in left (LA) and right (RA) atrial myocytes in WKY rats under 1 Hz stimulation (1Hz) and resting conditions (rest). **B:** Average  $[Na^+]_i$  in left (LA) and right (RA) atrial myocytes in SHR rats under 1 Hz stimulation (1Hz) and resting conditions (rest). **C:** Average  $[Na^+]_i$  in left (LA) and right (RA) atrial myocytes in SHR-NF rats under 1 Hz stimulation (1Hz) and resting conditions (rest). **D:** Average  $[Na^+]_i$  in left (LA) and right (RA) atrial myocytes in SHR-HF rats under 1 Hz stimulation (1Hz) and resting conditions (rest). n/N=number of cells/number of animals: WKY rats: 22/12 and 7/5 for left and right atrial myocytes, respectively. SHR rats: 13/6 and 18/12 for left and right atrial myocytes, respectively. SHR-NF: 7/3 and 5/3 for left and right atrial myocytes, respectively. SHR-HF: 6/3 and 13/9 for left and right atrial myocytes, respectively. Data were analyzed by Student's unpaired t-test.

Thus, SHR atrial myocytes exhibited a significant decrease in  $[Na^+]_i$  compared to WKY. Previous studies indicate elevated  $[Na^+]_i$  in ventricular myocytes in human heart failure and various animal models of heart failure (Despa & Bers 2013). Thus, we also performed measurements of  $[Na^+]_i$  in ventricular myocytes from old SHR and WKY. As can be seen from Figure 33A and B, left panels, no significant changes in  $[Na^+]_i$  neither at 1 Hz stimulation nor under resting conditions were observed between the two rat strains. In addition to that, comparison of ventricular myocytes from SHR-NF and SHR-HF also did not reveal any changes in  $[Na^+]_i$  (Figure 33A and B, right panels). Stimulation-dependent change in  $[Na^+]_i$  was similar between WKY and SHR ventricular myocytes (Figure 33C, left panel). However, we observed a significant reduction in delta  $[Na^+]_i$  when ventricular myocytes from SHR-NF were compared to SHR-HF (Figure 33C, right panel).

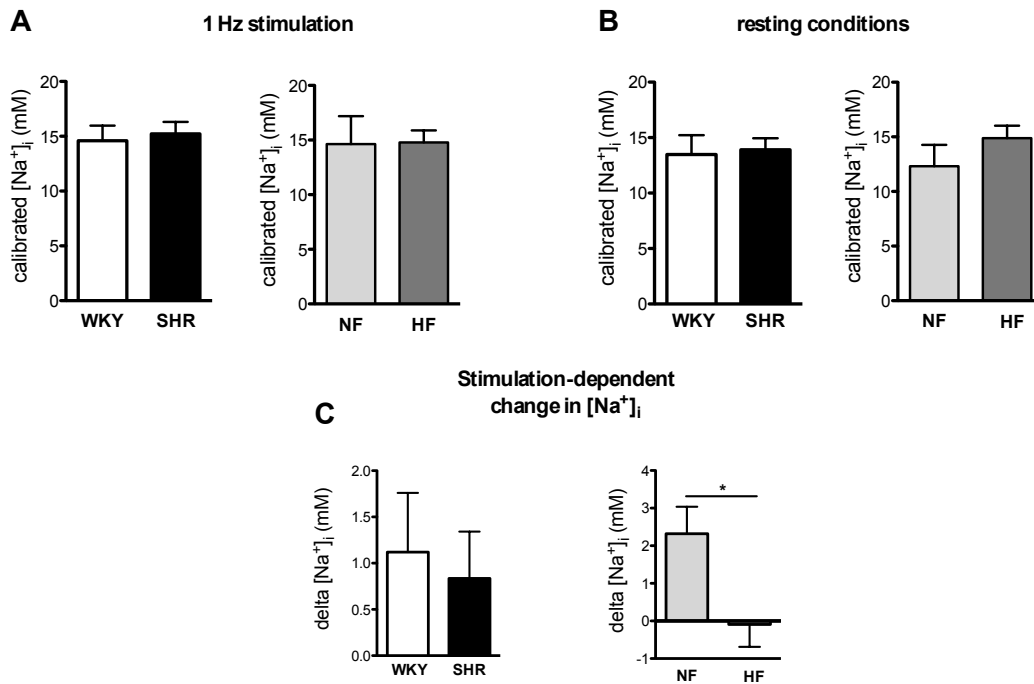


**Figure 33.  $[Na^+]_i$  in ventricular myocytes from WKY, SHR-NF and SHR-HF**

Average values of  $[Na^+]_i$  at 1 Hz stimulation (A) and under resting conditions (B). C: delta  $[Na^+]_i$  ( $[Na^+]_i$  at 1Hz – resting  $[Na^+]_i$ ). For comparison between WKY (n/N=9/8) and SHR (n/N=27/15) (left panels) and comparison between SHR-NF (n/N=10/6) and SHR-HF (n/N=17/9) (right panels), data were analyzed by Student's unpaired t-test, \* $p < 0.05$ .

Thus, the  $Na^+$  remodelling processes in the atrial myocytes from old SHR were not reflected in ventricular myocytes from the same animals, suggesting atria-specific ionic remodelling in hypertensive heart disease.

#### 5.2.4. Expression of $Na^+$ -handling proteins

To find the possible explanation for the decrease in  $[Na^+]_i$  in the atria, we performed western blot analysis of key  $Na^+$ -handling proteins.

In the left atria expression of  $Na^+$  channels and NCX was not different between WKY and SHR, whereas NHE expression was significantly increased in SHR (Figure 34a). During the transition from non-failing stage to heart failure no further changes in expression of  $Na^+$ -influx proteins in the left atrium were observed (Figure 34b).

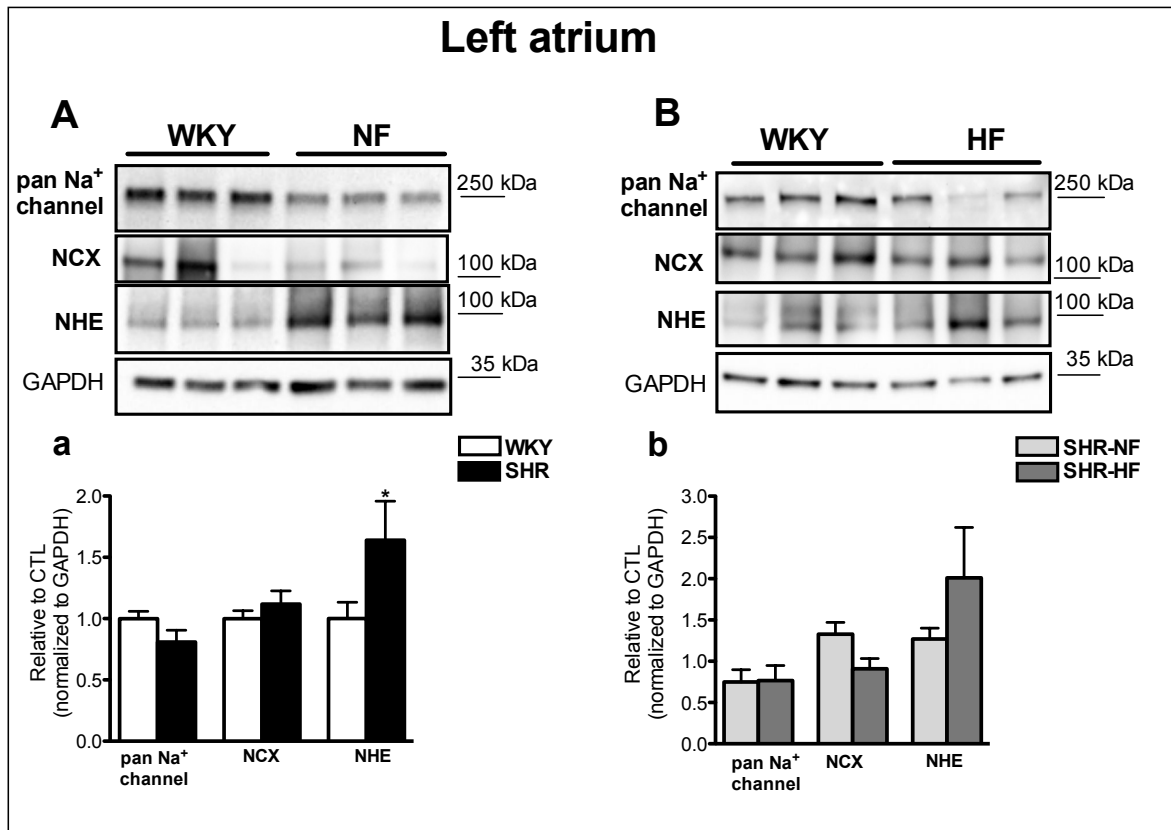


**Figure 34. Na<sup>+</sup> influx protein expression in left atrium from WKY, SHR-NF and SHR-HF**

**A,B:** Original immunoblots of pan Na<sup>+</sup>-channel, NCX and NHE in left atria from WKY, SHR-NF and SHR-HF. **(A-a)** Average values of protein expression in WKY (N=17) and SHR (N=14). **(B-b)** Same values for SHR-NF and SHR-HF (N=7 for each group). Expression was normalized to GAPDH. Note that GAPDH is identical for pan Na<sup>+</sup> channel, NCX and NHE, since they were stained on the same membrane. \* p<0.05, Student's unpaired t-test.

In the right atrium, Na<sup>+</sup> channels expression was not different between WKY and SHR. NCX and NHE expression was significantly higher in SHR (Figure 35a). Similarly to the left atrium, during the transition to heart failure no changes in the expression of Na<sup>+</sup> import proteins were present.



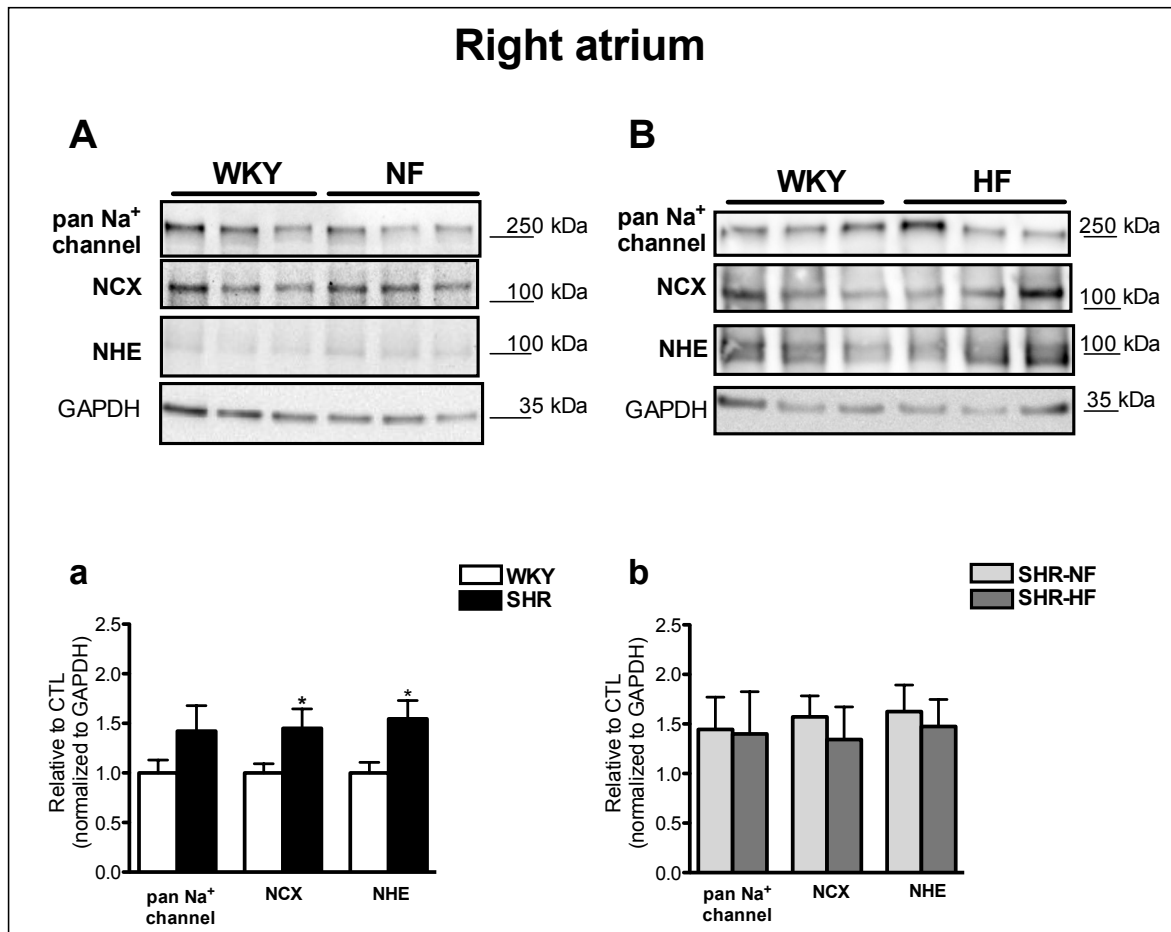


**Figure 35. Na<sup>+</sup> influx protein expression in right atrium from WKY, SHR-NF and SHR-HF**

**A, B:** Original immunoblots of Na<sup>+</sup> influx proteins in right atria from WKY, SHR-NF and SHR-HF. **(a)** Average values of protein expression in WKY (N=15) and SHR (N=12-13). **(b)** Same values for SHR-NF (N=6) and SHR-HF (N=6-7). Expression was normalized to GAPDH. Note that GAPDH is identical for pan Na<sup>+</sup> channel, NCX and NHE, since they were stained on the same membrane.

\* p<0.05, Student's unpaired t-test

Thus, we observed a significant increase in the expression of some Na<sup>+</sup> influx proteins in SHR when compared to WKY.

Western blot analysis of different NKA subunits revealed an increase in  $\alpha$  1 subunit expression in the left atrium, as indicated in Figure 36a. Expression of the  $\alpha$  2 and  $\alpha$  3 isoforms was not different between WKY and SHR. Expression of the  $\beta$  1 subunit of NKA and PLM were similar. The  $\alpha$  1/PLM ratio was markedly increased in SHR, suggesting higher NKA activity in SHR left atrium, compared to WKY.

During the transition from compensated left ventricular hypertrophy to heart failure (Figure 36b) no changes in the expression of the  $\alpha$  1 subunit was found, though, surprisingly,  $\alpha$  2 subunit expression was significantly reduced in failing SHR.  $\alpha$  3,  $\beta$  1 subunit and PLM expression were not significantly changed.

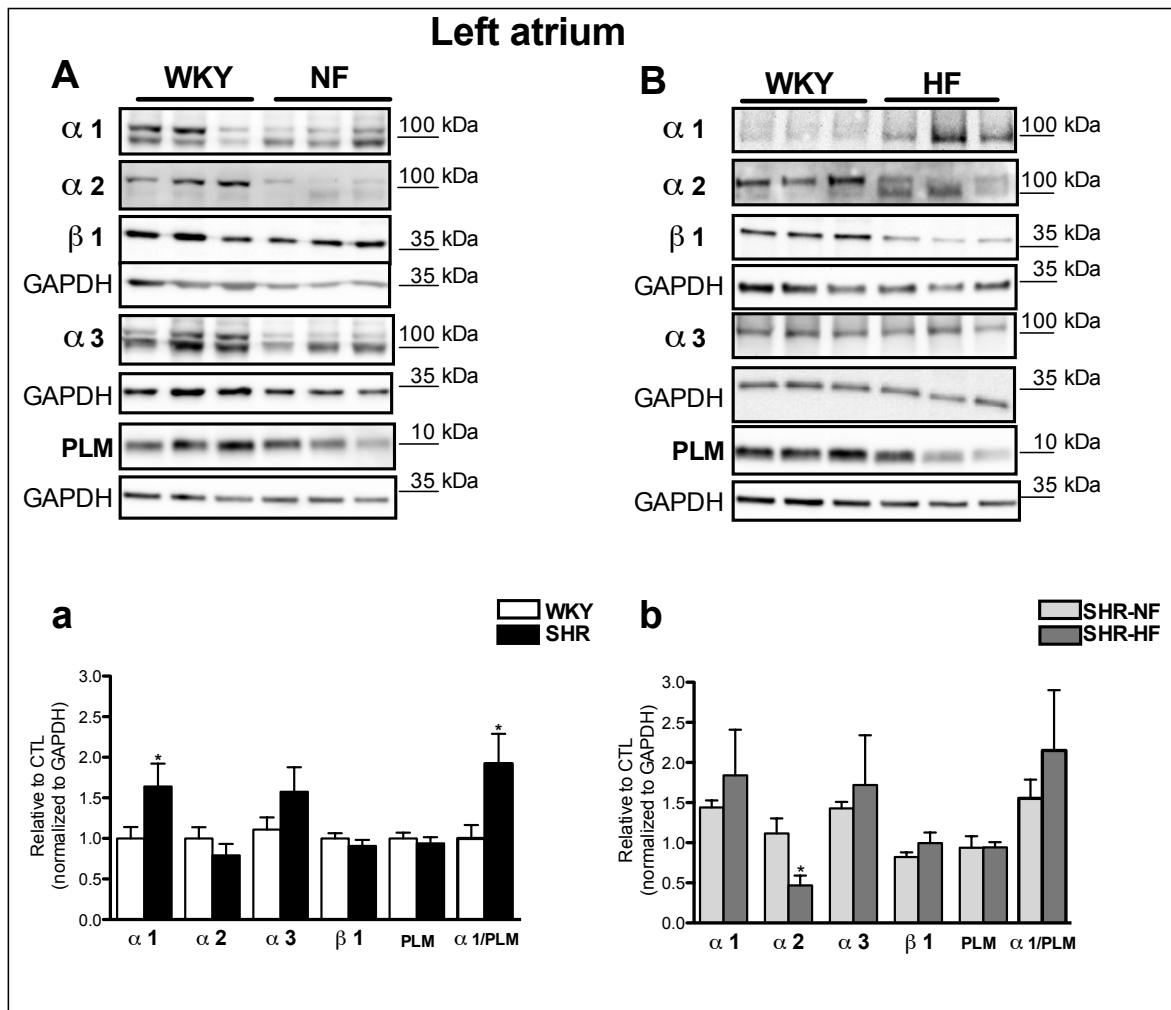


**Figure 36. Na<sup>+</sup> efflux protein expression in left atrium from WKY, SHR-NF and SHR-heart failure**

**A,B:** Original western blots of different Na<sup>+</sup>/K<sup>+</sup>-ATPase subunits and phospholemman in left atria from WKY, SHR-NF and SHR-HF. **(a)** Average values of protein expression in WKY (N=16) and SHR (N=14). **(b)** Same values for SHR-NF and SHR-HF. N=7 in each group. GAPDH served as a loading control. Note that GAPDH is identical for  $\alpha$  1,  $\alpha$  2 and  $\beta$  1, since they were stained on the same membrane \* p<0.05, Student's unpaired t-test

In the right atrium, similar changes in the expression of NKA subunits were observed (Figure 37a). Expression of  $\alpha$  1 and  $\alpha$  2 subunits was significantly increased in SHR. Expression of the  $\alpha$  3 isoform and the  $\beta$  1 subunit was unaltered. PLM expression was slightly but significantly lower, whereas the  $\alpha$  1/PLM ratio was remarkably higher in SHR, indicating a possible increase in NKA function in atrium from old SHR.

$\alpha$  1 subunit expression was not altered during the progression of the disease (Figure 37b), however,  $\alpha$  2 expression was markedly increased in failing SHR. No further changes in the expression of NKA subunits or PLM were found during the transition from compensated left ventricular hypertrophy to heart failure.

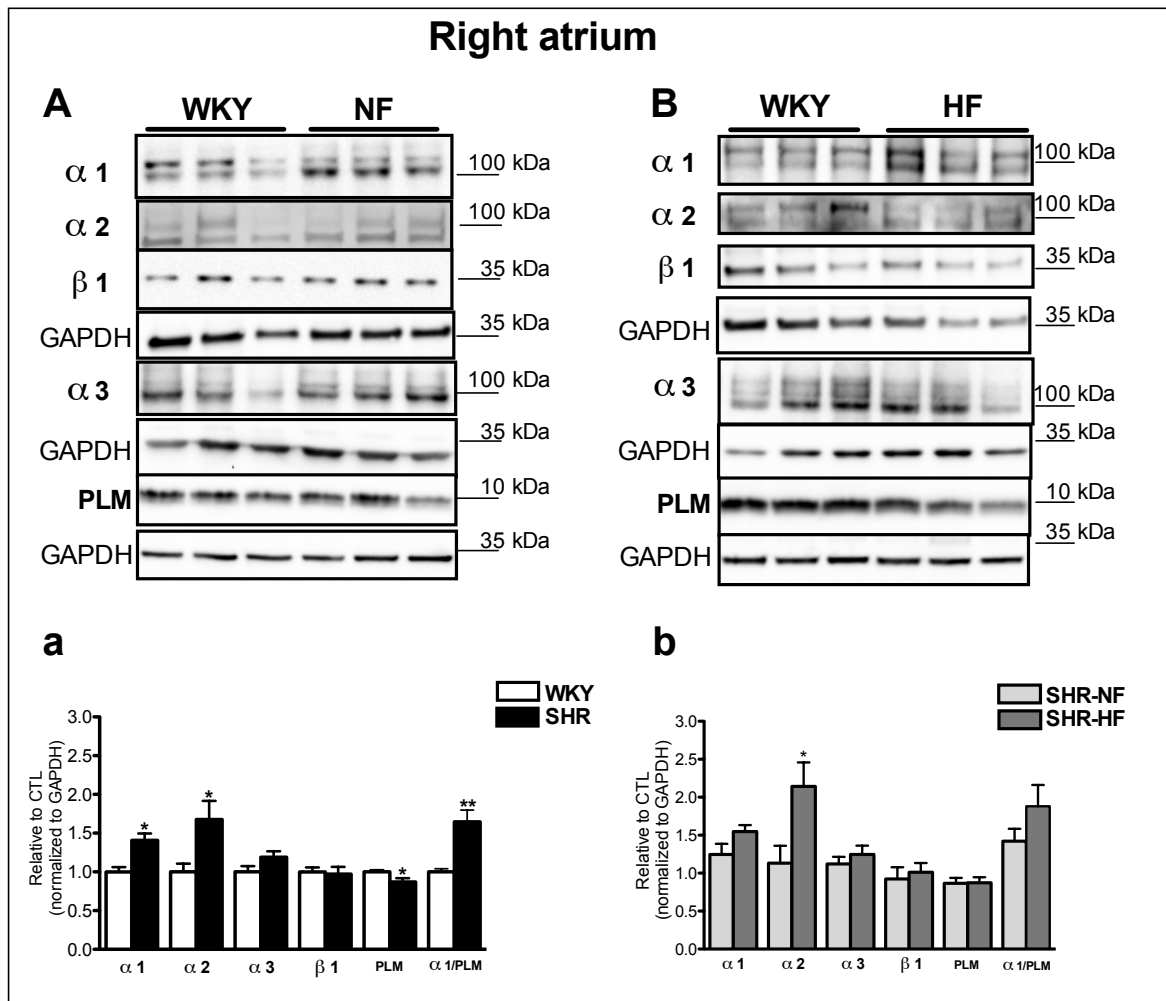


**Figure 37.  $\text{Na}^+$  efflux protein expression in right atrium from WKY, SHR-NF and SHR-HF**

**A,B:** Original western blots of different  $\text{Na}^+/\text{K}^+$ -ATPase subunits and phospholemman in right atria from WKY, SHR-NF and SHR-HF. **(a)** Average data of protein expression in WKY (N=15) and SHR (N=13). **(b)** Same values for SHR-NF (N=6) and SHR-HF (N=7). GAPDH served as a loading control. Note that GAPDH is identical for  $\alpha$  1,  $\alpha$  2 and  $\beta$  1, since they were stained on the same membrane. \*  $p < 0.05$ , Student's unpaired t-test.

Taken together, western blot data indicate an increase in the expression and, possibly, function of NKA and, thus, increased  $\text{Na}^+$  efflux. In addition, there might be a change in the expression of different  $\alpha$  subunits in atria of SHR during the transition from compensated left ventricular hypertrophy to heart failure.

To conclude, the following changes in the atria of SHR at the late stage of hypertensive heart disease were found:

- Left atrial hypertrophy
- Decline in the contractile function of atrial myocytes
- Decrease in  $[Na^+]_i$  in atrial myocytes
- Increase in the expression of NKA.
- Increase in the expression of NHE.

Transition from compensated left ventricular hypertrophy to heart failure in the atria of old SHR was associated with:

- Further increase in atrial hypertrophy
- Further reduction of the contractile function of atrial myocytes
- Unchanged  $[Na^+]_i$  in atrial myocytes
- Transition in the expression of different  $\alpha$  subunits of NKA.

### **5.3. Expression of Na<sup>+</sup>-handling proteins in human atrial fibrillation**

Atrial fibrillation is the most common arrhythmia in clinical practice and hypertension represents the most prevalent risk factor for atrial fibrillation (Andrade et al. 2014). Body of evidence indicates that atrial remodelling causes the development of this arrhythmic disorder and vice versa: atrial fibrillation induces atrial remodelling (“AF begets AF”) (Schotten et al. 2011). Data on Na<sup>+</sup> homeostasis and its role in atrial remodelling are limited. Thus, our next aim was to investigate the expression of major Na<sup>+</sup>-handling proteins in right atria from patients with sinus rhythm (SR), patients suffering from paroxysmal (pAF) and chronic atrial fibrillation (cAF). This project was done in collaboration with Prof. Dr. med. Dr. h.c. Ursula Ravens, Technical University of Dresden, who provided the right atrial tissue samples.

#### **5.3.1. Patient characteristics**

Patient groups characteristics are given in Table 31. For each group: sinus rhythm (SR), paroxysmal atrial fibrillation (pAF) and chronic atrial fibrillation (cAF), 6 samples were provided. All patients were male with an average age of ≈70 years. The indication for cardiac surgery for most of the SR patients was coronary artery disease, whereas in case of AF patients the distribution between coronary artery disease and valvular heart disease was almost equal.

Almost all of the patients were hypertensive. Symptoms of heart failure (NYHA III classification of heart failure, marked limitation of physical activity (Swedberg et al. 2005) were present in 4 patients of the SR group, in none of the pAF patients and in 5 patients with cAF. Hyperlipidemia was also present in each group: in 2 of the SR patients, in 4 of the pAF patients and in 3 of the cAF patients. One patient in the pAF group and one in the cAF group were suffering from diabetes.

The majority of the patients received β-blockers and ACE inhibitors or AT<sub>1</sub> blockers. Fifty percent of pAF patients and one of the cAF patients also received Ca<sup>2+</sup> channel blockers. In each group medication also included diuretics and statins. Two patients with cAF received digitalis.

**Table 31. Patient characteristics**

		SR (6)	pAF (6)	cAF (6)
	Gender	male	male	male
	Age, years (mean±SEM)	70.2±2.5	70.0±2.4	72.3±2
	BMI (mean±SEM)	25.9±3	27.9±0.9	25.3±1
Surgical procedure	Bypass grafting, n	5	3	2
	Valve replacement	1	1	2
	Bypass grafting and valve replacement	0	2	1
	Valve replacement and ASD	0	0	1
Pre-existing conditions	Hypertension, n	4	5	6
	Diabetes, n	0	1	1
	Hyperlipidemia, n	2	4	3
	NYHA III	4	0	5
Pre-medication	Digitalis, n	0	0	2
	ACE inhibitor, n	2	2	3
	AT <sub>1</sub> blocker, n	0	2	2
	β-blocker, n	3	5	5
	Ca <sup>2+</sup> channel blocker, n	0	3	1
	Diuretic, n	1	3	2
	Nitrate, n	0	2	0
	Statin, n	2	4	2

BMI indicates body mass index; ASD, atrial septal defect; NYHA III, New York heart association class III; ACE, angiotensin-converting enzyme; AT, angiotensin receptor

### 5.3.2. Western blot analysis of Na<sup>+</sup>-handling proteins

First, we performed western blot analysis of Na<sup>+</sup> influx proteins. Figure 38 presents expression of Na<sup>+</sup> channels, NCX and NHE. Expression of Na<sup>+</sup> channels was almost equal in pAF or cAF, as can be estimated from Figure 38Ba. Expression of NCX, as can be seen from Figure 38Bb, was not changed in pAF, whereas, in line with the previous study (El-Armouche et al. 2006), we observed an increase in cAF. However, this increase did not reach statistical significance ( $p=0.4$ ). NHE expression was unchanged in pAF or cAF, as evident from Figure 38Bc.



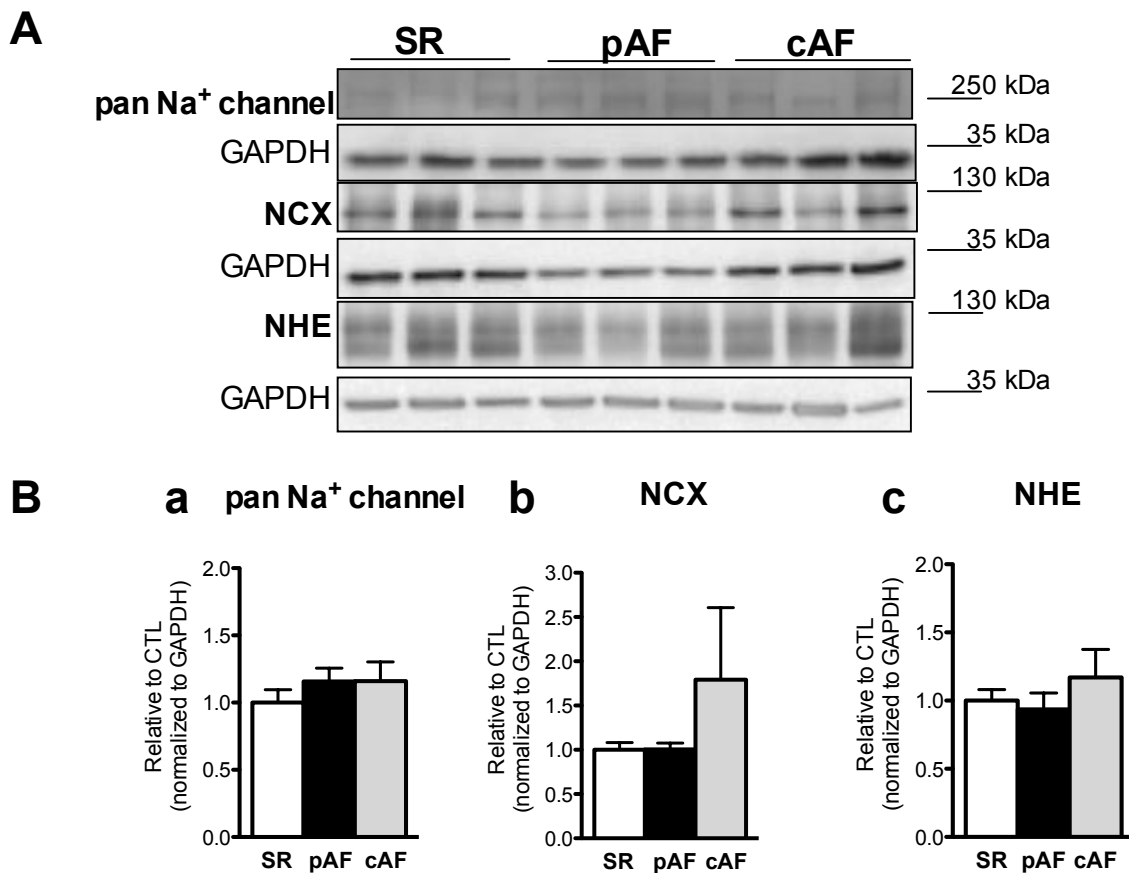


**Figure 38. Na<sup>+</sup> influx protein expression in right atrium in sinus rhythm (SR), paroxysmal atrial fibrillation (pAF) and chronic atrial fibrillation patients (cAF)**

**A:** Original western blots of Na<sup>+</sup> influx proteins: various isoforms of Na<sup>+</sup> channels (pan Na<sup>+</sup> channel), Na<sup>+</sup>/Ca<sup>2+</sup> exchanger (NCX) and Na<sup>+</sup>/H<sup>+</sup> exchanger (NHE) **B:** Averaged data of protein expression, normalized to GAPDH: **(a)**-pan Na<sup>+</sup> channel, **(b)**-NCX, **(c)**- NHE, normalized to GAPDH. Data were analyzed by one way ANOVA followed by Bonferroni's multiple comparison test.

Thus, we did not observe major changes in the expression of Na<sup>+</sup> influx proteins in paroxysmal or chronic atrial fibrillation.

Next, we analyzed expression of different NKA subunits and PLM, in order to estimate Na<sup>+</sup> efflux. Data are given in Figure 39.  $\alpha$  1 subunit expression was similar between SR and pAF or cAF, as can be seen from Figure 39Ba and b. Interestingly, we found a marked but statistically insignificant increase in the expression of the  $\alpha$  3 subunit in pAF

(Figure 39Bc), whereas in cAF expression of this subunit was only slightly higher in comparison to SR.

We observed a 25% reduction in  $\beta$  1 subunit expression in pAF. In cAF,  $\beta$  1 subunit expression was even more reduced: up to 50%, as can be seen from Figure 39Bd.  $\beta$  1 subunit is responsible for the correct folding of NKA complexes and trafficking of these complexes to the plasma membrane (Hasler et al. 1998). Thus, the significant reduction in the  $\beta$  1 subunit expression might suggest disturbed transport of newly synthesized NKA to the plasma membrane in atrial fibrillation.

Expression of PLM was not changed neither in pAF nor in cAF patients (Figure 39Be). We also calculated the  $\alpha$  1/PLM expression ratio to estimate the function of NKA. As indicated in Figure 39Bf, this ratio was not different in pAF or cAF patients.

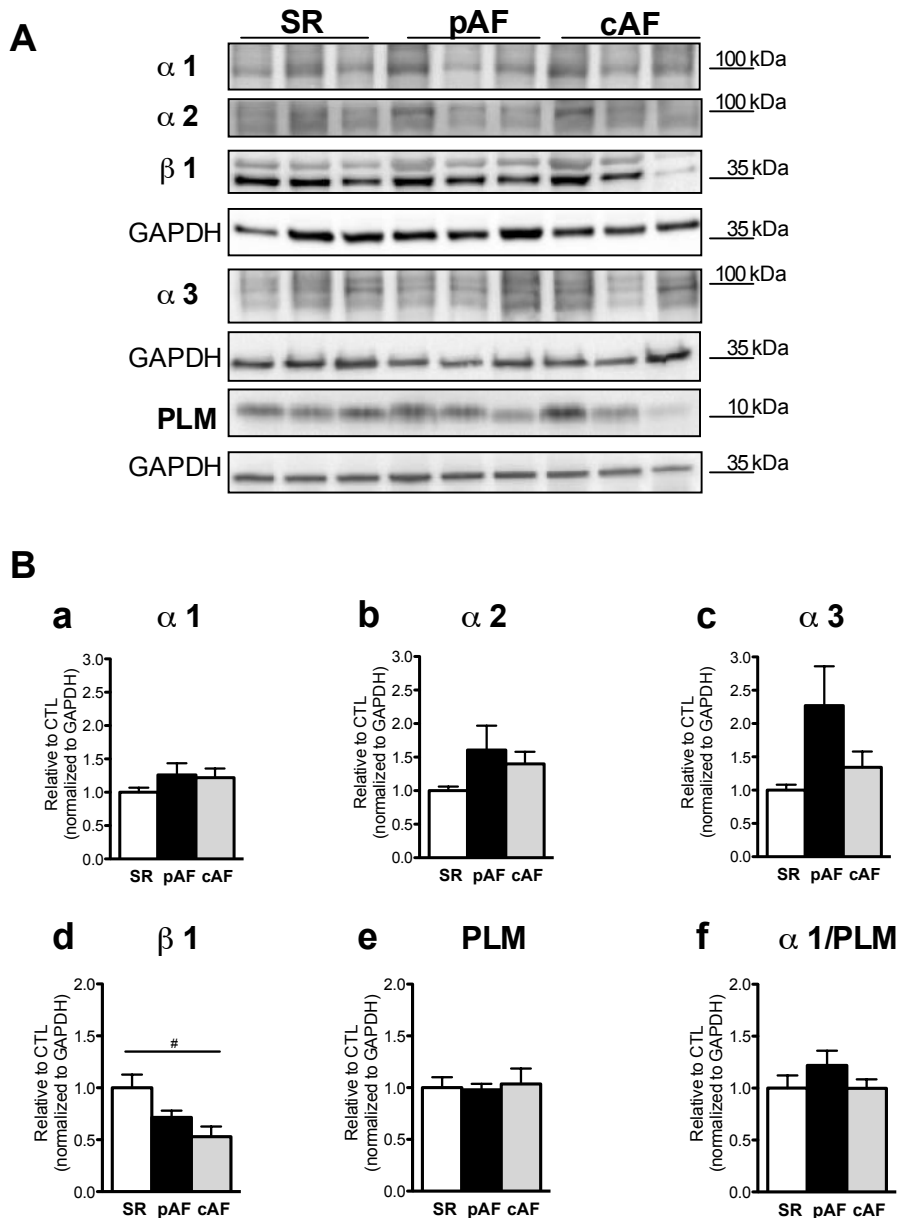


**Figure 39.  $\text{Na}^+$  efflux protein expression in right atrium in sinus rhythm (SR), paroxysmal atrial fibrillation (pAF) and chronic atrial fibrillation patients (cAF)**

**A:** Original western blots of different  $\text{Na}^+/\text{K}^+$ -ATPase subunits and phospholemman. **B:** Averaged data of protein expression, normalized to GAPDH: **(a)**-  $\alpha 1$  subunit, **(b)**  $\alpha 2$  subunit, **(c)**  $\alpha 3$  subunit, **(d)**  $\beta 1$  subunit, **(e)** phospholemman (PLM), **(f)**- $\alpha 1$  to PLM expression ratio. Data were analyzed by one way ANOVA followed by Bonferroni's, multiple comparison test, #  $p < 0.05$  cAF vs. SR.

To conclude, expression of different catalytic  $\alpha$  subunits was not affected in pAF and cAF, however, we observed a noticeable reduction in the expression of  $\beta$  1 subunit in cAF, which might suggest an impaired NKA function in atrial fibrillation.

#### **5.4. Effect of macitentan on blood pressure, heart rate, Ca<sup>2+</sup>-handling and endothelin-1 signalling proteins in left atria of SHR**

Endothelin-1 exhibits many pathological effects on the myocardium, including myocardial growth and fibrosis (Kerkelä et al. 2011). Activation of the endothelin-1 system also causes fibrotic changes in other organs and tissues (Iglarz & Clozel 2010). Moreover, endothelin-1 may induce Ca<sup>2+</sup>-dependent proarrhythmic events in myocardium (Kockskämper, Zima, et al. 2008). Inhibition of endothelin receptors was shown to be beneficial for treatment of various cardiovascular diseases (Duru et al. 2001). Previous studies from our laboratory and our collaboration partners revealed elevated expression of endothelin-1, increased endothelin-1 signalling and Ca<sup>2+</sup>-dependent proarrhythmic events in the atria of 6-8 months old SHR. Thus, the third aim of the thesis was to investigate the effect of endothelin receptor blockade on blood pressure, heart rate, expression and phosphorylation of key Ca<sup>2+</sup>-regulating proteins and endothelin-1 signalling in the left atrium of the SHR. Macitentan, a dual endothelin A and endothelin B receptor blocker with high tissue targeting properties (Iglarz et al. 2008), was used for this purpose.

Doxazosin is a selective alpha-1 adrenergic receptor antagonist. A previous study revealed a significant reduction in systolic blood pressure in SHR after 4 weeks of treatment with doxazosin (Hamada et al. 2012). As was shown in previous studies, doxazosin did not exert any major effects on cardiac remodelling (Varagic et al. 2001), (Asai et al. 2005). Since the aim of this study was to test the effect of macitentan treatment on atrial remodelling, doxazosin was chosen as a control drug in order to lower blood pressure independent of endothelin receptors.

This project was done in collaboration with Prof. Dr. Andreas Goette and Dr. Alicja Bukowska, Working Group of Molecular Electrophysiology, Medical Faculty, University of Magdeburg.

SHR rats at the age of 7-9 months were subdivided into three groups: control group (23 rats), macitentan-treated group (18 rats), doxazosin-treated group (18 rats). Rats were getting macitentan or doxazosin (30 mg/kg/day) with chow. The drug treatment was performed for 8 weeks. Within the 7-th or 8-th week of treatment rats were subjected to blood pressure and heart rate measurements. Afterwards, Dr. Alicja Bukowska

performed gravimetric assessment of hypertrophy and collected atrial tissue for further biochemical analysis.

#### 5.4.1. Blood pressure and heart rate measurements in SHR treated with macitentan or doxazosin

As can be seen from Figure 40A, diastolic blood pressure was increased by macitentan-treatment, whereas doxazosin did not influence it. Macitentan administration did not affect systolic blood pressure, as can be estimated from Figure 40B, while doxazosin significantly reduced systolic blood pressure in SHR. Interestingly, macitentan treatment significantly increased mean blood pressure in SHR, whereas doxazosin did not show any significant effect, as can be estimated from Figure 40C.

Heart rate was not affected by doxazosin or macitentan treatment, as can be seen in Figure 40D.

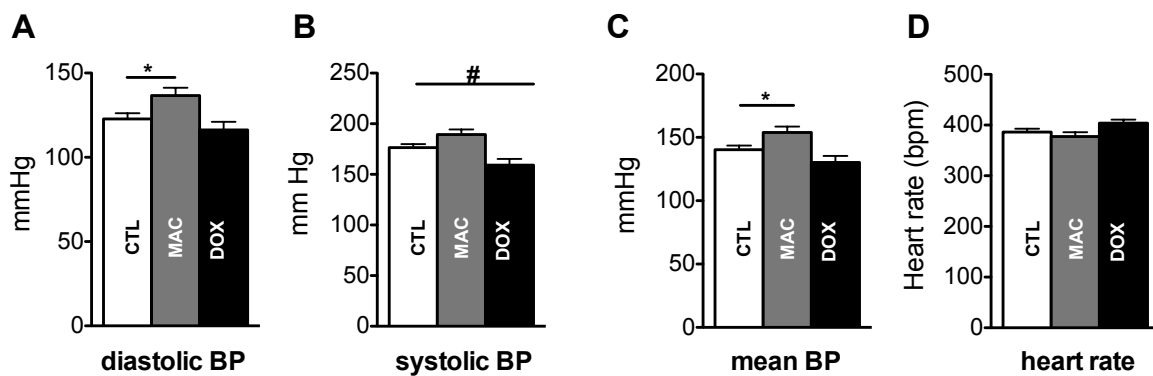


**Figure 40. Effect of macitentan treatment on blood pressure and heart rate in SHR**

A: diastolic blood pressure, B: systolic blood pressure, C: mean blood pressure, D: heart rate. N=number of rats: control group (CTL): N=23, doxazosin-treated group (DOX): N=18, macitentan-treated group (MAC): N=18. Data were analyzed by one-way ANOVA followed by Dunnett's test, \* $p < 0.05$  MAC vs. CTL, # $p < 0.05$  DOX vs. CTL.

#### **5.4.2. Effects of macitentan or doxazosin treatment on the expression and phosphorylation of Ca<sup>2+</sup>-handling proteins in left atrium of SHR**

The next step in this project was to characterize the expression and phosphorylation of major Ca<sup>2+</sup>-regulating proteins and proteins involved in endothelin-1 signalling in left atria of SHR.

First, we analyzed the expression of the  $\alpha$ 1C subunit of L-type Ca<sup>2+</sup>channels, the ryanodine receptor (RyR) and the Na<sup>+</sup>/Ca<sup>2+</sup> exchanger (NCX). RyR is phosphorylated by protein kinase A (PKA) at serine 2808 and by Ca<sup>2+</sup>/Calmodulin-dependent kinase II (CaMKII) at serine 2814. The phosphorylation of RyR results in an increase in Ca<sup>2+</sup> release out of the sarcoplasmic reticulum (Huke & Bers 2008).

Figure 41 presents original western blots (A) and averaged data (B) of protein expression in left atrium of SHR. Expression of  $\alpha$ 1C was unchanged by macitentan or doxazosin treatment (Figure 41Ba). NCX expression was also unaffected by drug treatment, as can be seen in Figure 2Bb. RyR expression (Figure 41Bc) and phosphorylation of RyR at serine 2808 by PKA (Figure 41Bd) was unaffected by either drug treatments, as shown in Figure 2Bd. Interestingly, we observed an approximately 50% increase in the phosphorylation of RyR by CaMKII at serine 2814 in macitentan-treated SHR. Doxazosin treatment revealed a similar effect on the phosphorylation at serine 2814 (Figure 41Be). However, these changes were not statistically significant.

Overall, neither macitentan nor doxazosin affected the expression of the  $\alpha$  1C subunit of L-type Ca<sup>2+</sup>channels and NCX. Phosphorylation and expression of RyR was also unaffected by both drugs, although with a tendency towards an increase in phosphorylation by CaMKII.

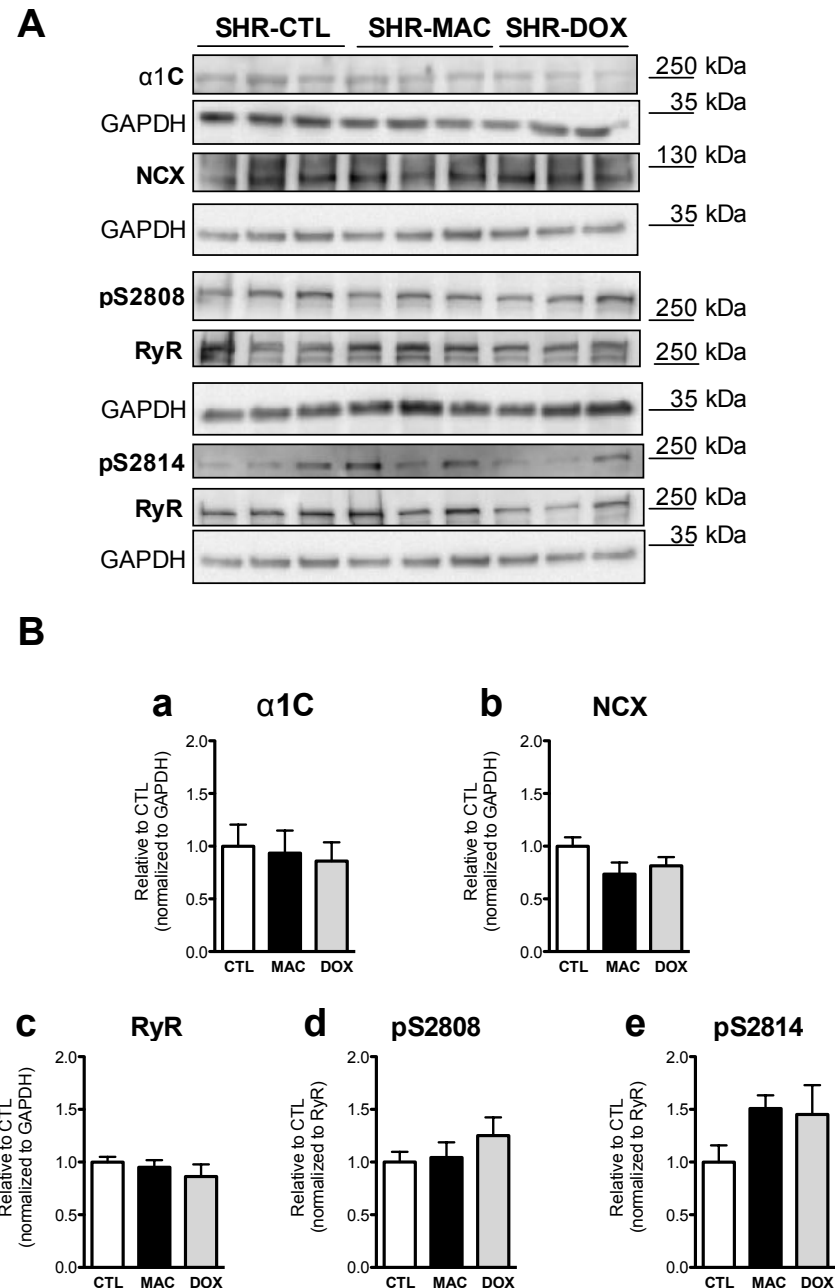


**Figure 41. Effects of macitentan or doxazosin administration on expression of  $\alpha$  1C subunit of L-type  $\text{Ca}^{2+}$  channels,  $\text{Na}^+/\text{Ca}^{2+}$  exchanger and ryanodine receptor in left atrium of SHR.**

**A:** Original western blots of  $\alpha$  1C subunit of L-type  $\text{Ca}^{2+}$  channel, NCX, ryanodine receptor and its phosphorylation at serine 2808 and serine 2814 in left atrium of SHR. **B:** Average data of protein expression, normalized to GAPDH. Phosphorylation of RyR was normalized to the expression of total protein. **a-** $\alpha$ 1C subunit of L-type  $\text{Ca}^{2+}$  channel **b-** $\text{Na}^+/\text{Ca}^{2+}$  exchanger (NCX), **c-**ryanodine receptor (RyR), **d-**phosphorylation of RyR at serine 2808 (pS2808), **e-**phosphorylation of RyR at serine 2814 (pS2814). Note that GAPDH for NCX and RyR is identical, since these proteins were stained on the same membrane. CTL = control group, MAC =



macitentan- treated group, DOX = doxazosin-treated group. N=6-9 samples per group. Data were analyzed by one-way ANOVA followed by Dunnett's test.

Next, we investigated the expression of sarcoplasmic (SR) Ca<sup>2+</sup>-handling proteins: sarcoplasmic Ca<sup>2+</sup>-ATPase (SERCA), its regulatory protein phospholamban (PLB) and calsequestrin (CSQ). Phospholamban is phosphorylated by PKA at serine 16, by CaMKII at threonine 17 and by protein kinase C (PKC) at serine 10. Phosphorylation of phospholamban results in its dissociation from SERCA and an increase in Ca<sup>2+</sup> reuptake into the SR (Kranias & Hajjar 2012).

SERCA expression, as can be estimated from Figure 42Ba, was unaffected by either drug treatment. Expression of PLB did not change under macitentan, whereas it was significantly reduced in doxazosin-treated rats (Figure 42Bb). For the estimation of SERCA activity we calculated the ratio SERCA/PLB. This ratio was almost unchanged, suggesting unaltered SERCA activity (Figure 42Bc). Expression of CSQ was unaltered by both drugs (Figure 42Bd). Phosphorylation of PLB at serine 16 was unchanged in macitentan-treated animals and there was a tendency towards an increase in its phosphorylation in doxazosin-treated rats (Figure 42Be). Phosphorylation of PLB by CaMKII at threonine 17 was not changed by either treatment (Figure 42Bf). Phosphorylation of PLB by PKC at serine 10 was also unaffected by either macitentan or doxazosin administration, as can be seen from Figure 42Bg. Thus, we observed a significant reduction in PLB expression by doxazosin treatment, however, no further changes in the expression or phosphorylation of SR Ca<sup>2+</sup>-handling proteins was found by either macitentan or doxazosin treatment.

In summary, the expression and phosphorylation of major Ca<sup>2+</sup>-handling proteins was overall unaffected by macitentan treatment.

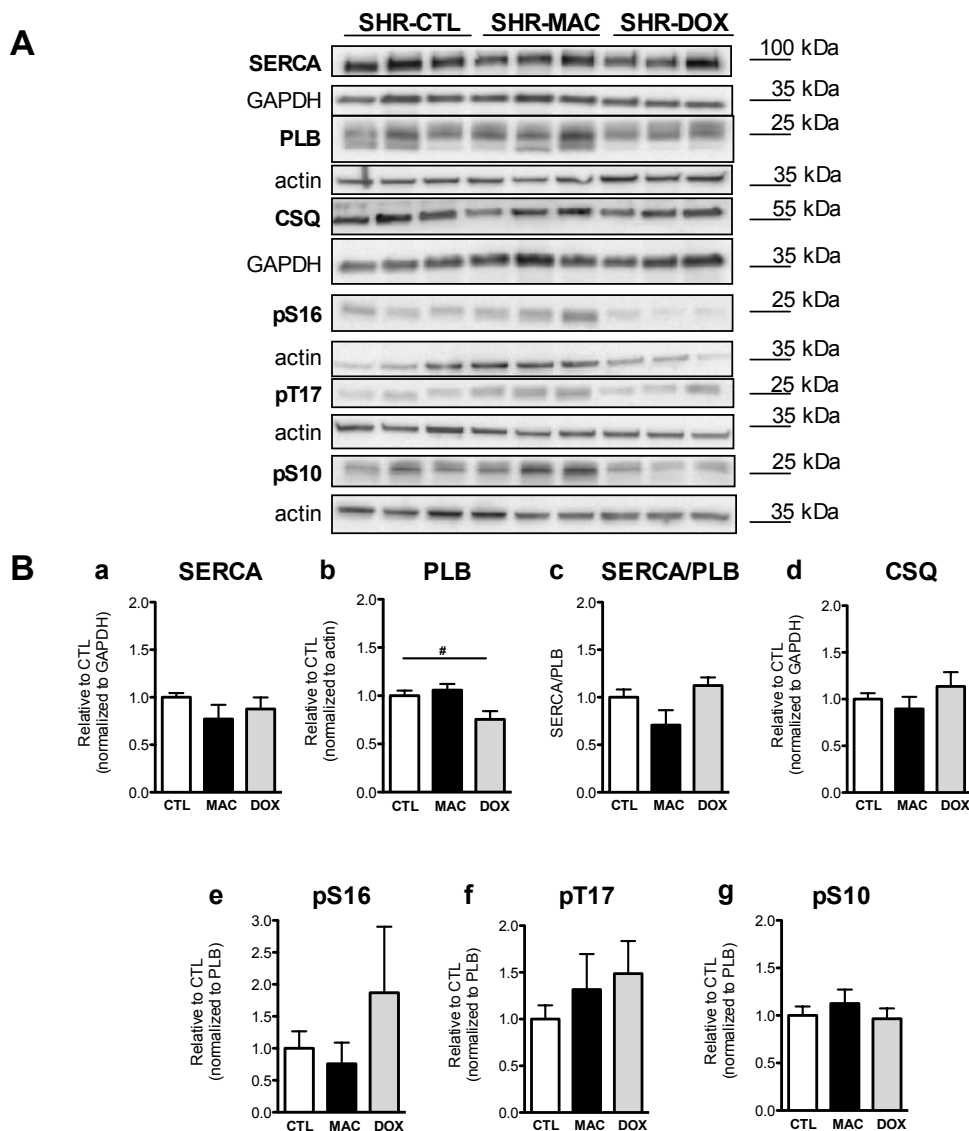


**Figure 42. Effects of macitentan or doxazosin treatment on the expression and phosphorylation of SR Ca<sup>2+</sup>-handling proteins.**

**A:** Original western blots of SR Ca<sup>2+</sup>-ATPase (SERCA), phospholamban (PLB), its phosphorylated forms and calsequestrin (CSQ) in left atrium of SHR. **B:** Averaged data of protein expression, normalized to GAPDH or actin. Phosphorylation of PLB was normalized to the expression of total protein. **a-** SR Ca<sup>2+</sup>-ATPase (SERCA), **b-** phospholamban (PLB), **c-** ratio of SERCA expression to PLB expression, **d-** calsequestrin (CSQ), **e-** phosphorylation of PLB by PKA at serine 16 (pS16), **f-** phosphorylation of PLB by CaMKII at threonine 17 (pT17), **g-** phosphorylation of PLB by PKC at serine 10 (pS10). CTL = control group, MAC = macitentan-treated group, DOX = doxazosin-treated group. N=6-9 samples per group. Data were analyzed by one-way ANOVA followed by Dunnett's test, #p<0.05 DOX vs. CTL.

### 5.4.3. Effects of macitentan or doxazosin treatment on the expression of proteins involved in endothelin-1 signalling

Next, we investigated the expression of major proteins involved in endothelin-1 signalling. Endothelin-1 binds to the endothelin A receptor (ET<sub>A</sub>R), abundantly expressed in the atrial myocardium (Thibault et al. 1994). The ET<sub>A</sub>R belongs to the family of Gq-coupled receptors. Activation of the ET<sub>A</sub>R causes activation of phospholipase C  $\beta$  (PLC  $\beta$ ). This enzyme catalyzes the hydrolysis of phosphatidylinositol bisphosphate (PIP<sub>2</sub>), producing inositol trisphosphate (IP<sub>3</sub>). IP<sub>3</sub> binds to the inositol trisphosphate receptor (IP<sub>3</sub>R) in the sarcoplasmic reticulum, producing Ca<sup>2+</sup> release from the SR (Drawnel et al. 2013), (Kockskämper, Zima, et al. 2008).

Thus, we investigated the expression of the ET<sub>A</sub>R, different isoforms of PLC $\beta$  and the IP<sub>3</sub>R. In addition to that we checked for the expression of the alpha 1 adrenergic receptor ( $\alpha$ 1AR). Since endothelin-1 signalling alters Ca<sup>2+</sup> handling, we investigated expression of CaMKII and its phosphorylation status.

Macitentan treatment increased the expression of the ET<sub>A</sub>R receptor, however, this increase did not reach statistical significance (Figure 43Ba,  $p=0.14$ ). Doxazosin application did not affect ET<sub>A</sub>R expression (Figure 43Ba).

Doxazosin treatment significantly reduced expression of the  $\alpha$ 1AR in SHR, while macitentan administration exhibited a slight but insignificant reduction in its expression, as indicated in Figure 43Bb.

There are two major isoforms of phospholipase C $\beta$  expressed in the myocardium: PLC $\beta$  1 and PLC $\beta$  3 (Filtz et al. 2009). As can be estimated from Figure 43Bc and d, the expression of these enzymes was not affected by macitentan or doxazosin treatment.

Next, we investigated expression of the IP<sub>3</sub>R receptor. Macitentan or doxazosin treatment did not induce any significant changes in the expression of the IP<sub>3</sub>R receptor, as can be estimated from Figure 43Be.

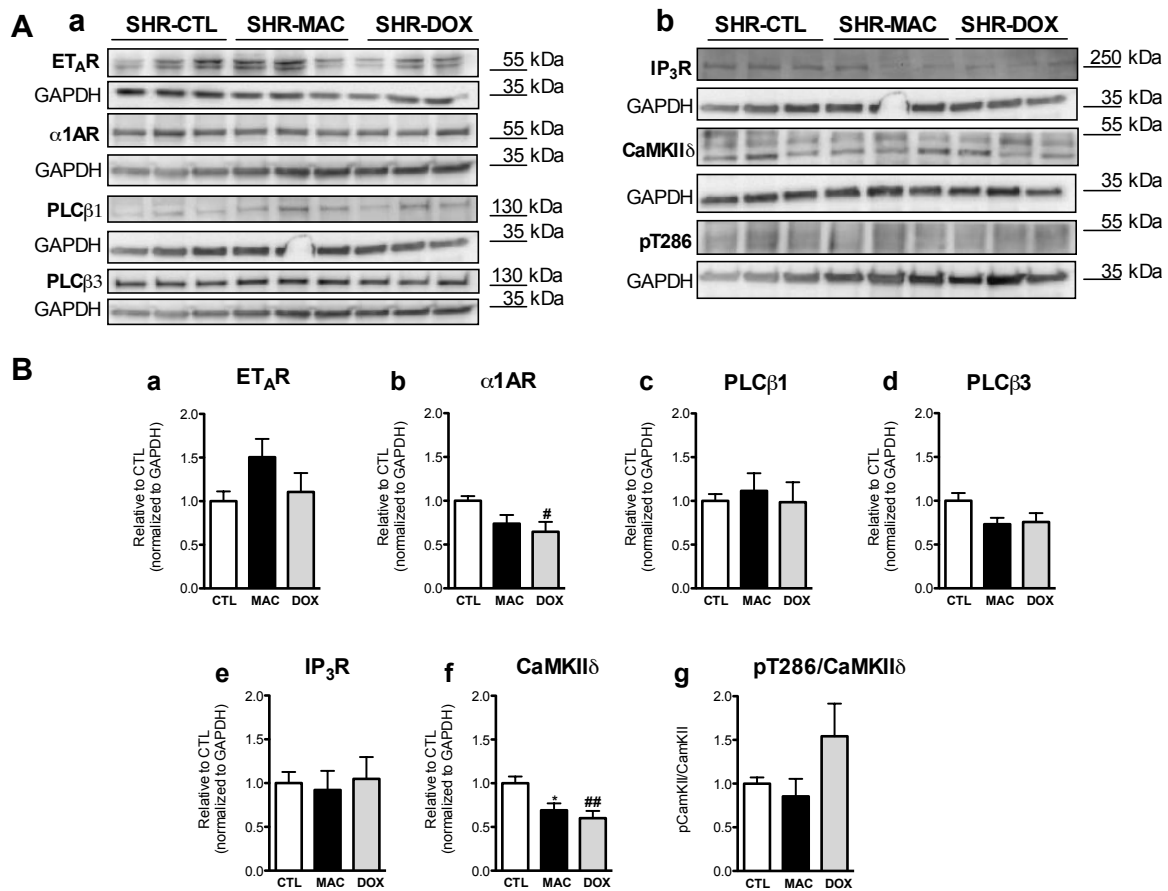


**Figure 43. Effects of macitentan or doxazosin treatment on the expression of proteins involved in endothelin-1 signalling.**

**A:** Original western blots of **(a)**: endothelin-A receptor (ET<sub>A</sub>R),  $\alpha$ <sub>1</sub> adrenergic receptor ( $\alpha$ 1AR), phospholipase C $\beta$ 1 (PLC  $\beta$ 1), phospholipase C $\beta$ 3 (PLC  $\beta$ 3). Note that GAPDH is identical for  $\alpha$ 1 AR and PLC  $\beta$  3 (panel A), as it was from the same blot. **(b)**: inositol trisphosphate receptor (IP<sub>3</sub>R), Ca<sup>2+</sup>/Calmodulin-dependent kinase II $\delta$  (CaMKII $\delta$ ), its phosphorylated form at threonine 286 (pT286). ) Note that GAPDH is identical for PLC  $\beta$ 1 and IP<sub>3</sub>R (panel B), as it was from the same blot. **B (a-g)**: Averaged data of protein expression, normalized to GAPDH. Expression of phosphorylated CaMKII was normalized to the expression of total protein. CTL = control group, MAC = macitentan-treated group, DOX = doxazosin-treated group. N=7-9 samples per group. Data were analyzed by one-way ANOVA followed by Dunnett's test. \*p<0.05 MAC vs. CTL, ## p<0.05 DOX vs. CTL.

There are different isoforms of CaMKII expressed in the body. CaMKII $\delta$  is the major cardiac isoform (Anderson et al. 2011). We observed a marked and significant decrease in the expression of CaMKII $\delta$  by macitentan treatment. The reduction of CaMKII $\delta$  expression under doxazosin treatment was even more pronounced, as can be estimated from Figure 43Bf.

The activity of CaMKII $\delta$  is regulated by its autophosphorylation at threonine 286. Macitentan treatment did not alter phosphorylation of this enzyme, whereas doxazosin treatment induced an increase in the phosphorylation, which was, however, not significant (Figure 43Bg). Thus, despite the changes in total CaMKII $\delta$  expression, its phosphorylation status was not significantly changed.

To conclude, macitentan treatment significantly reduced expression of CaMKII $\delta$ , though we have not observed any changes in two of its phosphorylation targets (RyR and PLB). The endothelin-1 signalling pathway (ET<sub>A</sub>R-PLC $\beta$ -IP<sub>3</sub>R) was not affected by macitentan treatment.

Taken together, the presented results indicate that macitentan treatment overall did not induce any major changes in expression of Ca<sup>2+</sup>-handling or endothelin-1 signalling proteins in atria of SHR.

## **6. Discussion**

The aim of the first part of this thesis was to find out, if SHR, as a model of hypertensive heart disease, exhibit signs of atrial ionic (in terms of Na<sup>+</sup> handling) and functional (in terms of contractility) remodelling in either early hypertension (3 and 7 months old rats) or in advanced hypertensive heart disease (in 15-23 months old rats), when heart failure develops.

In early hypertension no marked changes in Na<sup>+</sup> homeostasis and contractility were present, whereas in advanced hypertensive heart disease Na<sup>+</sup> homeostasis and contractility of atrial myocytes were impaired, indicating development of atrial ionic and functional remodelling, associated with progression of advanced hypertensive heart disease.

### **6.1. Cardiovascular changes, unaffected contractility and unchanged [Na<sup>+</sup>]<sub>i</sub> in early hypertension**

#### **6.1.1. Cardiovascular changes in early hypertension**

The collected data on blood pressure and gravimetric parameters confirmed early onset of hypertension. Hypertension caused left ventricular hypertrophy already in 3 months old SHR and later on, in 7 months old SHR, left ventricular hypertrophy became more prominent, in line with previous observations (Pfeffer et al. 1979), (Chan et al. 2011). The right ventricular weight was unaffected in SHR, in accordance with a previous study (Chan et al. 2011), indicating isolated left ventricular hypertrophy in early hypertension. In early hypertension no signs of atrial enlargement were observed. On the contrary, SHR exhibited bi-atrial hypotrophy but unchanged atrial myocyte size (Pluteanu et al. 2015). However, the reason for atrial hypotrophy remains unknown.

At the tissue level, 3 months old SHR exhibited higher mRNA expression of pro-fibrotic markers (collagen 1a and 13, CTGF) in the left atrium, as was shown by our previous study (Pluteanu et al. 2015). At the age of 7 months, expression of these markers was even more prominent, moreover, the histological assessment revealed increased degree of fibrosis in left atria of SHR, indicating an early onset of fibrotic changes. A previous

study by Choisy et al. also revealed increased fibrosis in the left atrium at around 3 months of age and these changes were even more prominent at 11 months of age (Choisy et al. 2007). As discussed previously, fibrosis impairs atrial contractility (Casaclang-Verzosa et al. 2008). A study of Dodd et al., for instance, revealed a decrease in atrial filling of left ventricle in vivo in SHR at the age of 15 weeks, indicating a possible impairment of atrial pumping function (Dodd et al. 2012). Another study found an increased left atrial pressure in 4-5 months old SHR (Noresson et al. 1979). The increase in pressure might cause the mechanical stress on the atrial walls, inducing the fibrotic changes (Díez 2007), (Casaclang-Verzosa et al. 2008).

Taken together, in early hypertension SHR developed progressive left ventricular hypertrophy but no signs of atrial hypertrophy. However, atrial fibrosis was markedly present in SHR, implying the presence of a pro-arrhythmogenic substrate in the atria of SHR in early hypertensive heart disease.

#### **6.1.2. Unaffected contractility of atrial myocytes in early hypertension**

Despite some signs of atrial structural remodelling, our findings did not reveal any changes in contractility of atrial myocytes in 7 months old SHR. Diastolic sarcomere length, fractional shortening ( $\approx 12\%$  in WKY vs.  $\approx 11\%$  in SHR) and kinetic parameters of contraction were similar between WKY and SHR. In addition to that, no changes in the contractility between left and right atrial myocytes were found.

Contractility of isolated cardiac myocytes could be affected by several factors, among them:  $\text{Ca}^{2+}$  and  $\text{Na}^{+}$  handling, cytoplasmic pH and phosphorylation status of myofilaments (Bers 2002), (Bers & Despa 2009), (Orchard & Kentish 1990), (Bountra & Vaughan-Jones 1989), (Solaro & Rarick 1998)

Our previous study (Pluteanu et al. 2015) revealed that global  $\text{Ca}^{2+}$  transients (which are mostly responsible for the myocyte contraction) were unaffected in atrial myocytes from 7 months old SHR, which is in line with our observation of unchanged contractility. Changes in intracellular pH could also affect contractility of cardiac myocytes: acidosis decreases the contractile force of the myocardium, whereas alkalosis has an opposite effect (Orchard & Kentish 1990), (Bountra & Vaughan-Jones 1989). NHE maintains intracellular pH in cardiac myocytes. It was shown that expression or function of NHE is increased in hypertension, hypertrophy, heart failure, and ischemia (Avkiran & Haworth 1999), (Wakabayashi et al. 2013). Thus, the expression of NHE might serve as an indirect estimation of pH status in the cytosol. We found that NHE expression was not

changed in the atria of SHR in early hypertension, suggesting that pH status in the cytosol of atrial myocytes was not affected, supporting our observation of unaltered contractility of atrial myocytes. However, we did not perform direct measurements of intracellular pH.

The phosphorylation status of myofilament proteins (in particular troponin I or myosin-binding protein C) is crucial for the contractility of cardiac myocytes (Solaro & Rarick 1998), (Layland et al. 2005). In human heart failure and in atrial fibrillation, the phosphorylation of those proteins (via changes in kinases or phosphatases activities) is changed, what impairs the contractile properties of the atrial myocytes (Bodor et al. 1997), (van der Velden et al. 2003), (El-Armouche et al. 2006). However, due to the fact that contractility of atrial myocytes was unchanged, it appears unlikely that phosphorylation of myofilament proteins was altered in early hypertension.

Taken together, in early hypertension intrinsic contractile properties of atrial myocytes were not affected in SHR.

### **6.1.3. Unchanged $[Na^+]_i$ in atrial myocytes in early hypertension**

There is a limited number of studies conducted on SHR to determine  $Na^+$  handling in the hearts of these rats. To the best of our knowledge, this study presents the first measurements of  $[Na^+]_i$  on isolated atrial myocytes from SHR.  $[Na^+]_i$  was measured by epifluorescence microscopy using the fluorescent dye SBFI. This method provides information only about bulk cytosolic  $Na^+$  concentration, but does not give information about changes in local  $[Na^+]_i$ .

Our results indicate unchanged  $[Na^+]_i$  in atrial myocytes from SHR in early hypertension (at both 3 and 7 months of age). At 3 months of age,  $[Na^+]_i$  was around 10 mM in WKY and SHR at 1 Hz stimulation, and around 7 mM at resting conditions. Later on, at the age of 7 months,  $[Na^+]_i$  was also not significantly different between two strains neither at 1 Hz stimulation ( $\approx 12$  mM in WKY vs.  $\approx 10$  mM in SHR), nor at the resting stage (10 mM in WKY vs. 9 mM in SHR). The comparison of  $[Na^+]_i$  in left vs. right atrial myocytes did not reveal any differences neither in WKY nor in SHR.

A study of Jelicks and Gupta revealed that in isolated Langendorff perfused hearts of 15-19 weeks old SHR,  $[Na^+]_i$  measured by nuclear magnetic resonance technique was higher than in WKY (Jelicks & Gupta 1994). However, a later study of Fowler et al. (Fowler 2005) found that  $[Na^+]_i$  in isolated ventricular myocytes from SHR at the age of 5 months



was unchanged. Thus, in early hypertension SHR did not exhibit any major changes in global  $[Na^+]_i$  in ventricular myocytes.

As was discussed previously, intracellular  $Na^+$  and  $Ca^{2+}$  concentration are tightly linked together in cardiac myocytes via NCX. The previous study of our group observed a decreased NCX function in left atrial myocytes from 7 months old SHR (Pluteanu et al. 2015). This reduction of NCX function, however, did not affect the global  $[Na^+]_i$ . Previous research revealed that in the ventricular myocytes there might be a  $[Na^+]_i$  gradient (Wendt Gallitelli et al. 1993), (Pieske & Houser 2003), (Despa et al. 2004). This gradient is generated by different subsarcolemmal co-localization and local activity of NCX and NKA in ventricular myocytes (Despa et al. 2004), (Pavlovic et al. 2013). However, the data on co-localization of  $Na^+$  transporters in atrial myocytes, as far as we know, are not yet available. Thus, even if the global  $[Na^+]_i$  is unchanged, some changes in the subsarcolemmal  $Na^+$  flux could be present in atrial myocytes, eventually affecting local  $Ca^{2+}$  handling. This speculation, however, should be verified by future research.

In conclusion, there were no significant changes in global  $[Na^+]_i$  in atrial myocytes from SHR in early hypertension.

#### **6.1.4. Subtle changes in $Na^+$ -handling protein expression in early hypertension**

Available data on the expression of  $Na^+$ -handling proteins in the atria are very scarce. Western blot analysis in our study did not reveal any major changes in the expression of  $Na^+$ -regulating proteins, though some alterations in their expression were observed in early hypertension.

At the age of 3 months, expression of the  $Na^+$  influx proteins was unaffected in the left atrium, however, we observed a significant increase in the expression of NCX and  $Na^+$  channels in the right atrium of SHR. This would suggest higher  $[Na^+]_i$ , due to an increase in  $Na^+$  influx. However,  $[Na^+]_i$  in atrial myocytes from 3 months old SHR was not higher compared to WKY. A study of Jäger et al. found a significant increase in NCX expression at the mRNA level in right atrium of hypertensive patients (Jäger et al. 2001). However, this study did not provide information about  $[Na^+]_i$  or protein expression. Thus, the increase in  $Na^+$  channel and NCX expression in right atrium in 3 months old SHR did not affect the overall  $Na^+$  influx in the atrial myocytes in early hypertension.

Expression of Na<sup>+</sup> efflux proteins was unchanged in SHR at the age of 3 months. Later in 7 months old SHR, expression of Na<sup>+</sup>-influx proteins was unaffected. However, we observed a significant reduction in the expression of the  $\alpha$  1 subunit of NKA in the left atrium of SHR at 7 months of age. As mentioned earlier,  $\alpha$  1 is the major catalytic isoform of NKA, responsible for most of the Na<sup>+</sup> extrusion (Shattock et al. 2015). However, we did not observe any changes in [Na<sup>+</sup>]<sub>i</sub>, particularly, not in left atrial myocytes from 7 months old SHR. We estimated NKA function by analyzing expression of its regulating protein PLM and calculating the  $\alpha$  1/PLM ratio. No changes in PLM expression or this ratio were observed, suggesting unchanged NKA function. PLM is phosphorylated by PKA at serine 68 and by PKC at serine 63. This, in turn, increases the pumping activity (Fuller et al. 2012). Therefore, a further study to evaluate the phosphorylation status of PLM and, thus, the activity of NKA, in the atria of SHR is needed. Another, and more direct approach for estimation of the NKA function would be the measurements of the NKA current by the patch clamp method.

Previous studies (Lee, S.W. et al. 1983), (Vrbjar et al. 2002) revealed a reduction in NKA function in ventricular myocytes from SHR at 5 and 9 months of age, respectively. However, the protein level of the pump was not altered. Interestingly, another study of Jäger et al. revealed unchanged  $\alpha$  1 mRNA level in the right atrium of hypertensive patients, whereas  $\alpha$  2 and  $\alpha$  3 isoforms were significantly increased (Jäger et al. 2001). Previous research indicates that in different models of hypertension and hypertrophy (Muller-Ehmsen et al. 2001), (Fedorova et al. 2004), there might be a shift in the expression of different  $\alpha$  subunit isoforms of the NKA. Thus, another possible explanation for the decrease in  $\alpha$  1 subunit expression in the left atrium of SHR might be a compensatory transition in the expression of  $\alpha$  isoforms towards increase in  $\alpha$  2 and  $\alpha$  3 expression. In other words, other isoforms of NKA might take over the function of the  $\alpha$  1 subunit and, thus, maintain [Na<sup>+</sup>]<sub>i</sub>.

It should be noted, however, that the western blot method used in this study has some limitations. Firstly, data on protein expression provide information about protein abundance only and does not give insight into a function of the protein. Secondly, determination of protein expression in our study was done in atrial homogenates, which might contain non-myocytes (fibroblasts and cardiac endothelial cells). Non-myocytes also express Na<sup>+</sup>-handling proteins, e.g. voltage-dependent Na<sup>+</sup> channels (Kaye & Kelly 1999), NCX (Kaye & Kelly 1999), NHE (Hattori et al. 2001) and NKA (Zahler et al. 1996).

Thus, the possibility exists that the observed increase in the expression of Na<sup>+</sup> channels and NCX could reflect changes in non-myocytes.

To conclude, despite reduced  $\alpha$  1 subunit expression and structural remodelling of the atria, Na<sup>+</sup> homeostasis and contractility of atrial myocytes were not markedly changed in the atria of SHR in early hypertension.

## **6.2. Progression of cardiovascular impairment, reduced atrial myocyte contractile function and decreased $[Na^+]_i$ in advanced hypertensive heart disease**

Our findings indicate that in advanced hypertensive heart disease SHR exhibited decreased contractile function of atrial myocytes, reduction in  $[Na^+]_i$  as well as changes in the expression of  $Na^+$ -handling proteins in the atria.

### **6.2.1. Cardiovascular changes**

We found that old SHR exhibited further progression of left ventricular hypertrophy and manifestation of right ventricular hypertrophy. We also observed increased lung weight and difficulties breathing, fluid retention in the thorax and a decrease in the body weight in many old SHR, indicating signs of heart failure. However, we did not perform functional measurements of cardiac function in vivo (e.g. by echocardiography). Instead, we divided SHR into non-failing and failing based on the absence or presence of lung edema, respectively. A number of previous studies confirmed a significant increase in lung weight in ageing SHR, which correlated with the onset of heart failure (Conrad et al. 1991), (Kapur et al. 2010). These studies also revealed that, starting with 15-18 months of age, old SHR exhibited systolic and diastolic dysfunction and structural changes, e.g. ventricular fibrosis. The study of Chan et al. found that fibrosis in the left ventricular free wall was followed by dilation of the left ventricle in 18 months old SHR. Moreover, as was shown in the same study many of the old SHR developed ascities together with increased liver weight, indicating the manifestation of right-sided heart failure (Chan et al. 2011). It should be noted, that the onset of the above mentioned signs of decreased cardiac performance developed gradually in SHR starting with 15 months of age, indicating that compensated left ventricular hypertrophy deteriorates into heart failure in old SHR.

We observed bi-atrial hypertrophy together with increased expression of hypertrophic and fibrotic markers in the left atrium of SHR (Goette A., Bukowska A., Kocksämper J, Pluteanu F., Nikonova Y., unpublished data). These observations are in line with the

studies by Lau et al and Dunn et al., in which bi-atrial hypertrophy was confirmed in 15 and 16 months old SHR, respectively, by echocardiography. The study of Lau et al. confirmed the bi-atrial hypertrophy on the cellular level by increased left and right atrial myocyte size. In addition, interstitial fibrosis was present in both atria of SHR (Lau et al. 2013), (Dunn et al. 1978). Moreover, SHR demonstrated high susceptibility to the development of atrial arrhythmias, indicating that ageing SHR develop structural (fibrosis) and functional (alterations in the electrophysiological properties of the atria) arrhythmogenic substrates (Choisy et al. 2007), (Lau et al. 2013).

To conclude, in advanced hypertensive heart disease SHR exhibited transition from compensated left ventricular hypertrophy to heart failure and this transition was accompanied by structural atrial remodelling.

#### **6.2.2. Reduction in contractile function of atrial but not ventricular myocytes in advanced hypertensive heart disease**

We observed a significant reduction in contractility of atrial myocytes from old SHR. During the transition from compensated left ventricular hypertrophy to heart failure atrial contractile function was even more impaired. These observations could be explained by unpublished findings from our lab (work by Dr. Florentina Pluteanu), which indicate that atrial myocytes from old SHR exhibited impaired  $Ca^{2+}$  handling. Starting with 8 months of age many SHR develop thrombi in left atrium, which indicate impairment of atrial contractile function in vivo (Brooks et al. 2010), (Scridon et al. 2013). Loss of atrial pumping function is also found in animal models of atrial fibrillation, human atrial fibrillation and heart failure (Schotten et al. 2011), (Wijesurendra & Casadei 2015), (Anter et al. 2009).

Thus, decrease in the contractile function of single atrial myocytes might cause the loss of atrial pumping function, which contributes to the decrease in ventricular filling and cardiac output and, thus, development of heart failure.

Despite the fact that in advanced hypertensive heart disease SHR develop left ventricular fibrosis and systolic dysfunction, the fractional shortening of isolated ventricular myocytes from old SHR was unchanged. Moreover, during the transition to heart failure, no impairment in the contractile function of ventricular myocytes was found. The study of Ward et al. found that the peak of  $Ca^{2+}$  transients measured in left ventricular trabeculae from failing SHR was even higher than in WKY. The authors also

suggested that in this animal model the decrease in contractile function of the ventricle was rather due to fibrosis than to impaired  $\text{Ca}^{2+}$  cycling (Ward et al. 2003). We also found a slight but significant decrease in the relaxation kinetics during the transition from compensated left ventricular hypertrophy to heart failure. This could be explained by prolongation of  $\text{Ca}^{2+}$  transients in ventricular myocytes in old SHR during the transition to heart failure, which would ultimately prolong the relaxation.

Taken together, the impairment of atrial myocyte contractility in SHR was not accompanied by depressed contractility of ventricular myocytes, indicating that atrial myocytes undergo atria-specific functional remodelling. Mechanisms underlying these alterations require further investigation. Impaired atrial myocyte contractility contributes to atrial contractile dysfunction, which causes reduced left ventricular filling and cardiac output, contributing to the development of heart failure.

### **6.2.3. Decrease in $[\text{Na}^+]_i$ in atrial but not ventricular myocytes from SHR in advanced hypertensive heart disease**

Another important and striking finding of this work was a significant reduction of  $[\text{Na}^+]_i$  in atrial myocytes from old SHR. This decrease could be explained by an increase in NKA expression, and, thus, an increase in  $\text{Na}^+$  export.

Previous studies of Greiser et al. (by measuring free  $[\text{Na}^+]_i$  using SBFI) and Akar et al. (by measuring total  $[\text{Na}^+]_i$  using electron probe microanalysis) also described reduced  $[\text{Na}^+]_i$  in the atria of animal models of atrial fibrillation (induced by rapid atrial pacing) (Greiser et al. 2014) (Akar et al. 2003). However, these studies explained the decrease in  $[\text{Na}^+]_i$  by reduced NCX function and, consequently, decreased  $\text{Na}^+$  influx. The study of Greiser et al. revealed that NKA expression was not changed. Moreover, the authors also found a decrease in the phosphorylation of PLM, which suggests a reduction of NKA function. However, it should be noted that the model of rapid atrial pacing could induce other changes in atrial structure and function than those in long-standing hypertension in SHR. Our own observations, on the contrary, revealed no changes in NCX expression and that the fractional contribution of NCX to  $\text{Ca}^{2+}$  removal was rather higher in SHR (unpublished data, work by Dr. Florentina Pluteanu). Decrease in  $[\text{Na}^+]_i$  may alter the trans-sarcolemmal  $[\text{Na}^+]_i$  gradient and, thus, stimulate  $\text{Ca}^{2+}$  export via NCX. As a result of it, the amplitude of  $\text{Ca}^{2+}$  transients declines, leading to impaired contractility.

However, in order to estimate the contribution of each Na<sup>+</sup> transporter to the Na<sup>+</sup> influx or efflux processes in the atria of SHR another study would be required. It should be noted, that during the transition from compensated left ventricular hypertrophy to heart failure no further changes in [Na<sup>+</sup>]<sub>i</sub> were found, suggesting that changes in atrial myocyte [Na<sup>+</sup>]<sub>i</sub> do not play any major role for this transition.

Many previous studies described elevated [Na<sup>+</sup>]<sub>i</sub> in ventricular myocytes in human heart failure and animal models of cardiac disease (Pogwizd 2003), (Pieske & Houser 2003), (Despa & Bers 2013), (Clancy et al. 2015). As mentioned previously, increased [Na<sup>+</sup>]<sub>i</sub> alters NCX function by favouring Ca<sup>2+</sup> influx and Na<sup>+</sup> efflux. Elevated Ca<sup>2+</sup>, in turn, could produce arrhythmias and activate other pathological remodelling processes in the myocardium. However, our findings did not reveal any significant changes in [Na<sup>+</sup>]<sub>i</sub> in ventricular myocytes from old SHR. In addition to that, during the progression to heart failure no changes in [Na<sup>+</sup>]<sub>i</sub> in ventricular myocytes were found. However, we found that the stimulation-dependent change in [Na<sup>+</sup>]<sub>i</sub> was significantly lower in ventricular myocytes from failing SHR. This observation requires further investigation.

A previous study also reported unaltered [Na<sup>+</sup>]<sub>i</sub> in ventricular myocytes from SHR, however, in 5 months old SHR (Fowler et al. 2007). Of note, the values for [Na<sup>+</sup>]<sub>i</sub> reported in that study (≈10 mM) are in the same range as the values measured in our study (≈13 mM).

Thus, it may be speculated that [Na<sup>+</sup>]<sub>i</sub> in ventricular myocytes from old SHR is not of particular importance for alterations in Ca<sup>2+</sup> handling and contractility observed in this model by previous studies (Brooksby et al. 1993), (Fowler et al. 2007), (Kapur et al. 2010).

Taken together, our data indicate that atrial myocytes undergo specific Na<sup>+</sup> handling remodelling in old SHR, which is not observed in ventricular myocytes from the same animals. Decreased [Na<sup>+</sup>]<sub>i</sub> in atrial myocytes may contribute to a reduction in the amplitude of Ca<sup>2+</sup> transients and, thus, contractility.

#### **6.2.4. Up-regulation of Na<sup>+</sup> influx protein expression in the atria in advanced hypertensive heart disease**

Despite the observed decrease in atrial myocyte [Na<sup>+</sup>]<sub>i</sub>, the expression of some Na<sup>+</sup> influx proteins was increased in the atria of old SHR. NCX expression was higher in the right atrium of SHR and expression of NHE was enhanced in both atria.

NCX couples  $\text{Ca}^{2+}$  and  $\text{Na}^{+}$  handling in the myocardium. Increased expression of NCX in the atria was found in human atrial fibrillation (El-Armouche et al. 2006), (Neef et al. 2010) (Voigt et al. 2012). One study also revealed increased NCX function in ventricular myocytes from failing SHR (Rodriguez et al. 2014). The increased  $\text{Ca}^{2+}$  leak from the sarcoplasmic reticulum, observed in atrial fibrillation together with enhanced NCX function (or expression) might increase the NCX current, causing delayed afterdepolarizations and, thus, arrhythmias. Thus, increased NCX expression might contribute to the development of pro-arrhythmic events in the atrial myocardium of SHR. It should be noted that NCX expression in left and right atria was not changed in 7 months old SHR. Thus, the observed increase in NCX expression might contribute to the electrical remodelling of the atria in advanced hypertensive heart disease.

Another important observation in this study was a significant increase in NHE expression in both atria of SHR. The major role of this transporter is the extrusion of protons and, thus, maintenance of the physiological  $\text{pH}_i$ . Many studies have shown, that NHE function and/or expression are increased in ventricular myocytes during ischemic injury, hypertrophy and heart failure (Karmazyn et al. 1999), (Cingolani & Ennis 2007), (Baartscheer 2003). In SHR, the NHE function was significantly increased in the papillary muscles and in the whole heart (Ennis et al. 1998), (Schussheim & Radda 1995). However, the data regarding NHE expression and function in the atria are still sparse.

Several mechanisms might be responsible for the increased expression and/or activation of NHE (Karmazyn et al. 1999): ischemia, elevated levels of angiotensin II and endothelin-1 and mechanical stress of the atrial tissue. Jayachandran et al. described both increased NHE activation and expression in a dog model of atrial fibrillation (Jayachandran, J.V. et al. 2000). The authors of that study also proposed that in the fibrillating atria there might be a decrease in the coronary flow and, as a consequence, ischemic changes with the subsequent activation of NHE (Jayachandran, V. et al. 1998), (Jayachandran, J.V. et al. 2000). A more recent study of van Bragt et al. showed that in a pig model of atrial fibrillation increased oxygen demand with insufficient oxygen supply are present, suggesting ischemic conditions in the atrium during atrial fibrillation (van Bragt et al. 2014). As discussed previously, old SHR are prone to atrial arrhythmias, thus, ischemic conditions might be present in the atria of the SHR. As a result, NHE overexpression might be an adaptive mechanism for the  $\text{pH}_i$  maintenance within atrial myocytes during ischemic conditions and atrial tachyarrhythmias. However, another



study for the estimation of NHE function and pH balance in the atria of these rats would be needed to clarify this issue.

Previous research revealed that activation of NHE by angiotensin II, endothelin 1,  $\alpha$  1 adrenergic receptor agonists, and stretching contribute to the pathological remodelling of the myocardium (reviewed in (Wakabayashi et al. 2013)). Two studies of Jessup et al. found an elevated level of angiotensin II in the ventricle of young SHR and, overall, the RAAS was shown to be dysregulated (Jessup, Trask, et al. 2008), (Jessup, Brosnihan, et al. 2008). In addition to that, atrial tissue of 7 months old SHR was found to be constantly exposed to the elevated level of local angiotensin II (Bukowska et al. 2013), indicating that NHE might be also involved in angiotensin II-mediated pathological remodelling in the atria of SHR. In addition, severe diastolic dysfunction of old SHR (Slama et al. 2004) might cause an increase in left atrial pressure and mechanical stress of the atrial tissue, which ultimately might result in the stimulation of NHE function. However, the study of Kockskämper et al. revealed that in the human atrial myocardium the stretch-induced increase in  $[Na^+]_i$  was not the result of NHE activation (Kockskämper, Lewinski, et al. 2008) and the mechanism responsible for this effect is not yet elucidated.

To conclude, overexpression of NHE in atria from old SHR observed in this study is a potential indicator for activation of various signalling pathways, which might be involved in atrial remodelling in advanced hypertensive heart disease. Thus, elucidation of these mechanisms could be an interesting direction for future research.

#### **6.2.5. Up-regulation of NKA expression in the atria in advanced hypertensive heart disease**

$\alpha$  1 is the dominant isoform of NKA, regulating the bulk  $[Na^+]_i$  (Despa & Bers 2007). Our findings indicate that expression of the  $\alpha$  1 subunit of NKA was significantly increased in both atria of SHR. In addition, expression of the  $\alpha$  2 isoform was elevated in right atrium together with decreased PLM expression, suggesting increased NKA activity and, thus, enhanced  $Na^+$  extrusion. We suggest that these changes are responsible for the reduced  $[Na^+]_i$  in atrial myocytes from old SHR. During the transition from compensated left ventricular hypertrophy to heart failure no further changes in the  $\alpha$  1 subunit expression were found, which is in line with unchanged  $[Na^+]_i$ . Interestingly, expression of the  $\alpha$  2 subunit was elevated in the right and decreased in the left atrium during this

transition. Recent studies have shown that the  $\alpha 2$  isoform plays an important role in ventricular myocytes. As shown by Despa et al. in rat ventricular myocytes,  $\alpha 2$  co-localizes with NCX (Despa & Bers 2007), and preferentially regulates  $\text{Ca}^{2+}$  removal by NCX (Correll et al. 2014). Moreover, changes in local  $\text{Na}^+$  concentration could regulate NCX activity and contractility of rat ventricular myocytes without changes in the bulk  $[\text{Na}^+]_i$  (Swift et al. 2010). Thus, similar processes could occur in atrial myocytes. However, by now data on the co-localization of  $\text{Na}^+$ -handling proteins in atrial myocytes are not available and the role of the  $\alpha 2$  isoform remains elusive.

The data regarding changes in the expression and function of NKA in various animal models of atrial fibrillation and heart failure differ. In a rat model of heart failure, the activity and the expression of the  $\alpha 2$  isoform were reduced in the ventricles (Swift et al. 2008). However, another study of Schwinger et al. revealed that in failing human ventricular myocardium expression of  $\alpha 1$ ,  $\alpha 3$  and  $\beta 1$  subunits were significantly reduced, whereas  $\alpha 2$  subunit expression remained unchanged and the activity of the pump was significantly reduced (Schwinger et al. 1999). Expression of PLM in failing ventricular myocardium was also significantly reduced together with an increase in its phosphorylation, so the NKA pumping function was suggested to be increased in that study, as a compensation for a decrease in  $\alpha 1$  and  $\alpha 2$  subunit expression (Bossuyt 2005). Studies on the expression or function of NKA in the atria show contradictory findings, however, the majority of them indicate that changes in NKA expression or function are not observed in human atrial fibrillation (reviewed in the next section).

Thus, the intracellular  $\text{Na}^+$  homeostasis was altered in the atria of SHR towards the maintenance of lower  $[\text{Na}^+]_i$ , presumably due to an increase in  $\alpha 1$  expression and, possibly, function of NKA.

In conclusion, long-standing hypertension in SHR caused atrial remodelling characterized by bi-atrial hypertrophy, decline in the contractile function, decreased  $[\text{Na}^+]_i$ , and increased expression of NHE and NKA. At the same time ventricular remodelling was characterized by progression of hypertrophy, unchanged contractile function of ventricular myocytes and unaltered  $[\text{Na}^+]_i$ . Presented results suggest that atrial remodelling might contribute to the development of ventricular remodelling and heart failure.

Figure 44 schematically presents the major findings of the study on the atrial remodelling in SHR in advanced hypertension.

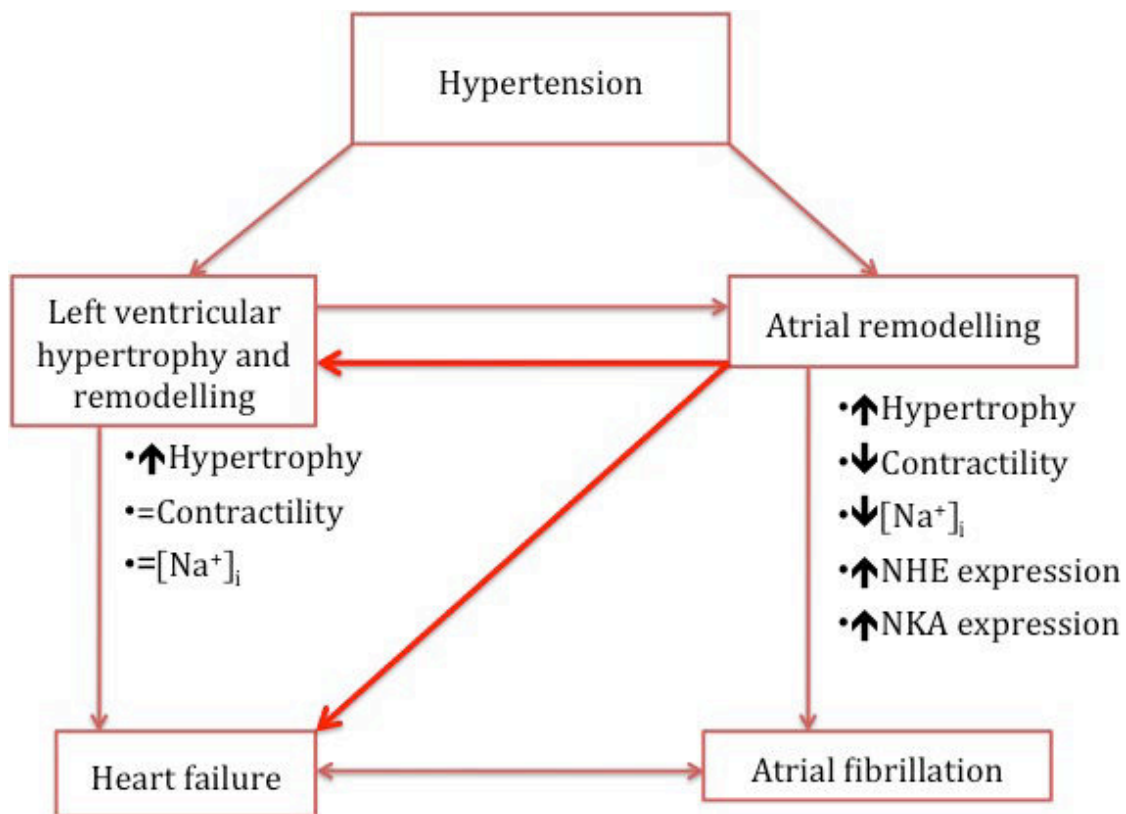


**Figure 44. Atrial remodelling in advanced hypertensive heart disease in SHR**

### **6.3. Unaltered expression of Na<sup>+</sup>-handling proteins in human atrial fibrillation**

The aim of the second part of the thesis was to characterize expression of Na<sup>+</sup>-handling proteins in the atria of patients suffering from paroxysmal (pAF) or chronic atrial fibrillation (cAF). Expression of Na<sup>+</sup> influx proteins was largely unaltered in atrial fibrillation, whereas expression of the  $\beta$  1 subunit of NKA was reduced in cAF.

In our study we analyzed expression of all alpha subunits of Na<sup>+</sup> channel by using an antibody raised to detect all alpha isoforms of voltage-gated Na<sup>+</sup> channels. Our data indicate that the expression of all alpha subunit isoforms of Na<sup>+</sup> channels was unchanged in pAF or cAF. In human atrial myocardium six different isoforms of alpha subunits of voltage-gated Na<sup>+</sup> channels are present: Na<sub>v</sub>1.1-Na<sub>v</sub>1.6 with Na<sub>v</sub>1.5 being the major cardiac isoform (Kaufmann et al. 2013). In cAF, as was shown by Sossalla et al., there is a transition in the expression of different alpha isoforms of Na<sup>+</sup> channels towards neuronal isoforms (Na<sub>v</sub>1.1 and Na<sub>v</sub>1.6) and a reduction in the expression of the major cardiac isoform Na<sub>v</sub>1.5 (Sossalla et al. 2010). Thus, our data provide information only about the total expression of all alpha isoforms and could not detect the changes in the expression of particular isoforms.

NCX expression was unaltered in pAF, whereas we observed a tendency towards an increase in NCX expression in cAF. Previous studies (El-Armouche et al. 2006), (Neef et al. 2010), (Voigt et al. 2012) found a significant increase in NCX expression in cAF. Moreover, NCX function was increased in cAF (Neef et al. 2010), whereas in pAF its expression and function were unaltered (Voigt et al. 2012). Increased NCX expression and function (together with increased Ca<sup>2+</sup> leak from the sarcoplasmic reticulum) has an important impact on the atrial electrophysiology: it facilitates the development of delayed afterdepolarizations and, thus, induces arrhythmias (Voigt et al. 2012). As discussed previously, NCX expression was significantly increased in the right atrium of old SHR, when atrial functional and structural remodelling had manifested.

Expression of NHE was unaltered in either pAF or cAF. The data regarding NHE expression in human AF are limited. Jayachandran et al. described both increased NHE activation and expression in dog rapid pacing atrial fibrillation (J. V. Jayachandran et al. 2000). A more recent study of van Bragt et al. showed that in a pig model of atrial

fibrillation oxygen demand with insufficient oxygen supply are present, indicating the presence of ischemic conditions in the atrium during atrial fibrillation (van Bragt et al. 2014). Ischemia would potentially lead to an increase in NHE expression or function (Avkiran & Haworth 2003), (Imahashi et al. 2007). Moreover, we observed increased NHE expression in both atria of old SHR. In our study on human atrial myocardium, we did not perform analysis of NHE function and thus, alterations in NHE function in human AF cannot be excluded.

Expression of the various  $\alpha$  subunits of NKA was unaltered in atrial fibrillation, however,  $\beta$  1 subunit expression was significantly decreased in cAF. The data on NKA function and expression in human AF and animal models of AF vary. For instance, Workman et al. found that NKA current in cAF was unchanged (Workman et al. 2003). In a sheep model of AF unchanged  $\alpha$  1 expression and an increase in  $\beta$  1 expression was observed (Maixent et al. 2002). Another study using a rabbit model of rapid atrial pacing found unchanged expression of the  $\alpha$  1 subunit together with a reduction in PLM phosphorylation and, thus, a decrease in NKA function (Greiser et al. 2014). Thus, the data on NKA expression and function in atrial fibrillation are variable. In human heart failure expression of the  $\beta$  1 subunit was significantly reduced in left ventricle (Schwinger et al. 1999), which is in line with our finding of decreased  $\beta$  1 expression in cAF. The  $\beta$  1 subunit of NKA is necessary for trafficking of the pump and proper insertion of NKA into the plasma membrane (Geering 2001). Thus, its down-regulation would provide evidence for impaired NKA function. On the other hand, expression of the regulatory protein PLM was unchanged, suggesting that NKA function is not markedly affected during atrial fibrillation. However, another western blot study should be done in order to analyze the phosphorylation of PLM in human atrial fibrillation.

Taken together, the presented results indicate that there are no major changes in the expression of  $\text{Na}^+$ -handling proteins in human atrial fibrillation, except for reduced expression of the  $\beta$  1 subunit of NKA. The functional relevance of this change is probably negligible, since NKA function/current is not altered in human atrial fibrillation, as was shown by Workman et al. (Workman et al. 2003). Whether  $[\text{Na}^+]_i$  is changed in atrial myocytes in human atrial fibrillation remains to be determined.

Interestingly, in SHR model the expression and the function of NKA was also decreased in the atria, however, due to the reduction in  $\alpha$  1 expression. In line with our findings in SHR, expression of  $\text{Na}^+$  channels was also unchanged in atrial fibrillation. However, a

significant increase in NHE and NCX expression, observed in SHR, was not seen in human atrial fibrillation.

Thus, the expression pattern of Na<sup>+</sup>-handling proteins in the atria of SHR and in human atrial fibrillation was different.

## **6.4. Macitentan treatment did not markedly affect atrial Ca<sup>2+</sup> remodelling in SHR**

### **6.4.1. Macitentan treatment did not lower blood pressure in SHR**

The aim of this project was to test the hypothesis that inhibition of endothelin receptors (ETR) reverses or reduces the atrial proarrhythmic remodelling in SHR in terms of Ca<sup>2+</sup> handling and endothelin-1 signalling proteins expression. We found that macitentan treatment for 8 weeks did not markedly affect hemodynamic parameters, expression of Ca<sup>2+</sup>-handling proteins and proteins involved in the endothelin-1 signalling pathway in the atria of SHR.

Macitentan significantly increased diastolic and mean blood pressure in SHR. This observation is interesting. Macitentan inhibits both types of ET receptors (ETR): ET<sub>A</sub>R and ET<sub>B</sub>R (Iglarz et al. 2008). ET<sub>B</sub> is abundantly expressed in endothelial cells, where its activation causes increased production of NO and PGI<sub>2</sub>, which act as vasodilators (Horinouchi et al. 2013). Thus, inhibition of ET<sub>B</sub>R by Macitentan theoretically could cause reduced production of vasodilators and, thus, an increase in diastolic blood pressure.

Interestingly, Macitentan treatment significantly reduced mean arterial blood pressure in another rat model of hypertension: Dahl salt-sensitive rats (Bolli et al. 2012). Macitentan administration for 8 weeks caused a significant reduction in diastolic blood pressure in patients with essential systemic hypertension (Kholdani et al. 2014). The treatment with bosentan (another dual endothelin receptor antagonist) did not affect the blood pressure in young SHR (from 12 to 16 weeks of age) (Li & Schiffrin 1995). Another study by Nishikibe et al. also found that an ETR antagonist did not lower blood pressure in 18-19 weeks and 40 weeks (10 months) old SHR (Nishikibe et al. 1993). However, in patients with essential hypertension bosentan administration resulted in a decrease in diastolic blood pressure (Krum et al. 1998). Thus, the observed increase in diastolic blood pressure by macitentan administration in SHR requires further investigation.

We observed a significant reduction in systolic blood pressure in SHR by doxazosin. doxazosin is a selective  $\alpha$  1 adrenergic blocker. Inhibition of  $\alpha$  1 adrenergic receptors results in the lowering of intracellular Ca<sup>2+</sup> concentration in the vascular smooth muscle

cells and, thus, dilatation of the blood vessels and a decrease in blood pressure (O'Connell et al. 2014). Many previous studies confirmed the reduction in systolic blood pressure by doxazosin in SHR (Hamada et al. 2012), (Asai et al. 2005). Thus, the observed decrease in the systolic blood pressure by doxazosin in SHR is in line with previous studies.

In summary, treatment of SHR with doxazosin but not macitentan lowered blood pressure.

#### **6.4.2. Macitentan treatment did not alter expression of key Ca<sup>2+</sup>-handling proteins in left atria of SHR**

Previous observations from our laboratory revealed that 7 months old SHR exhibited impaired Ca<sup>2+</sup> handling and altered expression of some Ca<sup>2+</sup> regulating proteins: decreased expression of the L-type Ca<sup>2+</sup> channel, the RyR and increased phosphorylation of the RyR at serine 2808 (Pluteanu et al. 2015). Moreover, atrial myocytes from SHR exhibited an increased response to endothelin-1 with elevation of Ca<sup>2+</sup> transients and the development of proarrhythmic events. Some components of the endothelin-1 signalling pathway were upregulated on the mRNA or protein level in left atria of 7 months old SHR (Pluteanu et al. 2013). Thus, we proposed that inhibition of ETR would affect expression of some key Ca<sup>2+</sup>-handling proteins in the atria of SHR. We found, however, that expression of most Ca<sup>2+</sup>-regulating proteins was not altered by macitentan administration.

Expression of the  $\alpha$  1 subunit of L-type Ca<sup>2+</sup> channels, the RyR and its phosphorylation status, and NCX was not changed. Thus, sarcolemmal Ca<sup>2+</sup> entry and Ca<sup>2+</sup> release from the SR were most probably unaffected by macitentan treatment. Expression of SERCA, PLB, its phosphorylation and CSQ expression were also not significantly affected by macitentan, suggesting unaltered Ca<sup>2+</sup> reuptake into the SR. Thus, the Ca<sup>2+</sup> cycle in atrial myocytes on the protein expression level was not affected by inhibition of endothelin receptors in SHR.

Doxazosin treatment also did not markedly affect expression of Ca<sup>2+</sup>-handling proteins, except for a 20% decrease in PLB expression. The potential functional relevance of this alteration is, however, difficult to predict.

We did not observe any changes in the activity of PKA or CaMKII, as indirectly shown by unchanged phosphorylation of their targets: RyR and PLB. Interestingly, expression of CaMKII was significantly reduced by both macitentan and doxazosin. CaMKII plays a



critical role in endothelin-1-mediated hypertrophic effects (Zhu et al. 2000) and adverse cardiac remodelling (Anderson et al. 2011). Thus, inhibition of the ETR could decrease CaMKII expression and prevent some aspects of cardiac remodelling. However, the autophosphorylation of CaMKII and the phosphorylation of two important targets of CaMKII, (RyR and PLB), was not altered, suggesting that the CaMKII activity was unaffected. It should be noted, that we did not perform analysis of phosphatase expression or activity and, thus, we can not exclude the possibility that changes in phosphatases function occurred in parallel. Furthermore, local regulation of phosphatases and kinases was not addressed in this study.

In summary, macitentan administration did not induce any major changes in the expression or phosphorylation of Ca<sup>2+</sup>-handling proteins.

#### **6.4.3. Expression of proteins involved in endothelin-1 signalling is not affected by macitentan treatment**

Activation of ET<sub>A</sub>R causes production of two important second messengers: IP<sub>3</sub> and diacylglycerol (DAG). We analyzed expression of some proteins involved in the endothelin signalling cascade and we found that expression of ET<sub>A</sub>R, PLCβ and IP<sub>3</sub>R was unchanged. Another part of this pathway includes activation of PKC by DAG. PKC phosphorylates various proteins, such as NHE, NCX, L-Type Ca<sup>2+</sup> channels and PLB, stimulating a positive inotropic response and development of pro-arrhythmogenic events in the myocardium (Drawnel et al. 2013), (Kockskämper, Zima, et al. 2008). In our study, we did not focus on the DAG-PKC cascade, although we analyzed the phosphorylation of PLB by PKC at serine 10 and found that it was unchanged by macitentan. Thus, it can be assumed that the activity of PKC was not altered by macitentan. Similar to macitentan, doxazosin also did not affect phosphorylation of PLB by PKC at serine 10.

ET<sub>A</sub>R and α 1 adrenergic receptor belong to the Gq-coupled receptor family. We found that macitentan treatment slightly enhanced expression of the ET<sub>A</sub>R (by almost 50%, although this effect was statistically not significant). Chronic treatment with GPCR antagonists, as in case of macitentan, often results in up-regulation of the receptors due to increased protein synthesis of the receptor or receptor trafficking to the plasma membrane (Hendriks-Balk et al. 2008). Thus, the observed increase in the expression of ET<sub>A</sub>R by macitentan treatment is in line with such a mechanism. In case of doxazosin administration, however, we observed a decrease in α 1 adrenergic receptor expression.

In line with our observation, a study by Wikberg et al. found that  $\alpha$  1 adrenergic receptor antagonists can down-regulate this receptor in vascular smooth muscle cells (Wikberg et al. 1983). However, as was shown by Zhang et al., prazosin (another  $\alpha$ 1 adrenoceptor antagonist) up-regulated  $\alpha$  1 adrenergic receptor expression in rat heart and spleen (Zhang et al. 2002). Another study by Yono et al. found an up-regulation of the  $\alpha$  1 adrenergic receptor expression on the mRNA level in rat heart (Yono et al. 2004) . Thus, both up- and down-regulation of  $\alpha$  1 adrenergic receptors have been observed following its inhibition.

Taken together, our findings indicate that the blockade of ETRs with macitentan did not lower the blood pressure or alter expression of key  $\text{Ca}^{2+}$ -handling, and endothelin-1 signalling proteins in the atria of 7 months old SHR.

## 7. References

- Aiello, E.A. et al., 2005. Endothelin-1 stimulates the Na<sup>+</sup>/Ca<sup>2+</sup> exchanger reverse mode through intracellular Na<sup>+</sup> (Na<sup>+</sup><sub>i</sub>)-dependent and Na<sup>+</sup><sub>i</sub>-independent pathways. *Hypertension*, 45(2), pp.288–293.
- Akar, J.G. et al., 2003. Intracellular chloride accumulation and subcellular elemental distribution during atrial fibrillation. *Circulation*, 107(13), pp.1810–1815.
- Anderson, M.E., Brown, J.H. & Bers, D.M., 2011. CaMKII in myocardial hypertrophy and heart failure. *Journal of Molecular and Cellular Cardiology*, 51(4), pp.468–473.
- Andrade, J. et al., 2014. The clinical profile and pathophysiology of atrial fibrillation: relationships among clinical features, epidemiology, and mechanisms. *Circulation Research*, 114(9), pp.1453–1468.
- Anter, E., Jessup, M. & Callans, D.J., 2009. Atrial fibrillation and heart failure: treatment considerations for a dual epidemic. *Circulation*, 119(18), pp.2516–2525.
- Aronsen, J.M., Swift, F. & Sejersted, O.M., 2013. Cardiac sodium transport and excitation–contraction coupling. *Journal of Molecular and Cellular Cardiology*, 61, pp.11–19.
- Asai, T. et al., 2005. Different effects on inhibition of cardiac hypertrophy in spontaneously hypertensive rats by monotherapy and combination therapy of adrenergic receptor antagonists and/or the angiotensin II type 1 receptor blocker under comparable blood pressure reduction. *Hypertension research : official journal of the Japanese Society of Hypertension*, 28(1), pp.79–87.
- Avkiran, M., 2003. Basic biology and pharmacology of the cardiac sarcolemmal sodium/hydrogen exchanger. *Journal of Cardiac Surgery*, 18 Suppl 1, pp.3–12.
- Avkiran, M. & Haworth, R.S., 1999. Regulation of cardiac sarcolemmal Na<sup>+</sup>/H<sup>+</sup> exchanger activity by endogenous ligands. Relevance to ischemia. *Annals of the New York Academy of Sciences*, 874, pp.335–345.
- Avkiran, M. & Haworth, R.S., 2003. Regulatory effects of G protein-coupled receptors on cardiac sarcolemmal Na<sup>+</sup>/H<sup>+</sup> exchanger activity: signalling and significance. *Cardiovascular Research*, 57(4), pp.942–952.
- Baartscheer, A., 2003. Increased Na<sup>+</sup>/H<sup>+</sup>-exchange activity is the cause of increased [Na<sup>+</sup>]<sub>i</sub> and underlies disturbed calcium handling in the rabbit pressure and volume overload heart failure model. *Cardiovascular Research*, 57(4), pp.1015–1024.
- Baartscheer, A. & van Borren, M., 2008. Sodium Ion Transporters as New Therapeutic Targets in Heart Failure. *Cardiovascular & Hematological Agents in Medicinal Chemistry*, 6(4), pp.229–236.
- Benjamin, E.J. et al., 1995. Left Atrial Size and the Risk of Stroke and Death : The Framingham Heart Study. *Circulation*, 92(4), pp.835–841.

- Berridge, M.J., Bootman, M.D. & Roderick, H.L., 2003. Calcium signalling: dynamics, homeostasis and remodelling. *Nature Reviews Molecular Cell Biology*, 4(7), pp.517–529.
- Bers, D.M., 2002. Cardiac excitation-contraction coupling. *Nature*, 415(6868), pp.198–205.
- Bers, D.M. & Despa, S., 2009. Na<sup>+</sup> transport in cardiac myocytes; Implications for excitation-contraction coupling. *IUBMB Life*, 61(3), pp.215–221.
- Bers, D.M., Despa, S. & Bossuyt, J., 2006. Regulation of Ca<sup>2+</sup> and Na<sup>+</sup> in Normal and Failing Cardiac Myocytes. *Annals of the New York Academy of Sciences*, 1080(1), pp.165–177.
- Bianchi, G. et al., 1974. Blood Pressure Changes Produced by Kidney Cross-Transplantation between Spontaneously Hypertensive Rats and Normotensive Rats. *Clinical Science*, 47(5), pp.435–448.
- Bing, O.H.L. et al., 2002. Studies of Prevention, Treatment and Mechanisms of Heart Failure in the Aging Spontaneously Hypertensive Rat. *Heart Failure Reviews*, 7(1), pp.71–88.
- Blatter, L.A. et al., 2003. Local calcium gradients during excitation–contraction coupling and alternans in atrial myocytes. *The Journal of Physiology*, 546(1), pp.19–31.
- Bodor, G.S. et al., 1997. Troponin I phosphorylation in the normal and failing adult human heart. *Circulation*, 96(5), pp.1495–1500.
- Bolli, M.H. et al., 2012. The Discovery of N-[5-(4-Bromophenyl)-6-[2-[(5-bromo-2-pyrimidinyl)oxy]ethoxy]-4-pyrimidinyl]-N'-propylsulfamide (Macitentan), an Orally Active, Potent Dual Endothelin Receptor Antagonist. *Journal of Medicinal Chemistry*, 55(17), pp.7849–7861.
- Bootman, M.D. et al., 2011. Atrial cardiomyocyte calcium signalling. *BBA - Molecular Cell Research*, 1813(5), pp.922–934.
- Bootman, M.D. et al., 2006. Calcium signalling during excitation-contraction coupling in mammalian atrial myocytes. *Journal of Cell Science*, 119(Pt 19), pp.3915–3925.
- Bosch, R.F. et al., 1999. Ionic mechanisms of electrical remodeling in human atrial fibrillation. *Cardiovascular Research*, 44(1), pp.121–131.
- Bossuyt, J., 2005. Expression and Phosphorylation of the Na-Pump Regulatory Subunit Phospholemman in Heart Failure. *Circulation Research*, 97(6), pp.558–565.
- Bountra, C. & Vaughan-Jones, R.D., 1989. Effect of intracellular and extracellular pH on contraction in isolated, mammalian cardiac muscle. *The Journal of Physiology*, 418(1), pp.163–187.
- Brooks, W.W. et al., 2010. Transition from compensated hypertrophy to systolic heart failure in the spontaneously hypertensive rat: Structure, function, and transcript analysis. *Genomics*, 95(2), pp.84–92.

- Brooksby, P., Levi, A.J. & Jones, J.V., 1993. Investigation of the mechanisms underlying the increased contraction of hypertrophied ventricular myocytes isolated from the spontaneously hypertensive rat. *Cardiovascular Research*, 27(7), pp.1268–1277.
- Bukowska, A., Hartmann, A. & Chilukoti, R.K., 2013. Atrial tachyarrhythmia causes atrial imbalance of the Ace/Ace2 ratio in aged and hypertensive rats. *European Heart Journal*, 34(suppl 1), P4989-P4989.
- Burstein, B. & Nattel, S., 2008. Atrial Fibrosis: Mechanisms and Clinical Relevance in Atrial Fibrillation. *JAC*, 51(8), pp.802–809.
- Bylund, D.B. et al., 1994. International Union of Pharmacology nomenclature of adrenoceptors. *Pharmacological Reviews*, 46(2), pp.121–136.
- Camm, A.J. et al., 2012. A proposal for new clinical concepts in the management of atrial fibrillation. *American Heart Journal*, 164(3), pp.292–302.e1.
- Carson, P.E. et al., 1993. The influence of atrial fibrillation on prognosis in mild to moderate heart failure. The V-HeFT Studies. The V-HeFT VA Cooperative Studies Group. *Circulation*, 87(6 Suppl), pp.VI102–10.
- Casaclang-Verzosa, G., Gersh, B.J. & Tsang, T.S.M., 2008. Structural and Functional Remodeling of the Left Atrium. *Journal of the American College of Cardiology*, 51(1), pp.1–11.
- Chan, V. et al., 2011. Cardiovascular changes during maturation and ageing in male and female spontaneously hypertensive rats. *Journal of cardiovascular pharmacology*, 57(4), pp.469–478.
- Chen, P.S. et al., 2014. Role of the Autonomic Nervous System in Atrial Fibrillation: Pathophysiology and Therapy. *Circulation Research*, 114(9), pp.1500–1515.
- Chen-Izu, Y. et al., 2015. Na<sup>+</sup> channel function, regulation, structure, trafficking and sequestration. *The Journal of Physiology*, 593(6), pp.1347–1360.
- Choisy, S.C.M. et al., 2007. Increased Susceptibility to Atrial Tachyarrhythmia in Spontaneously Hypertensive Rat Hearts. *Hypertension*, 49(3), pp.498–505.
- Cingolani, H.E. & Ennis, I.L., 2007. Sodium-Hydrogen Exchanger, Cardiac Overload, and Myocardial Hypertrophy. *Circulation*, 115(9), pp.1090–1100.
- Clancy, C.E. et al., 2015. Deranged sodium to sudden death. *The Journal of Physiology*, 593(6), pp.1331–1345.
- Conrad, C.H. et al., 1991. Impaired myocardial function in spontaneously hypertensive rats with heart failure. *The American journal of physiology*, 260(1 Pt 2), pp.H136–45.
- Coppini, R. et al., 2013. Regulation of intracellular Na<sup>+</sup> in health and disease: pathophysiological mechanisms and implications for treatment. *Global Cardiology Science and Practice*, 2013(3), p.30.

- Correll, R.N. et al., 2014. Overexpression of the Na<sup>+</sup>/K<sup>+</sup> ATPase 2 But Not 1 Isoform Attenuates Pathological Cardiac Hypertrophy and Remodeling. *Circulation Research*, 114(2), pp.249–256.
- David, G., Barrett, J.N. & Barrett, E.F., 1997. Spatiotemporal gradients of intra-axonal [Na<sup>+</sup>] after transection and resealing in lizard peripheral myelinated axons. *The Journal of Physiology*, 498(2), pp.295–307.
- Despa, S., 2002. Intracellular Na<sup>+</sup> Concentration Is Elevated in Heart Failure But Na/K Pump Function Is Unchanged. *Circulation*, 105(21), pp.2543–2548.
- Despa, S. & Bers, D.M., 2007. Functional analysis of Na<sup>+</sup>/K<sup>+</sup>-ATPase isoform distribution in rat ventricular myocytes. *AJP: Cell Physiology*, 293(1), pp.C321–C327.
- Despa, S. & Bers, D.M., 2013. Na<sup>+</sup> transport in the normal and failing heart — Remember the balance. *Journal of Molecular and Cellular Cardiology*, pp.1–9.
- Despa, S. et al., 2004. Na/K Pump-Induced [Na]<sub>i</sub> Gradients in Rat Ventricular Myocytes Measured with Two-Photon Microscopy. *Biophysical Journal*, 87(2), pp.1360–1368.
- Diamond, J.A. & Phillips, R.A., 2005. Hypertensive Heart Disease. *Hypertension research : official journal of the Japanese Society of Hypertension*, 28(3), pp.191–202.
- Diarra, A., Sheldon, C. & Church, J., 2001. In situ calibration and [H<sup>+</sup>] sensitivity of the fluorescent Na<sup>+</sup> indicator SBFI. *AJP: Cell Physiology*, 280(6), pp.C1623–33.
- Díez, J., 2007. Mechanisms of Cardiac Fibrosis in Hypertension. *The Journal of Clinical Hypertension*, 9(7), pp.546–550.
- Dobrev, D. & Nattel, S., 2010. New antiarrhythmic drugs for treatment of atrial fibrillation. *The Lancet*, 375(9721), pp.1212–1223.
- Dodd, M.S. et al., 2012. In vivo alterations in cardiac metabolism and function in the spontaneously hypertensive rat heart. *Cardiovascular Research*, 95(1), pp.69–76.
- Doggrell, S.A. & Brown, L., 1998. Rat models of hypertension, cardiac hypertrophy and failure. *Cardiovascular Research*, 39(1), pp.89–105.
- Donoso, P., Mill, J.G., O'Neill, S.C. & Eisner, D.A., 1992. Fluorescence measurements of cytoplasmic and mitochondrial sodium concentration in rat ventricular myocytes. *The Journal of Physiology*, 448(1), pp.493–509.
- Drawnel, F.M., Archer, C.R. & Roderick, H.L., 2013. The role of the paracrine/autocrine mediator endothelin-1 in regulation of cardiac contractility and growth. *British Journal of Pharmacology*, 168(2), pp.296–317.
- Drazner, M.H., 2011. The progression of hypertensive heart disease. *Circulation*, 123(3), pp.327–334.

- Dunn, F.G., Pfeffer, M.A. & Frohlich, E.D., 1978. ECG alterations with progressive left ventricular hypertrophy in spontaneous hypertension. *Clinical and experimental Hypertension*, 1(1), pp.67–86.
- Duru, F. et al., 2001. Endothelin and cardiac arrhythmias: do endothelin antagonists have a therapeutic potential as antiarrhythmic drugs? *Cardiovascular Research*, 49(2), pp.272–280.
- El-Armouche, A. et al., 2006. Molecular determinants of altered  $\text{Ca}^{2+}$  handling in human chronic atrial fibrillation. *Circulation*, 114(7), pp.670–680.
- Ennis, I.L. et al., 1998. Enalapril induces regression of cardiac hypertrophy and normalization of pHi regulatory mechanisms. *Hypertension*, 31(4), pp.961–967.
- Fedorova, O.V. et al., 2004. Coordinated shifts in Na/K-ATPase isoforms and their endogenous ligands during cardiac hypertrophy and failure in NaCl-sensitive hypertension. *Journal of hypertension*, 22(2), p.389.
- Felker, G.M. et al., 2003. The problem of decompensated heart failure: Nomenclature, classification, and risk stratification. *American Heart Journal*, 145(2), pp.S18–S25.
- Ferreira, J. & Santos, M., 2015. Heart Failure and Atrial Fibrillation: From Basic Science to Clinical Practice. *International Journal of Molecular Sciences*, 16(2), pp.3133–3147.
- Filtz, T.M. et al., 2009. Gq-initiated cardiomyocyte hypertrophy is mediated by phospholipase C $\beta$ 1b. *FASEB journal : official publication of the Federation of American Societies for Experimental Biology*, 23(10), pp.3564–3570.
- Fischer, T.H. et al., 2015. Late  $I_{\text{Na}}$  increases diastolic SR- $\text{Ca}^{2+}$ -leak in atrial myocardium by activating PKA and CaMKII. *Cardiovascular Research*, 107(1), pp.184–196.
- Fowler, M.R., 2005. Decreased  $\text{Ca}^{2+}$  extrusion via  $\text{Na}^+/\text{Ca}^{2+}$  exchange in epicardial left ventricular myocytes during compensated hypertrophy. *AJP: Heart and Circulatory Physiology*, 288(5), pp.H2431–H2438.
- Fowler, M.R., 2007. Age and hypertrophy alter the contribution of sarcoplasmic reticulum and  $\text{Na}^+/\text{Ca}^{2+}$  exchange to  $\text{Ca}^{2+}$  removal in rat left ventricular myocytes. *Journal of Molecular and Cellular Cardiology*, 42(3), pp.582–589.
- Fuller, W. et al., 2012. Regulation of the cardiac sodium pump. *Cellular and Molecular Life Sciences*, 70(8), pp.1357–1380.
- Geering, K., 2001. The Functional Role of  $\beta$  Subunits in Oligomeric P-Type ATPases. *Journal of bioenergetics and biomembranes*, 33(5), pp.425–438.
- Greene, R.J. & Harris, N.D., 2008. Pathology and therapeutics for pharmacists: a basis for clinical pharmacy practice. :Pharmaceutical Press; 2008, pp.209-210, p.186.
- Greiser, M. et al., 2014. Tachycardia-induced silencing of subcellular  $\text{Ca}^{2+}$  signaling in atrial myocytes. *Journal of Clinical Investigation*, 124(11), pp.4759–4772.

- Hamada, N. et al., 2012. Disrupted regulation of ghrelin production under antihypertensive treatment in spontaneously hypertensive rats. *Circulation journal : official journal of the Japanese Circulation Society*, 76(6), pp.1423–1429.
- Harootunian, A.T. et al., 1989. Fluorescence ratio imaging of cytosolic free Na<sup>+</sup> in individual fibroblasts and lymphocytes. *Journal of Biological Chemistry*, 264(32), pp.19458–19467.
- Hasler, U. et al., 1998. Role of  $\beta$ -Subunit Domains in the Assembly, Stable Expression, Intracellular Routing, and Functional Properties of Na,K-ATPase. *Journal of Biological Chemistry*, 273(46), pp.30826–30835.
- Hattori, R. et al., 2001. NHE and ICAM-1 expression in hypoxic/reoxygenated coronary microvascular endothelial cells. *AJP: Heart and Circulatory Physiology*, 280(6), pp.H2796–803.
- Healey, J.S. & Connolly, S.J., 2003. Atrial fibrillation: hypertension as a causative agent, risk factor for complications, and potential therapeutic target. *The American journal of cardiology*, 91(10), pp.9–14.
- Heijman, J. et al., 2014. Cellular and molecular electrophysiology of atrial fibrillation initiation, maintenance, and progression. *Circulation Research*, 114(9), pp.1483–1499.
- Heineke, J. & Molkenin, J.D., 2006. Regulation of cardiac hypertrophy by intracellular signalling pathways. *Nature Reviews Molecular Cell Biology*, 7(8), pp.589–600.
- Hendriks-Balk, M.C. et al., 2008. Regulation of G protein-coupled receptor signalling: Focus on the cardiovascular system and regulator of G protein signalling proteins. *European Journal of Pharmacology*, 585(2-3), pp.278–291.
- Hisamitsu, T., Nakamura, T.Y. & Wakabayashi, S., 2012. Na<sup>+</sup>/H<sup>+</sup> Exchanger 1 Directly Binds to Calcineurin A and Activates Downstream NFAT Signaling, Leading to Cardiomyocyte Hypertrophy. *Molecular and Cellular Biology*, 32(16), pp.3265–3280.
- Horinouchi, T. et al., 2013. Endothelin Receptor Signaling: New Insight Into Its Regulatory Mechanisms. *Journal of Pharmacological Sciences*, 123(2), pp.85–101.
- Houser, S.R. et al., 2012. Animal models of heart failure: a scientific statement from the American Heart Association. *Circulation Research*, 111(1), pp.131–150.
- Huke, S. & Bers, D.M., 2008. Ryanodine receptor phosphorylation at Serine 2030, 2808 and 2814 in rat cardiomyocytes. *Biochemical and biophysical research communications*, 376(1), pp.80–85.
- Iglarz, M. & Clozel, M., 2010. At the heart of tissue: endothelin system and end-organ damage. *Clinical science (London, England : 1979)*, 119(11), pp.453–463.
- Iglarz, M. et al., 2008. Pharmacology of macitentan, an orally active tissue-targeting dual endothelin receptor antagonist. *The Journal of pharmacology and experimental therapeutics*, 327(3), pp.736–745.



- Imahashi, K. et al., 2007. Overexpression of the Na<sup>+</sup>/H<sup>+</sup>exchanger and ischemia-reperfusion injury in the myocardium. *AJP: Heart and Circulatory Physiology*, 292(5), pp.H2237–H2247.
- Ito, S., Ohta, T. & Nakazato, Y., 1997. Changes in intracellular Na<sup>+</sup> concentration evoked by nicotinic receptor activation in the guinea-pig adrenal chromaffin cells. *Neuroscience letters*, 238(3), pp.111–114.
- January, C.T. & Fozzard, H.A., 1988. Delayed afterdepolarizations in heart muscle: mechanisms and relevance. *Pharmacological Reviews*, 40(3), pp.219–227.
- Jayachandran, J.V. et al., 2000. Atrial fibrillation produced by prolonged rapid atrial pacing is associated with heterogeneous changes in atrial sympathetic innervation. *Circulation*, 101(10), pp.1185–1191.
- Jayachandran, V. et al., 1998. Chronic atrial fibrillation from rapid atrial pacing is associated with reduced atrial blood flow: A positron emission tomography study. *Circulation*, 98(17), pp.209–209.
- Jäger, H. et al., 2001. Expression of sodium pump isoforms and other sodium or calcium ion transporters in the heart of hypertensive patients. *Biochimica et biophysica acta*, 1513(2), pp.149–159.
- Jelicks, L.A. & Gupta, R.K., 1994. Nuclear-Magnetic-Resonance Measurement of Intracellular Sodium in the Perfused Normotensive and Spontaneously Hypertensive Rat-Heart. *American journal of hypertension*, 7(5), pp.429–435.
- Jessup, J.A., Brosnihan, K.B., et al., 2008. Differential effect of low-dose thiazides on the renin angiotensin system in genetically hypertensive and normotensive rats. *Journal of the American Society of Hypertension*, 2(2), pp.106–115.
- Jessup, J.A., Trask, A.J., et al., 2008. Localization of the novel angiotensin peptide, angiotensin-(1-12), in heart and kidney of hypertensive and normotensive rats. *AJP: Heart and Circulatory Physiology*, 294(6), pp.H2614–H2618.
- Johnson, I. & Spence, M., 2010. The molecular probes handbook. :Life Technologies Corporation; 2010, pp.835-836, p.881, pp.905-906.
- Kahan, T., 1998. The importance of left ventricular hypertrophy in human hypertension. *Journal of hypertension. Supplement : official journal of the International Society of Hypertension*, 16(7), pp.S23–9.
- Kahan, T. & Bergfeldt, L., 2005. Left ventricular hypertrophy in hypertension: its arrhythmogenic potential. *Heart (British Cardiac Society)*, 91(2), pp.250–256.
- Kapur, S. et al., 2010. Early development of intracellular calcium cycling defects in intact hearts of spontaneously hypertensive rats. *AJP: Heart and Circulatory Physiology*, 299(6), pp.H1843–H1853.
- Karmazyn, M. et al., 1999. The myocardial Na<sup>+</sup>-H<sup>+</sup> exchange: structure, regulation, and its role in heart disease. *Circulation Research*, 85(9), pp.777–786.

- Katz, A.M., 2010. *Physiology of the Heart*. : Lippincott Williams &Wilkins; 2010, p.475.
- Kaufmann, S.G. et al., 2013. Distribution and function of sodium channel subtypes in human atrial myocardium. *Journal of Molecular and Cellular Cardiology*, pp.1–9.
- Kaye, D.M. & Kelly, R.A., 1999. Expression and regulation of the sodium-calcium exchanger in cardiac microvascular endothelial cells. *Clinical and Experimental Pharmacology and Physiology*, 26(8), pp.651–655.
- Kemp, C.D. & Conte, J.V., 2012. The pathophysiology of heart failure. *Cardiovascular Pathology*, 21(5), pp.365–371.
- Kerkelä, R. et al., 2011. Key roles of endothelin-1 and p38 MAPK in the regulation of atrial stretch response. *American journal of physiology. Regulatory, integrative and comparative physiology*, 300(1), pp.R140–9.
- Kholidani, C.A., Fares, W.H. & Trow, T.K., 2014. Macitentan for the treatment of pulmonary arterial hypertension. *Vascular health and risk management*, 10, pp.665–673.
- Kockskämper, J. et al., 2001. Activation and Propagation of Ca<sup>2+</sup> Release during Excitation-Contraction Coupling in Atrial Myocytes. *Biophysical Journal*, 81(5), pp.2590–2605.
- Kockskämper, J., Lewinski, von, D., et al., 2008. The slow force response to stretch in atrial and ventricular myocardium from human heart: Functional relevance and subcellular mechanisms. *Progress in Biophysics and Molecular Biology*, 97(2-3), pp.250–267.
- Kockskämper, J., Zima, A.V., et al., 2008. Emerging roles of inositol 1,4,5-trisphosphate signaling in cardiac myocytes. *Journal of Molecular and Cellular Cardiology*, 45(2), pp.128–147.
- Kodavanti, U.P. et al., 2000. The Spontaneously Hypertensive Rat as a Model of Human Cardiovascular Disease: Evidence of Exacerbated Cardiopulmonary Injury and Oxidative Stress from Inhaled Emission Particulate Matter. *Toxicology and Applied Pharmacology*, 164(3), pp.250–263.
- Kohlhaas, M. et al., 2010. Elevated Cytosolic Na<sup>+</sup> Increases Mitochondrial Formation of Reactive Oxygen Species in Failing Cardiac Myocytes. *Circulation*, 121(14), pp.1606–1613.
- Korantzopoulos, P., Kolettis, T. & Goudevenos, J., 2003. Atrial fibrillation in hypertension: an established association with several unresolved issues. *Cardiology*, 100(2), pp.105–106.
- Kranias, E.G. & Hajjar, R.J., 2012. Modulation of cardiac contractility by the phospholamban/SERCA2a regulatome. *Circulation Research*, 110(12), pp.1646–1660.

- Krum, H. et al., 1998. The Effect of an Endothelin-Receptor Antagonist, Bosentan, on Blood Pressure in Patients with Essential Hypertension. *New England Journal of Medicine*, 338(12), pp.784–791.
- Lau, D.H. et al., 2013. Atrial arrhythmia in ageing spontaneously hypertensive rats: unraveling the substrate in hypertension and ageing. M. Rota, ed. *PLoS ONE*, 8(8), p.e72416.
- Layland, J., Solaro, R.J. & Shah, A.M., 2005. Regulation of cardiac contractile function by troponin I phosphorylation. *Cardiovascular Research*, 66(1), pp.12–21.
- Lee, B.L., Sykes, B.D. & Fliegel, L., 2012. Structural and functional insights into the cardiac Na<sup>+</sup>/H<sup>+</sup> exchanger. *Journal of Molecular and Cellular Cardiology*, pp.1–8.
- Lee, S.W. et al., 1983. Decrease in Na<sup>+</sup>,K<sup>+</sup>-ATPase activity and [3H]ouabain binding sites in sarcolemma prepared from hearts of spontaneously hypertensive rats. *Hypertension*, 5(5), pp.682–688.
- Levi, A.J., Lee, C.O. & Brooksby, P., 1994. Properties of the fluorescent sodium indicator “SBFI” in rat and rabbit cardiac myocytes. *Journal of Cardiovascular Electrophysiology*, 5(3), pp.241–257.
- Levy, D. et al., 1996. The Progression From Hypertension to Congestive Heart Failure. *JAMA*, 275(20), pp.1557–1562.
- Li, J.S. & Schiffrin, E.L., 1995. Effect of chronic treatment of adult spontaneously hypertensive rats with an endothelin receptor antagonist. *Hypertension*, 25(4 Pt 1), pp.495–500.
- Louch, W.E., Sheehan, K.A. & Wolska, B.M., 2011. Methods in cardiomyocyte isolation, culture, and gene transfer. *Journal of Molecular and Cellular Cardiology*, 51(3), pp.288–298.
- Maisel, W.H. & Stevenson, L.W., 2003. Atrial fibrillation in heart failure: epidemiology, pathophysiology, and rationale for therapy. *The American journal of cardiology*, 91(6), pp.2–8.
- Maixent, J.-M. et al., 2002. Remodeling of Na,K-ATPase, and membrane fluidity after atrial fibrillation in sheep. *Journal of receptor and signal transduction research*, 22(1-4), pp.201–211.
- Malkoff, J., 2005. Non-invasive blood pressure for mice and rats. *Animal Lab News*.
- Mancia, G. et al., 2014. 2013 ESH/ESC Practice Guidelines for the Management of Arterial Hypertension. *Blood pressure*, 23(1), pp.3–16.
- Mayyas, F. et al., 2010. Association of left atrial endothelin-1 with atrial rhythm, size, and fibrosis in patients with structural heart disease. *Circulation: Arrhythmia and Electrophysiology*, 3(4), pp.369–379.

- McLenachan, J.M. et al., 1987. Ventricular Arrhythmias in Patients with Hypertensive Left Ventricular Hypertrophy. *New England Journal of Medicine*, 317(13), pp.787–792.
- Millane, T. et al., 2000. ABC of heart failure. Acute and chronic management strategies. *BMJ (Clinical research ed.)*, 320(7234), pp.559–562.
- Minta, A. & Tsien, R.Y., 1989. Fluorescent indicators for cytosolic sodium. *Journal of Biological Chemistry*, 264(32), pp.19449–19457.
- Muller-Ehmsen, J. et al., 2001. Region specific regulation of sodium pump isoform and Na,Ca-exchanger expression in the failing human heart--right atrium vs left ventricle. *Cellular and molecular biology (Noisy-le-Grand, France)*, 47(2), pp.373–381.
- Neef, S. et al., 2010. CaMKII-dependent diastolic SR Ca<sup>2+</sup> leak and elevated diastolic Ca<sup>2+</sup> levels in right atrial myocardium of patients with atrial fibrillation. *Circulation Research*, 106(6), pp.1134–1144.
- Nishikibe, M. et al., 1993. Antihypertensive effect of a newly synthesized endothelin antagonist, BQ-123, in a genetic hypertensive model. *Life Sciences*, 52(8), pp.717–724.
- Noresson, E., Ricksten, S.E. & Thoren, P., 1979. Left atrial pressure in normotensive and spontaneously hypertensive rats. *Acta physiologica Scandinavica*, 107(1), pp.9–12.
- Okamoto, K. & Aoki, K., 1963. Development of a strain of spontaneously hypertensive rats. *Japanese circulation journal*, 27, pp.282–293.
- Orchard, C.H. & Kentish, J.C., 1990. Effects of Changes of pH on the Contractile Function of Cardiac-Muscle. *The American journal of physiology*, 258(6), pp.C967–C981.
- O'Connell, T.D. et al., 2014. Cardiac alpha1-adrenergic receptors: novel aspects of expression, signaling mechanisms, physiologic function, and clinical importance. *Pharmacological Reviews*, 66(1), pp.308–333.
- Patel, M.R. et al., 2011. Rivaroxaban versus Warfarin in Nonvalvular Atrial Fibrillation. *New England Journal of Medicine*, 365(10), pp.883–891.
- Pavlovic, D., Fuller, W. & Shattock, M.J., 2013. Novel regulation of cardiac Na pump via phospholemman. *Journal of Molecular and Cellular Cardiology*, pp.1–11.
- Pfeffer, J.M. et al., 1979. Cardiac function and morphology with aging in the spontaneously hypertensive rat. *The American journal of physiology*, 237(4), pp.H461–8.
- Pieske, B. & Houser, S.R., 2003. [Na<sup>+</sup>]<sub>i</sub> handling in the failing human heart. *Cardiovascular Research*, 57(4), pp.874–886.
- Pluteanu, F. et al., 2013. Atrial endothelin-1 signalling in hypertensive rats. *European Heart Journal*, 34 (suppl 1), P5040-5040.

- Pluteanu, F. et al., 2015. Early subcellular Ca<sup>2+</sup> remodelling and increased propensity for Ca<sup>2+</sup> alternans in left atrial myocytes from hypertensive rats. *Cardiovascular Research*, 106(1), pp.87–97.
- Pogwizd, S., 2003. Intracellular Na in animal models of hypertrophy and heart failure: contractile function and arrhythmogenesis. *Cardiovascular Research*, 57(4), pp.887–896.
- Rodriguez, J.S. et al., 2014. Increased Na<sup>+</sup>/Ca<sup>2+</sup> exchanger expression/activity constitutes a point of inflection in the progression to heart failure of hypertensive rats. N. Ashton, ed. *PLoS ONE*, 9(4), p.e96400.
- Schägger, H., 2006. Tricine-SDS-PAGE. *Nature Protocols*, 1 (1), pp.16-22.
- Schotten, U. et al., 2010. Enhanced Late Na<sup>+</sup> Currents in Atrial Fibrillation. *JAC*, 55(21), pp.2343–2345.
- Schotten, U. et al., 2011. Pathophysiological mechanisms of atrial fibrillation: a translational appraisal. *Physiological reviews*, 91(1), pp.265–325.
- Schussheim, A. & Radda, G., 1995. Altered Na<sup>+</sup>-H<sup>+</sup>-exchange activity in the spontaneously hypertensive perfused rat heart. *Journal of Molecular and Cellular Cardiology*, 27(8), pp.1475–1481.
- Schwinger, R.H.G. et al., 1999. Reduced Sodium Pump 1, 3, and 1-Isoform Protein Levels and Na<sup>+</sup>,K<sup>+</sup>-ATPase Activity but Unchanged Na<sup>+</sup>-Ca<sup>2+</sup> Exchanger Protein Levels in Human Heart Failure. *Circulation*, 99(16), pp.2105–2112.
- Scridon, A. et al., 2013. Left atrial endocardial fibrosis and intra-atrial thrombosis - landmarks of left atrial remodeling in rats with spontaneous atrial tachyarrhythmias. *Romanian journal of morphology and embryology = Revue roumaine de morphologie et embryologie*, 54(2), pp.405–411.
- Scridon, A. et al., 2012. Unprovoked atrial tachyarrhythmias in aging spontaneously hypertensive rats: the role of the autonomic nervous system. *AJP: Heart and Circulatory Physiology*, 303(3), pp.H386–H392.
- Seravalle, G., Mancia, G. & Grassi, G., 2014. Role of the sympathetic nervous system in hypertension and hypertension-related cardiovascular disease. *High blood pressure & cardiovascular prevention : the official journal of the Italian Society of Hypertension*, 21(2), pp.89–105.
- Shah, A.M. & Lam, C.S.P., 2014. Function over form? Assessing the left atrium in heart failure. *European Heart Journal*, 36(12), pp.711-714.
- Shanks, J. & Herring, N., 2013. Peripheral cardiac sympathetic hyperactivity in cardiovascular disease: role of neuropeptides. *AJP: Regulatory, Integrative and Comparative Physiology*, 305(12), pp.R1411–R1420.
- Sharp, P. & Villano, J.S., 2012. The laboratory rat. : CRC Press; 2012, p.15

- Shattock, M.J. et al., 2015. Na<sup>+</sup>/Ca<sup>2+</sup>exchange and Na<sup>+</sup>/K<sup>+</sup>-ATPase in the heart. *The Journal of Physiology*, 593(6), pp.1361–1382.
- Slama, M. et al., 2004. Long-term left ventricular echocardiographic follow-up of SHR and WKY rats: effects of hypertension and age. *AJP: Heart and Circulatory Physiology*, 286(1), pp.H181–5.
- Smyrniak, I. et al., 2010. Comparison of the T-tubule system in adult rat ventricular and atrial myocytes, and its role in excitation-contraction coupling and inotropic stimulation. *Cell Calcium*, 47(3), pp.210–223.
- Solaro, R.J. & Rarick, H.M., 1998. Troponin and Tropomyosin Proteins That Switch on and Tune in the Activity of Cardiac Myofilaments. *Circulation Research*, 83(5), pp.471–480.
- Sossalla, S. et al., 2010. Altered Na<sup>+</sup> Currents in Atrial Fibrillation. *JAC*, 55(21), pp.2330–2342.
- Swedberg, K. et al., 2005. Guidelines for the diagnosis and treatment of chronic heart failure: executive summary (update 2005). *European Heart Journal*, 26(11), pp.1115–1140.
- Swift, F. et al., 2008. Altered Na<sup>+</sup>/Ca<sup>2+</sup>-exchanger activity due to downregulation of Na<sup>+</sup>/K<sup>+</sup>-ATPase  $\alpha$ 2-isoform in heart failure. *Cardiovascular Research*, 78(1), pp.71–78.
- Swift, F. et al., 2010. Functional coupling of  $\alpha$ 2-isoform Na<sup>+</sup>/K<sup>+</sup>-ATPase and Ca<sup>2+</sup> extrusion through the Na<sup>+</sup>/Ca<sup>2+</sup>-exchanger in cardiomyocytes. *Cell Calcium*, 48(1), pp.54–60.
- Thibault, G. et al., 1994. Endothelin-stimulated secretion of natriuretic peptides by rat atrial myocytes is mediated by endothelin A receptors. *Circulation Research*, 74(3), pp.460–470.
- Triposkiadis, F. et al., 2009. The Sympathetic Nervous System in Heart Failure. *JAC*, 54(19), pp.1747–1762.
- Trippodo, N.C. & Frohlich, E.D., 1981. Similarities of genetic (spontaneous) hypertension. Man and rat. *Circulation Research*, 48(3), pp.309–319.
- Tsukamoto, O. & Kitakaze, M., 2013. It is time to reconsider the cardiovascular protection afforded by RAAS blockade -- overview of RAAS systems. *Cardiovascular Drugs and Therapy*, 27(2), pp.133–138.
- van Bragt, K.A. et al., 2014. Atrial supply-demand balance in healthy adult pigs: coronary blood flow, oxygen extraction, and lactate production during acute atrial fibrillation. *Cardiovascular Research*, 101(1), pp.9–19.

- van der Velden, J. et al., 2003. Increased  $\text{Ca}^{2+}$ -sensitivity of the contractile apparatus in end-stage human heart failure results from altered phosphorylation of contractile proteins. *Cardiovascular Research*, 57(1), pp.37–47.
- Vanecková, I., 2002. Function of the isolated perfused kidney in young and adult spontaneously hypertensive and Dahl salt-sensitive rats. *Kidney & blood pressure research*, 25(5), pp.315–321.
- Varagic, J., Susic, D. & Frohlich, E.D., 2001. Low-dose ACE with alpha- or beta-adrenergic receptor inhibitors have beneficial SHR cardiovascular effects. *Journal of cardiovascular pharmacology and therapeutics*, 6(1), pp.57–63.
- Vaughan-Jones, R.D., Spitzer, K.W. & Swietach, P., 2009. Intracellular pH regulation in heart. *Journal of Molecular and Cellular Cardiology*, 46(3), pp.318–331.
- Voigt, N. et al., 2012. Enhanced sarcoplasmic reticulum  $\text{Ca}^{2+}$  leak and increased  $\text{Na}^{+}$ - $\text{Ca}^{2+}$  exchanger function underlie delayed afterdepolarizations in patients with chronic atrial fibrillation. *Circulation*, 125(17), pp.2059–2070.
- Vrbjar, N. et al., 2002. Sodium and ATP affinities of the cardiac  $\text{Na}^{+}$ , $\text{K}^{+}$ -ATPase in spontaneously hypertensive rats. *General Physiology and Biophysics*, 21(3), pp.303–313.
- Walker, J.M. 1994. The bicinchoninic acid (BCA) assay for protein quantification. *Methods in Molecular Biology*, 32, pp. 5-8.
- Wakabayashi, S., Hisamitsu, T. & Nakamura, T.Y., 2013. Regulation of the cardiac  $\text{Na}^{+}/\text{H}^{+}$  exchanger in health and disease. *Journal of Molecular and Cellular Cardiology*, 61(C), pp.68–76.
- Wakili, R. et al., 2011. Recent advances in the molecular pathophysiology of atrial fibrillation. *Journal of Clinical Investigation*, 121(8), pp.2955–2968.
- Wang, T.J. et al., 2003. Temporal relations of atrial fibrillation and congestive heart failure and their joint influence on mortality: the Framingham Heart Study. *Circulation*, 107(23), pp.2920–2925.
- Ward, M.L. et al., 2003. Reduced contraction strength with increased intracellular  $[\text{Ca}^{2+}]$  in left ventricular trabeculae from failing rat hearts. *The Journal of Physiology*, 546(2), pp.537–550.
- Weber, K.T. & Brilla, C.G., 1991. Pathological hypertrophy and cardiac interstitium. Fibrosis and renin-angiotensin-aldosterone system. *Circulation*, 83(6), pp.1849–1865.
- Wendt Gallitelli, M.F., Voigt, T. & Isenberg, G., 1993. Microheterogeneity of subsarcolemmal sodium gradients. Electron probe microanalysis in guinea-pig ventricular myocytes. *The Journal of Physiology*, 472(1), pp.33–44.

- Wijesurendra, R.S. & Casadei, B., 2015. Atrial fibrillation: effects beyond the atrium? *Cardiovascular Research*, 105(3), pp.238–247.
- Wikberg, J. et al., 1983. Norepinephrine-Induced Down Regulation of Alpha-1-Adrenergic Receptors in Cultured Rabbit Aorta Smooth-Muscle Cells. *Life Sciences*, 33(14), pp.1409–1417.
- Workman, A.J., Kane, K.A. & Rankin, A.C., 2003. Characterisation of the Na, K pump current in atrial cells from patients with and without chronic atrial fibrillation. *Cardiovascular Research*, 59(3), pp.593–602.
- Yanagisawa, M. et al., 1988. A novel potent vasoconstrictor peptide produced by vascular endothelial cells. *Nature*, 332(6163), pp.411-415.
- Yono, M. et al., 2004. Doxazosin treatment causes differential alterations of alpha 1-adrenoceptor subtypes in the rat kidney, heart and aorta. *Life Sciences*, 75(21), pp.2605–2614.
- Zahler, R. et al., 1996. Na-K-ATPase alpha-isoform expression in heart and vascular endothelia: cellular and developmental regulation. *AJP: Cell Physiology*, 270(1), pp.C361–C371.
- Zeng, J. & Rudy, Y., 1995. Early afterdepolarizations in cardiac myocytes: mechanism and rate dependence. *Biophysical Journal*, 68(3), pp.949–964.
- Zhang, L. et al., 2002. Alpha-1 adrenoceptor up-regulation induced by prazosin but not KMD-3213 or reserpine in rats. *British Journal of Pharmacology*, 135(7), pp.1757–1764.
- Zhu, W. et al., 2000. Ca<sup>2+</sup>/calmodulin-dependent kinase II and calcineurin play critical roles in endothelin-1-induced cardiomyocyte hypertrophy. *Journal of Biological Chemistry*, 275(20), pp.15239–15245.



## 8. Abbreviations

Abbreviation	Full text
[Ca <sup>2+</sup> ]	Calcium concentration
[Na <sup>+</sup> ] <sub>i</sub>	Intracellular sodium concentration
AF	Atrial fibrillation
ANOVA	Analysis of variance
APS	Ammoniumpersulfate
ATP	Adenosine triphosphate
BCA	Bicinchoninic acid
BDM	2,3-Butanedione 2-Monoxime
bpm	Beats per minute
Br-Ph Blue	Bromophenol blue sodium salt
BSA	Bovine serum albumin
cAF	Chronic atrial fibrillation
CaMKII	Ca <sup>2+</sup> /calmodulin-dependent protein kinase II
CICR	Ca <sup>2+</sup> -induced Ca <sup>2+</sup> release
CSQ	Calsequestrin
ddH <sub>2</sub> O	Double distilled water
CTGF	Connective tissue growth factor
DMSO	Dimethyl sulfoxide
DTT	Dithiothreitol

e.g.	exempli gratia
ECC	Excitation-contraction coupling
EDTA	Ethylenediaminetetraacetic acid
EGTA	Ethylene glycol tetraacetic acid
Eppendorf tube	Eppendorf (microcentrifuge) tube
ET <sub>A</sub> R	Endothelin-A receptor
ET <sub>B</sub> R	Endothelin-B receptor
ETR	Endothelin receptor
GAPDH	Glyceraldehyde 3-phosphate dehydrogenase
GPCR	G-protein coupled receptor
HEPES	4-(2-hydroxyethyl)-1-piperazineethanesulfonic acid
HF	Heart failure
HRP	Horseradish peroxidase
Hz	The Hertz unit of frequency
IgG	Immunoglobulin G
IP <sub>3</sub>	Inositol 1,4,5-trisphosphate
IP <sub>3</sub> R	Inositol 1,4,5-trisphosphate receptor
kDa	Kilo Dalton
LTCC	L-type calcium channel
mmHg	Millimeter of mercury
NaCl	Sodium chloride
NADH	Nicotineamide adenine dinucleotide

NADPH	Nicotineamide adenine dinucleotide phosphate
NCX	Sodium-calcium exchanger
NF	Non-failing stage
NHE	Sodium-hydrogen exchanger
NKA	Sodium-potassium ATPase
nM	Nanomolar
NP-40	Tergitol-type NP-40
PAA/BIS	Polyacrylamide/N,N'-methylene-bisacrylamide
PAA/BIS 30%	30% acrylamide/bis-acrylamide, 29:1 (3.3% crosslinker) solution
pAF	Paroxysmal atrial fibrillation
PIP <sub>2</sub>	Phosphatidylinositol 4,5-bisphosphate
PKA	Protein kinase A
PKC	Protein kinase C
PLB	Phospholamban
PLC $\beta$	Phospholipase C $\beta$
PLM	Phospholemman
PMSF	Phenylmethylsulfonyl fluoride
Ponceau S	Ponceau S, Acid Red 112
pPLB S16	Phospholamban phosphorylated at serine 16
pPLB Th17	Phospholamban phosphorylated at threonine 17
pPLB S10	Phospholamban phosphorylated at serine 10
pRyR S 2808	Ryanodine receptor phosphorylated at serine 2808

pRyR S 2814	Ryanodine receptor phosphorylated at serine 2814
q.s.	Quantum satis
RAAS	Renin-angiotensin-aldosterone system
rpm	Revolutions per minute
RT	Room temperature
RyR	Ryanodine receptor
SBFI	Sodium-binding benzofuran isophthalate
SDS	Sodium dodecyl sulfate
SDS-PAGE	Sodium dodecyl sulfate polyacrylamide gel electrophoresis
SEM	Standard error of the mean
SERCA	Sarcoplasmic reticulum Ca <sup>2+</sup> ATPase
SHR	Spontaneously hypertensive rats
TBS	Tris buffered solution
TBST buffer	Tris-buffered saline and Tween 20 buffer
TEMED	Tetramethylethylenediamine
Tris	Tris(hydroxymethyl)aminomethane
Tween 20	Polysorbate 20
VPR	Volume Pressure Recording
vs.	Versus
WKY	Wistar Kyoto rats

## 9. List of Figures

Figure 1. Electrocardiographic recording of sinus rhythm and the onset of an atrial fibrillation episode.....	13
Figure 2. Role of atrial remodelling in the initiation of atrial fibrillation .....	17
Figure 3. Interconnection between heart failure and atrial fibrillation .....	19
Figure 4. Association and potential connections between hypertension, heart failure and atrial fibrillation.....	20
Figure 5. Excitation-contraction coupling in ventricular myocyte .....	25
Figure 6. Na <sup>+</sup> involvement in excitation-contraction coupling in ventricular myocyte.....	28
Figure 7. The onsets of cardiovascular changes during the lifespan of SHR .....	35
Figure 8. CODA system for measurements of blood pressure and heart rate.....	40
Figure 9. Langendorff system for isolation of cardiac myocytes. ....	44
Figure 10. SBF1 molecule (TEFLABS, <a href="http://www.teflabs.com">www.teflabs.com</a> ).....	45
Figure 11. SBF1 molecule and the fluorescent spectrum of SBF1.....	46
Figure 12 Setup for [Na <sup>+</sup> ] and contractility measurements .....	50
Figure 13. Chamber system.....	51
Figure 14. Video image of an atrial myocyte with region of interest for measurement of sarcomere shortening. ....	52
Figure 15. Analysis of twitch .....	53
Figure 16. Cardiovascular characteristics of 3 and 7 months old rats .....	68
Figure 17. Contractility of atrial myocytes in 7 months old rats .....	69
Figure 18. Comparison of left and right atrial myocyte contractility in 7 months old rats.....	70
Figure 19. [Na <sup>+</sup> ] <sub>i</sub> in 3 and 7 months old animals.....	72
Figure 20. Comparison of [Na <sup>+</sup> ] <sub>i</sub> between left and right atrial myocytes in 7 months old animals .....	73
Figure 21. Expression of Na <sup>+</sup> influx proteins in left and right atrium from 3 months old rats.....	74
Figure 22. Expression of Na <sup>+</sup> efflux proteins in left and right atrium from 3 months old rats.....	76
Figure 23. Expression of Na <sup>+</sup> influx proteins in left and right atrium from 7 months old rats.....	77
Figure 24. Expression of Na <sup>+</sup> efflux proteins in left and right atrium from 7 months old rats .....	78
Figure 25. Cardiovascular characteristics of 15-23 months old WKY and SHR.....	81
Figure 26. Cardiovascular characteristics of SHR-NF and SHR-HF.....	82
Figure 27 Sarcomere length (SL) shortening in atrial myocytes from WKY, SHR-NF and SHR-HF .....	83
Figure 28. Comparison of left and right atrial myocyte contractility in 15-23 months old WKY and SHR.....	85

Figure 29. Comparison of left and right atrial myocyte contractility in SHR-NF and SHR-HF.....	86
Figure 30. Sarcomere length (SL) shortening in ventricular myocytes from WKY, SHR-NF and SHR-HF .....	88
Figure 31. $[Na^+]_i$ in atrial myocytes from WKY, SHR-NF and SHR-HF .....	90
Figure 32. Comparison of intracellular $Na^+$ concentration between left and right atrial myocytes in WKY, SHR-NF and SHR-HF rats .....	91
Figure 33. $[Na^+]_i$ in ventricular myocytes from WKY, SHR-NF and SHR-HF .....	92
Figure 34. $Na^+$ influx protein expression in left atrium from WKY, SHR-NF and SHR-HF .....	93
Figure 35. $Na^+$ influx protein expression in right atrium from WKY, SHR-NF and SHR-HF.....	94
Figure 36. $Na^+$ efflux protein expression in left atrium from WKY, SHR-NF and SHR-heart failure .....	95
Figure 37. $Na^+$ efflux protein expression in right atrium from WKY, SHR-NF and SHR-HF .....	97
Figure 38. $Na^+$ influx protein expression in right atrium in sinus rhythm (SR), paroxysmal atrial fibrillation (pAF) and chronic atrial fibrillation patients (cAF).....	102
Figure 39. $Na^+$ efflux protein expression in right atrium in sinus rhythm (SR), paroxysmal atrial fibrillation (pAF) and chronic atrial fibrillation patients (cAF).....	104
Figure 40. Effect of macitentan treatment on blood pressure and heart rate in SHR .....	107
Figure 41. Effects of macitentan or doxazosin administration on expression of $\alpha$ 1C subunit of L-type $Ca^{2+}$ channels, $Na^+/Ca^{2+}$ exchanger and ryanodine receptor in left atrium of SHR.....	109
Figure 42. Effects of macitentan or doxazosin treatment on the expression and phosphorylation of SR $Ca^{2+}$ -handling proteins.....	111
Figure 43. Effects of macitentan or doxazosin treatment on the expression of proteins involved in endothelin-1 signalling.....	113
Figure 44. Atrial remodelling in advanced hypertensive heart disease in SHR.....	128

## 10. List of tables

Table 1. Basic Tyrode's solution (without Ca <sup>2+</sup> ) 1l, pH 7.4 .....	41
Table 2. Cardioplegic solution.....	41
Table 3. Cannulation solution.....	41
Table 4. Ca <sup>2+</sup> - free solution.....	42
Table 5. Enzyme solution .....	42
Table 6. Stop solution (0.5 mM Ca <sup>2+</sup> ).....	42
Table 7. 1 mM Ca <sup>2+</sup> solution .....	42
Table 8. 1.5 mM Ca <sup>2+</sup> solution.....	42
Table 9. 2 mM Ca <sup>2+</sup> solution .....	43
Table 10. Scheme of atrial myocytes adaptation to physiological Ca <sup>2+</sup> concentration.....	44
Table 11. Recording solution, pH 7.4 .....	48
Table 12. Solution A for SBFI calibration (145 mM Na <sup>+</sup> ), pH 7.2 .....	49
Table 13. Solution B for SBFI calibration (145 mM K <sup>+</sup> ), pH 7.2.....	49
Table 14. Homogenization (lysis) buffer .....	55
Table 15. Composition of 8% running gel for SDS-PAGE (10 ml) .....	56
Table 16. Composition of 4% stacking gel for SDS-PAGE (5 ml).....	57
Table 17. 10% Ammoniumpersulphate (APS).....	57
Table 18. 1.5 M Tris-HCL pH 8.8 .....	57
Table 19. 0.5 M Tris-HCL pH 6.8 .....	57
Table 20. Composition of 16% and 14% Tris-tricine running gel (12 ml).....	57
Table 21. 3 M Tris HCl/SDS (3x) pH 8.45.....	58
Table 22. Lämmli buffer 4x.....	59
Table 23. Running buffer for Glycine-SDS-PAGE .....	59
Table 24. Cathode buffer for Tricine-SDS-PAGE pH 8.25 .....	60
Table 25. Anode buffer for Tricine-SDS-PAGE pH 8.9 .....	60
Table 26. 10x Transfer buffer 1l.....	60
Table 27. 20x TBS buffer pH 7.5.....	61
Table 28. Investigated proteins and primary antibodies .....	62
Table 29. Secondary antibodies .....	64
Table 30. Stripping buffer pH 2.2.....	65

## 11. Publications

### 11.1. Original papers

2014

Walther S., Pluteanu F., Renz S., **Nikonova Y.**, Maxwell J.T., Yang L., Schmidt K., Edwards J.N., Wakula P., Groschner K., Maier L.S., Spiess J., Blatter L.A., Pieske B., Kockskämper J., 2014, Urocortin stimulates nitric oxide production in ventricular myocytes via Akt-and PKA-mediated phosphorylation of eNOS at serine 1177. *AJP: Heart and Circulatory Physiology*, 307(5), pp.H689–H700

2015

Pluteanu F., Heß J., Plackic J., **Nikonova Y.**, Preisenberger J., Bukowska A., Schotten U., Rinne A., Kienitz M., Schäfer M.K.-H., Weihe E., Goette A., Kockskämper J., 2015 Early subcellular Ca<sup>2+</sup> remodelling and increased propensity for Ca<sup>2+</sup> alternans in left atrial myocytes from hypertensive rats. *Cardiovascular Research*, 106 (1) pp. 87-97.



## 11.2. Abstracts and poster presentations

2011

Plutenau F., Heß J., **Nikonova Y.**, Plackic J., Kockskämper J., Atrial calcium handling in spontaneously hypertensive rats, Herbsttagung der Deutschen Gesellschaft für Kardiologie – Herz- und Kreislaufforschung e.V. (DGK), Düsseldorf, Germany, 06.10.11-08.10.11

2012

Pluteanu F., Kiess T., Sack C., **Nikonova Y.**, Plackic J., Roderick H.L., Kockskämper J., Endothelin-1 alters calcium transients in atrial myocytes from spontaneously hypertensive rats, 91. Jahrestagung der Deutschen Physiologischen Gesellschaft e.V., Dresden, Germany, 22.03.12-25.03.12

2014

Pluteanu F., Preisenberger J., Heß J., **Nikonova Y.**, Plackic J., Kockskämper J., Altered  $Ca^{2+}$  homeostasis and  $Ca^{2+}$  alternans in left atrial myocytes of spontaneously hypertensive rats, 58<sup>th</sup> annual Biophysical society meeting, San-Francisco, California, USA, 15.02.14-18.02.14

Plackic J., Pluteanu F., **Nikonova Y.**, Preisenberger J., Kockskämper J., Subcellular calcium handling during transition from hypertrophy to heart failure in ventricular myocytes of spontaneously hypertensive rats, 80. Jahrestagung der Deutschen Gesellschaft für Pharmakologie und Toxikologie, Hannover, Germany, 01.04.14-03.04.14

2015

**Nikonova Y.**, Pluteanu F., Plackic J., Herzog B., Kockskämper J., Left atrial hypertrophy and reduced contractility and intracellular sodium concentration in atrial myocytes from hypertensive rats during the development of heart failure, Herbsttagung der Deutschen Gesellschaft für Kardiologie – Herz- und Kreislaufforschung e.V. (DGK), Berlin, Germany, 08.10.15-10.10.15

2016

Bukowska A., Kockskämper J., **Nikonova Y.**, Pluteanu F., Chilukoti R.K., Wolke C., Lendeckel U., Goette A., Anti-inflammatory effects of endothelin receptor blockade on the atrial tissue in spontaneously hypertensive rats, accepted abstract for poster presentation, Frontiers in Cardiovascular Biology, European Society for Cardiology, Florence, Italy, 08.07.16-10.07.16

## **Curriculum vitae**

This page contains personal information. It is therefore excluded from online publication.

Diese Seite enthält persönliche Daten. Sie ist daher nicht Bestandteil der Online-Veröffentlichung.

## 12. Acknowledgements

First of all, I would like to thank my supervisor Prof. Dr. Jens Kockskämper for giving me the opportunity to do my PhD studies in his group. I am very grateful for his patience and also for keeping me motivated during the difficult moments in my research process. I am very grateful for the opportunities that he gave me to go to several national conferences and international meetings. I am very appreciated for his warm welcome when I first came to Marburg as a diploma student to his lab and later, when I returned to Marburg to do my PhD studies.

I would like to thank Prof. Dr. Moritz Bünemann, Prof. Dr. Carsten Culmsee and Dr. Cornelius Krasel for their questions, suggestions, comments and feedback during my progress reports.

I am very grateful to Dr. Florentina-Cornelia Pluteanu for teaching me the basics of the western blot method, for many pieces of advice, regarding experiments, lab organization, and maintenance.

I would like to thank in particular my colleague and friend Jelena Plackic for all the advice, tips, suggestions, and scientific discussions. Without her encouragement and positive energy, I could have hardly imagined my everyday lab routine. She was always a great support.

Special thanks to Judit Preisenberger and Tobias Kiess for being great and supportive colleagues.

I would like to thank Anna Holzapfel, Eleni Knefeli, Birgit Herzog for their help with experiments. Many thanks to all my "Wahlpflichtstudents": Julia Lukassowitz, Natalie Leman, Michael Kurz, David Celik, Hanna Hähl, Jonas Reichert, Alya Mouzayen and Sara Roggenbuck.

I would like to thank Sandra Engel, Katharina Elsässer for their help with ordering the laboratory equipment.

Special thanks to Emma Esser for her friendliness and great help with the paperwork and all the formalities.

Many thanks to Ulrich Korell for technical help.

I am deeply grateful to my colleague and good friend Gaye Tanriöver for being around, encouraging and supporting me, especially during my writing process.

Many thanks to all my colleagues at the Institute of Pharmacology and Clinical Pharmacy.

I would like to thank in particular my friends in Marburg: Maria Solovey and Svetlana Kuzmina for being around and helping me to get through my difficult times.

Many thanks to Dr. Liudmila Pavlova for the moral support and useful advice.

Very special thanks to Jan-Patrick Rotter for his help, moral and humour support.

Without my parents and my beloved sister Anna Nikonova, I would not even dare move to Marburg and start my PhD studies. You were far away, but I always felt your love.

Огромное спасибо моим любимым родителям и любимой сестре Анне Никоновой за всё, что вы для меня сделали и делаете до сих пор.

Thanks to all my friends for believing in me.

## ERKLÄRUNG

Ich versichere, dass ich meine Dissertation

„Atrial remodelling in hypertensive heart disease: role of Na<sup>+</sup> homeostasis and contractility“

selbständig ohne unerlaubte Hilfe angefertigt und mich dabei keiner anderen als der von mir ausdrücklich bezeichneten Quellen bedient habe. Alle vollständig oder sinngemäß übernommenen sind Zitate als solche gekennzeichnet.

Die Dissertation wurde in der jetzigen oder einer ähnlichen Form noch bei keiner anderen Hochschule eingereicht und hat noch keinen sonstigen Prüfungszwecken gedient.

Marburg, den 31.03.2016

.....  
(Yulia Nikonova)